Green's Function for Multiterminal Josephson Junctions

Yury Holubeu

Mentor, Supervisor: Dr. Kiryl Piasotski
Karlsruhe Institute of Technology (KIT)

Co-supervisor: Prof. Thomas Van Riet
KU Leuven, Department of Physics
and Astronomy

Contents

Abstract

The study develops Green's function formalism for the description of the quantum dot that is coupled to an arbitrary number of superconducting leads. Such formalism allows computing the bound states and current numerically for arbitrary combinations of the microscopic parameters. The Andreev levels and supercurrent as a function of phase differences are shown for the two- and three-terminal Josephson junctions with the quantum dot. The dependence of the levels on the change of on-site energy of the dot, superconductive gap, and the coupling strength are plotted. The results are approximated by analytical formulas for two- and three-terminal junctions, and they are applied to calculate the diode efficiency of the latter. This approach has been extended from the case of a dot to a general continuous three-dimensional non-superconducting central domain with couplings to superconductors at different points. The expression of density of states is provided. Our methods can be applied to the analysis of spin-qubits and the creation of superconductive diodes.

Last compilation: January 29, 2025.

Summary

The analysis of multiterminal Josephson junctions (MTJJ) is at the forefront of research in condensed matter physics. The potential applications of such structures vary from topological quantum computations to dissipationless nanoelectronics. This work attempts to provide a framework, within which tunneling properties of MTJJ can be obtained algorithmically beyond the tunneling limit. First, we review the fundamental properties of superconductivity, such as Josephson relations, the BCS model, and Andreev states. Then we provide an introduction to the methods for calculating current, discuss the concept of Green's function (GF) and Nambu notation, finishing the review with two examples of MTJJ. After that, a detailed description of the GF formalism is presented, which was developed by the authors for a quantum dot (QD) with Zeeman interaction coupled to an arbitrary number of superconducting leads. By using the Nambu formalism, we combine the effects of couplings to the superconductive terminals to the effective self-energy, which allows us to obtain the full GF of the dot and superconductors. From such formulas, the expressions of the tunneling density of states and the current are established. The final formulas for numerical calculations and some examples of the code are provided. The validity of our approach is tested in the case of two-terminal junctions by finding the analytical expressions for the Andreev levels and the current as a function of phase difference. Further, we establish these quantities for the three-terminal Josephson junction and provide numerical results. Additionally, the diode efficiency as a function of the transparency of the junction is calculated. Finally, we extend the GF formalism to the case of continuous three-dimensional non-superconductive region and provide a formula for the density of states. Our method allows one to determine the dependence of the Zeeman splitting of bound states on the terminal phases, which can be applied to analyze possible ways of manipulating the Andreev spin qubit.

Introduction

Over the past century, the field of superconductivity has evolved from a niche interest of a few specialists to a cornerstone of condensed matter physics, distinguished by eight Nobel Prizes and the development of hundreds of methods and proposed applications. Superconductivity (SC), a phenomenon characterized by persistent current or zero electrical resistance at low temperatures, was first discovered in 1911 by the Dutch scientist Kamerlingh Onnes. Since then several genius theoretical approaches had been proposed before the most famous theory of condensed matter, the theory of superconductivity by Bardeen-Cooper-Schrieffer (BCS), was formulated in 1957 [41]. This theory explained the phenomenon by the new state of electrons, in which one of them pairs up with another having the opposite spin and direction of movement (known as "Cooper pairs"). These pairs are thousand times larger than the atomic difference of the material lattice and exist only because of their effective interaction, mediated by the material. In the BCS framework, the main parameter of a superconductor is a complex-valued function $\boldsymbol{\Delta} = \Delta e^{i\varphi}$, called "the gap function". Its amplitude Δ is responsible for the minimal energy of excitations of the condensate and the φ, called "the phase", plays the same role as the phase of a wave-function in quantum mechanics.

Soon it was realized that superconductive wires not only allow ow current to be transferred without energy loss, but also can be used to build special devices with unique properties. In 1962 Brian Josephson predicted the law of supercurrent flow through a weak coupling between two superconductors [42]. Such current flows at equilibrium and depends on the phases of the superconductors and such couplings are known as superconductor-normal metal-superconductor (SNS) contacts. In 1963 Alexander Andreev proposed a peculiar process of transformation of an electron to a hole (absence of an electron) if it falls on the border between normal region and superconductor [43]. Such process produces lower energy states in the normal region between superconductors, similar to bound states in potential wells in quantum mechanics. These discoveries were the fundamental breakthrough and established a new part of condensed matter theory, which is sometimes referred to as "mesoscopic physics of superconductors". The development of this field led to the creation of numerous gadgets, while more devices were theoretically predicted, e.g. fast switches and transistors [94], semiconductors [58], nanotubes [87], ferromagnets [86], graphene [85], topological insulators [84], quantum optics [55], high-speed digital electronics [54] or creation of artificial atoms [51].

The important direction in the tunneling physics is the analysis of multiterminal Josephson junctions (MTJJ). Such devices are the generalization of the SNS contact for more than two superconductors, typically for three (3TJJ) or for four (4TJJ) terminals, and for a different central region. They may be of interest for topological quantum information processing applications [61, 60], provide a possibility of engineering topologically protected matter of dimension higher than three [33, 34, 7], can be used for establishing ultralong quantum correlations [28], and potentially be a part of magnetic field sensors [35], thermal circulators [36], etc. Another hot-studied topic is the diode effect in the MTJJ [7, 12]. This occurs in some configurations of phases, when the critical current in one terminal is stronger than in the others (becomes direction-dependent), similar to an electronic diode but without energy dissipation. Another recently proposed application is connected to creation of Andreev spin qubits. In such setups, the Andreev levels are brought to the state in which spin-1/2 persists over a long time, thus being a quantum

5

bit [57]. Special materials with spin-orbit (SO) and Zeeman couplings allow for quantum operations and read-out of spin states. In November 2024, it was proposed to make an Andreev spin qubit with three-terminal Josephson junction and their coupling was analyzed [37].

For achieving such engineering possibilities, several theoretical methods have been developed. The best-known approaches can be categorized into three types. The first one is the tight-binding numerical approach, when the mode is discretized into sites and efficient matrix algorithms are used for the numerical solving of the discretized equations of motion. It played a key role in the creation of the popular Python library for the computation of electron transport Kwant [81, 82]. It is closely related to the second type of methods: the Green's function (GF) class of approaches [109, 108]. This is a vast class of methods, ranging from quantum field theory applications to the tight-binding GF. The third celebrated class of methods is the scattering matrices approach. It originates from the 1980s, when the Bogoliubov equations, which directly follow from the BCS model, were used to study reflectance at boundaries and bound states in junctions [80]. Further on, in the 1990s, Carlo Beenakker proposed his celebrated determinantal method [71], which has been successfully applied to describe uncountable number of models.

The present thesis pursues two main goals: to provide a general formalism that can be applied systematically to any type of MTJJ and to obtain some non-trivial properties of a three-terminal system. Methodology-wise, we describe a general approach to the analysis of discrete and continuous multiterminal junctions, while application-wise we demonstrate the method by revealing the physical properties of a QD coupled to several SC leads. This is achieved through providing analytical and numerical results of the bound states and current, showing the influence of microscopic input parameters of the model on the macroscopic quantities. The knowledge of how exactly the spin splitting of the levels depends on the phase differences of the SC leads can be used for a realization of a spin qubit and properties of the tunneling current can be used for increasing the diode efficiency.

The structure of the thesis is as follows. First, in Sec. 1, we provide an overview of the most fundamental methods that will be used later in our work. Sec. 2 is dedicated to the description of the multiterminal QD model. We show how GF formalism can be developed and provide formulas for the bound states and the current. Then, we present the numerical results for S-QD-S junction and 3-terminal junction. Later, in Sec. A, we generalize our theory to continuous models. We start with a simplified model to make the formulas comprehensible and then provide a version for a general case. Finally, several supplementary sections are provided in Sec. B: the glossary in Sec. B.1 and a mind map of the reviewed models in Sec. B.2, and the key formulas of our theory in Sec. B.3. We finish by two reviews of scattering matrix approach B.4 and of Majorana states B.5, derivations for the discrete B.6.1 and for continuous B.6.2 GF formalisms, and examples of the Python code in Sec. B.7, which was used to obtain the plots.

1 A Short Review of Basic Concepts and Methods

In this section we will increase the arsenal to be used for our main attack: description of the multiterminal junction (see Sec. 2 and Sec. A.2). However, due to the volume restrictions of this thesis, only key points will be presented with references to the original works.

1.1 The Basics of Superconductivity, Josephson Effect, Andreev States

The Josephson Effect

The Josephson effect is typically discussed in the setup called SNS contact or Josephson junction (JJ), which is shown in Fig. 1. On the left, we have a superconductor with phase ϕ_L and density of Cooper pairs n_{s1} and the analogous one on the right. The normal region between them is a short one, so the Cooper pairs from different SC "feel" each other. By this we mean that their wavefunctions overlap, thus there can be a tunneling. Instead of N there can be an insulator (I) or other materials, as will be reviewed later. There are
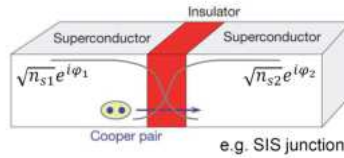

Figure 1: Josephson junction. Credit: [55]

two famous laws for a such supercurrent: the first Josephson equation (or current-phase relation, or CPR) and the second Josephson equation (or voltage-phase relation), which are as follows:

$$I = I_c \sin \varphi, \tag{1.1}$$

$$\dot{\varphi} = \frac{2\pi}{\Phi_0} V. \tag{1.2}$$

Here I_c is the critical current, which can be obtained from the Josephson coupling energy E_J of the junction $I_c = (2e/\hbar)E_J$; the phase $\varphi := \phi_L - \phi_R$ is the phase difference of the two superconductors; V is a electrostatic potential difference, which can also be applied; $\Phi_0 = h/2e$ is the magnetic-flux quantum. This equations can be obtained in several ways, ranging from solving Schrödinger equation for a 2×2 Hamiltonian [20, 49] to the calculation of susceptibility by using Green's functions of the microscopic theory of superconductivity [107] (to be reviewed below). It is important to understand that Josephson current takes place in thermodynamic equilibrium. Often JJ is realized when the proximity effect occurs, which consists of the overlapping of the wavefunction of Cooper pairs in the normal region. Such regions can also exhibit superconductivity, which in these cases is referred to as a "proximity induced".

The generalization of the equation (1.1) for the case of other contacts and accounting for various phenomena is the result of hundreds of studies conducted over the past 60

years. For example, the critical supercurrent I_c as a function of temperature is often obtained by the prominent formula known as "Ambegaokar-Baratoff relation":

$$I_0 = \frac{\pi\Delta}{2eR} \operatorname{th} \frac{\Delta}{2T}, \tag{1.3}$$

where R is the resistance of N region. This is the maximal current that can occur in the junction and often CPR are normalized to it (see Fig. 3) Besides, some junctions have not a sine(φ), but a modification. For example, there are so-called "π-junctions" or "φ-junctions" [45]. A detailed review of CPRs was done by Golubov et al. [68]. Another important physical effects can be seen by calculating and measuring current-voltage curves, the review of which can be found in [67].

There are several reasons why Josephson junctions are important. With JJ, it is possible create superconducting circuits, which could realize qubits (make so-called "transmon qubit") and see the phenomena of their interaction with light. This field is known as "circuit quantum electrodynamics". A perfect introduction to it is provided by Blais et al. [52]. Another important direction is that two JJ can be combined in a loop and the penetration of flux through it, well-known SQUID, produces the flux quantization, Fraunhofer pattern of the current and other effects [20]. This leads to many applications, for example, in sensing of magnetic field, MRI in medicine etc.

The BCS Hamiltonian

The key idea of the BCS theory it is that at low temperature electrons in some metals form a broad pairs (so-called Cooper pairs) because of the exchange of lattice vibration (which is described in the framework of condensed matter by special quasi-particle "phonon"). This can be expressed by a famous mean-field Hamiltonian that effectively describes interactions near the Fermi level. It can be constructed as follows. As usual, we start by writing the first term of a kinetic energy, which we count from the Fermi level, since at low temperatures the majority of electron states in metals are occupied. Then we add a hermitian potential term with two parts. The first part has two creation operators that create a Cooper pair, and the second one that annihilate the same pair. The BCS Hamiltonian for 3D continuous superconductor has the form [41, 3]:

$$\begin{aligned}
\mathcal{H}_{\mathrm{BCS}} := \int d\mathbf{r}\, \psi_\alpha^\dagger(\mathbf{r}) \left[\frac{1}{2m^*} \left(\mathbf{p} - \frac{e}{c}\mathbf{A}(\mathbf{p}) \right)^2 - \mu \right] \psi_\alpha(\mathbf{r}) - \\
- \frac{1}{2} \int d\mathbf{r} d\mathbf{r}' \left\{ \psi_\alpha^\dagger(\mathbf{r})\psi_\beta^\dagger(\mathbf{r}')\Delta_{\beta\alpha}(\mathbf{r}',\mathbf{r}) + \bar\Delta_{\alpha\beta}(\mathbf{r},\mathbf{r}')\psi_\beta(\mathbf{r}')\psi_\alpha(\mathbf{r}) \right\}.
\end{aligned} \tag{1.4}$$

Here the operator[1] $\psi_\alpha^\dagger(\mathbf{r})$ creates a normal electron with spin $\beta = +, -$; the momenta $\mathbf{P} = \mathbf{p} - \frac{e}{c}\mathbf{A}(\mathbf{p})$ takes into account existence of the vector potential $\mathbf{A}$ from an electromagnetic field; μ is the Fermi energy. In this notation the second term uses the matrix order parameter, which satisfies $\bar\Delta_{\alpha\beta}(\mathbf{r},\mathbf{r}') = -\Delta_{\alpha\beta}(\mathbf{r},\mathbf{r}')^*$, since the Hamiltonian is hermitian. The $\alpha, \beta \in \{\uparrow, \downarrow\}$ are the spin components, over which the summation is assumed. We will refer to the BCS Hamiltonian as "s-wave superconductor", because of the trivial angular dependence (the notation is the same as in quantum mechanics, where there are s, p, d orbitals).

---

[1]Relation of them to a wave-function is reviewed in Sec. 1.3.

BCS Hamiltonian is often used in the discretized version, when it is assumed that there are just points in space, like atoms, that can interact with each other with different strength. This is especially useful for tunneling models, where it was applied, for example, to create a popular software package [81]. The discrete version of the BCS Hamiltonian looks as follows:

$$H_{\text{BCS}} := \sum_{k\sigma} \xi_k c^\dagger_{k\sigma} c_{k\sigma} + \sum_k \left(\Delta c^\dagger_{k\uparrow} c^\dagger_{-k\downarrow} + \text{h.c.} \right). \tag{1.5}$$

Here $c^\dagger_{k\sigma}$ creates an electron with spin σ at the single-particle energy level ξ_k. Usually ξ_k is calculated from chemical potential, i.e. $\xi_k := \epsilon_k - \mu$, and $\Delta_\nu = |\Delta| \exp(i\phi)$ is the complex superconducting order parameter. The meaning of terms of a such Hamiltonian is the same: $c^\dagger_{k\uparrow} c^\dagger_{-k\downarrow}$ creates a Cooper pair (two operators create two electrons), and the h.c.$(c^\dagger_{k\uparrow} c^\dagger_{-k\downarrow}) = c_{k\uparrow} c_{-k\downarrow}$ annihilates it. By indices k and $\uparrow, \downarrow$ we mean a special value of spin and momenta, so operators with these different indices cannot be obtained one from another by any mathematical transformations. Such expression is more compact than the previous one (1.4).

More details of the BCS theory and its extensions can be found in the celebrated textbooks [106, 107, 117].

The Nambu Basis in Superconductivity

The BCS Hamiltonian and its extensions are usually written in the so-called "Nambu basis", which will be discussed now. This notation is often used in articles about tunneling models and makes the form of equations much more compact. To understand its significance, one can attempt performing some calculations suggested in Appendix B.6.2 and B.6.1 in non-Nambu notation and compare the amount of writing.

The typical expression of the BCS Hamiltonian (1.4) is long. For the case of $\mathbf{A} = 0$ we can rewrite it in a more compact way [1, 66]

$$\mathcal{H} = \int_{-\infty}^{\infty} dx \hat{\psi}^\dagger(x) h^{(0)} \hat{\psi}(x) + \frac{1}{2} \int_{-\infty}^{\infty} dx \left[\hat{\psi}^\dagger(x) \hat{\Delta}(x) \left(\hat{\psi}^\dagger(x) \right)^T + \text{ h.c. } \right], \tag{1.6}$$

by a two-component spinor $\hat{\psi}(x) := \left(\hat{\psi}_\uparrow(x), \hat{\psi}_\downarrow(x) \right)^T$ and $h^{(0)} := \frac{p^2}{2m} - \mu$. Spin components $\sigma = \uparrow, \downarrow$ of $\hat{\psi}(x)$ are the field operators obeying the fermionic anticommutation relations

$$\left\{ \hat{\psi}_\sigma(x), \hat{\psi}_{\sigma'}(x') \right\} = 0, \qquad \left\{ \hat{\psi}_\sigma(x), \hat{\psi}^\dagger_{\sigma'}(x') \right\} = \delta_{\sigma,\sigma'} \delta(x - x'). \tag{1.7}$$

It is more compact now, but it can be rewritten even in more symmetric form:

$$\mathcal{H} = \frac{1}{2} \int_{-\infty}^{\infty} dx \hat{\psi}^\dagger(x) H \hat{\psi}(x), \qquad H := \begin{pmatrix} \frac{p^2}{2m} - \mu & \Delta \\ \Delta^* & -\frac{p^2}{2m} + \mu \end{pmatrix}. \tag{1.8}$$

This formalism is called a "reduced Nambu basis" and $\hat{\Psi}(x)$ is called a "Nambu spinor". Now we have a definitely nice and compact expression.

For the discrete models, this notation can be introduced in a similar way[2]. Now the discrete Nambu spinor is defined as

$$\psi_{\mathbf{k}} := \begin{pmatrix} c_{\mathbf{k}\uparrow} \\ c^\dagger_{-\mathbf{k}.\downarrow} \end{pmatrix}. \tag{1.9}$$

---

[2]See Sec. 14.4.1 in [111].

Its conjugate is $\psi_{\mathbf{k}}^{\dagger} = \left(c_{\mathbf{k}\uparrow}^{\dagger}, c_{-\mathbf{k}\downarrow} \right)$ and both of them satisfy $\left\{ \psi_{\mathbf{k}\alpha}, \psi_{\mathbf{k}'\beta}^{\dagger} \right\} = \delta_{\alpha\beta}\delta_{\mathbf{k},\mathbf{k}'}$. The kinetic energy in (1.5) can be written as

$$\sum_{\mathbf{k}} \epsilon_{\mathbf{k}} \left(c_{\mathbf{k}\uparrow}^{\dagger}c_{\mathbf{k}\uparrow} - c_{-\mathbf{k}\downarrow}c_{-\mathbf{k}\downarrow}^{\dagger} \right) = \left(c_{\mathbf{k}\uparrow}^{\dagger}, c_{-\mathbf{k}\downarrow} \right) \begin{bmatrix} \epsilon_{\mathbf{k}} & 0 \\ 0 & -\epsilon_{\mathbf{k}} \end{bmatrix} \begin{pmatrix} c_{\mathbf{k}\uparrow} \\ c_{-\mathbf{k}\downarrow}^{\dagger} \end{pmatrix}, \qquad (1.10)$$

where the minus in term $c_{-\mathbf{k}\downarrow}c_{-\mathbf{k}\downarrow}^{\dagger}$ originates from anticommutive change of the fermions. The total Hamiltonian can be rewritten in terms of matrix multiplications by Pauli matrices as:

$$\epsilon_{\mathbf{k}} \sum_{\sigma} c_{\mathbf{k}\sigma}^{\dagger}c_{\mathbf{k}\sigma} + \left[\bar{\Delta}c_{-\mathbf{k}\downarrow}c_{\mathbf{k}\uparrow} + c_{\mathbf{k}\uparrow}^{\dagger}c_{-\mathbf{k}\downarrow}^{\dagger}\Delta \right] = \left(c_{\mathbf{k}\uparrow}^{\dagger}, c_{-\mathbf{k}\downarrow} \right) \begin{bmatrix} \epsilon_{\mathbf{k}} & \Delta \\ \bar{\Delta} & -\epsilon_{\mathbf{k}} \end{bmatrix} \begin{pmatrix} c_{\mathbf{k}\uparrow} \\ c_{-\mathbf{k}\downarrow}^{\dagger} \end{pmatrix}$$

$$\equiv \psi_{\mathbf{k}}^{\dagger} \begin{bmatrix} \epsilon_{\mathbf{k}} & \Delta_1 - i\Delta_2 \\ \Delta_1 + i\Delta_2 & -\epsilon_{\mathbf{k}} \end{bmatrix} \psi_{\mathbf{k}} \equiv \qquad (1.11)$$

$$\equiv \psi_{\mathbf{k}}^{\dagger} \left[\epsilon_{\mathbf{k}}\tau_3 + \Delta_1\tau_1 + \Delta_2\tau_2 \right] \psi_{\mathbf{k}},$$

where we have introduced Δ_1, Δ_2 such that $\Delta \equiv \Delta_1 - i\Delta_2, \bar{\Delta} \equiv \Delta_1 + i\Delta_2$ and

$$\vec{\tau} \equiv (\tau_1, \tau_2, \tau_3) := \left(\begin{bmatrix} 0 & 1 \\ 1 & 0 \end{bmatrix}, \begin{bmatrix} 0 & -i \\ i & 0 \end{bmatrix}, \begin{bmatrix} 1 & 0 \\ 0 & -1 \end{bmatrix} \right). \qquad (1.12)$$

The Nambu notation is often referred to as "particle-hole space", since here the first component means particle, and the second one means a hole. A good example of models analyzed with the help of this formalism can be found in [83, 4]. Another example of the Hamiltonian in the Nambu space is the Eq. (B.71).

Now, suppose there is a term in Hamiltonian that also has spin-dependent terms (e.g. (B.69)). Now, the so-called "extended Nambu notation" should be used, which is defined as follows:

$$\mathcal{H} = \frac{1}{2} \int_{-\infty}^{\infty} dx \, \hat{\Psi}^{\dagger}(x) H \hat{\Psi}(x), \qquad \hat{\Psi}(x) := \begin{pmatrix} \hat{\psi}(x) \\ i\sigma_y(\hat{\psi}^{\dagger}(x))^T \end{pmatrix} \equiv \begin{pmatrix} \psi_+ \\ \psi_- \\ \psi_-^{\dagger} \\ -\psi_+^{\dagger} \end{pmatrix},$$

$$H := \begin{pmatrix} h^{(0)} & \Delta(x) \\ \Delta^*(x) & -\sigma_y h^{(0)*}\sigma_y \end{pmatrix}. \qquad (1.13)$$

Now the tensor product between two Pauli σ- and τ-matrices of different types is assumed and the resulting matrix Hamiltonian has a 4×4 dimension. Another property, which is widely used in derivations, it the relation of symmetry:

$$\mathcal{C} \left[\Psi^{\dagger}(x) \right]^T = \Psi(x), \qquad \mathcal{C} := \tau_y \sigma_y = \begin{pmatrix} 0 & 0 & 0 & -1 \\ 0 & 0 & 1 & 0 \\ 0 & 1 & 0 & 0 \\ -1 & 0 & 0 & 0 \end{pmatrix}.$$

and the commutation relation:

$$\left\{ \Psi_a(x), \Psi_b(x') \right\} = \mathcal{C}_{ab}\delta(x - x'), \qquad \left\{ \Psi_a(x), \Psi_b^{\dagger}(x') \right\} = \delta_{ab}\delta(x - x').$$

The Nambu fields of the same field do not satisfy the usual fermionic anticommutative relations. Instead, the $\mathcal{C}_{ab}\delta(x - x')$ matrix appears and this is used in many derivations. The Hamiltonian possesses chiral symmetry:

$$\mathcal{C}\mathcal{H}_{\mathrm{n}}(p, x)\mathcal{C} = -\mathcal{H}_{\mathrm{n}}^*(p, x). \tag{1.14}$$

All of this can be checked by easy matrix multiplications.

We will finish discussing Nambu notation with commenting on its features. There is a second way of defying the spinor $\hat{\Psi}(\boldsymbol{x})$, the charge conjugation $\mathcal{C}$ and the Hamiltonian $\mathcal{H}$ matrices: $\hat{\Psi}(\boldsymbol{x}) := \begin{pmatrix} \hat{\psi}(\boldsymbol{x}) \\ [\hat{\psi}^\dagger(\boldsymbol{x})]^T \end{pmatrix}$, $\mathcal{C} := \begin{pmatrix} 0 & \mathbb{1} \\ \mathbb{1} & 0 \end{pmatrix}$ and $\mathcal{H}(p, x) := \begin{pmatrix} \left[\frac{p^2}{2m} - \mu\right] & i\Delta\sigma_y \\ -i\Delta^*\sigma_y & -\left[\frac{p^2}{2m} - \mu\right] \end{pmatrix}$, were $\mathbb{1}$ is a unit matrix. Here the matrix $i\sigma_y$ is in another part. These definitions, although valid, are not as popular as the ones presented above. Another feature is that often transformations in the Nambu basis produce some constant terms, which we neglect, since they do not play role in physics of the system. Also, there is a tricky minus in the last component of the Nambu spinor in (1.13). To understand which role it plays and to get used to the Nambu notation we have provided calculations for our model in Appendix B.6.2 and B.6.1.

The Bogoliubov-de Gennes Equations

A typical way of obtaining some physical properties of the BCS model 1.4 is by transforming the electron operators ψ to an expression with new fermion operators γ_n by the famous Bogoliubov transformation. This transformation mixes the creation and annihilation operators: $\psi_\alpha(\mathbf{r}) = \sum_n \left\{ u_n(\mathbf{r}, \alpha)\gamma_n + v_n(\mathbf{r}, \alpha)\gamma_n^\dagger \right\}$. Here the $\{u_n(\mathbf{r}, \alpha), v_n(\mathbf{r}, \alpha)\}$ are the wavefunctions of a particle and a hole, which form a complete set of orthogonal states $\{u_n, v_n\}$, and γ-s obey Fermion anti-commutation relations: $\left\{ \gamma_n, \gamma_{n'}^\dagger \right\} = \delta_{n,n'}$ and $\{\gamma_n, \gamma_{n'}\} = 0$. This transformation diagonalizes the BCS Hamiltonian, $\mathcal{H} = E_s + \sum_n \varepsilon_n \gamma_n^\dagger \gamma_n$ (here n runs over all positive energy states and E_s is the ground-state energy). They obey the Bogoliubov or Bogoliubov-de Gennes (BdG) equations:

$$\varepsilon u(\mathbf{r}, \alpha) = +\left(\frac{1}{2m^*}\left(\varphi - \frac{e}{c}\mathbf{A}(\mathbf{r}) \right)^2 - \mu \right) u(\mathbf{r}, \alpha) + \Delta_{\alpha\beta}(\mathbf{r}, \varphi)\, v(\mathbf{r}, \beta), \tag{1.15}$$

$$\varepsilon v(\mathbf{r}, \alpha) = -\left(\frac{1}{2m^*}\left(\varphi - \frac{e}{c}\mathbf{A}(\mathbf{r}) \right)^2 - \mu \right) v(\mathbf{r}, \alpha) + \Delta_{\alpha\beta}^\dagger(\mathbf{r}, \varphi)\, u(\mathbf{r}, \beta). \tag{1.16}$$

Here ε is an eigenvalue (number) and in last term, the sum over β is assumed. These equations are a mean-field qusiclassical approximation and provide a powerful tool for numerous models (they allow one to take into account local electronic structure, disorder, magnetic field, to name a few) [70].

The Andreev Reflection and States

An important simplification of the Bogoliubov equations can be obtained for the problem of heat transport of an inhomogeneous superconductor. For this case after transformation $|\varphi(\mathbf{r})\rangle = e^{i\mathbf{p}_F \cdot \mathbf{r}/\hbar} |\Psi_{\mathbf{p}}(\mathbf{r})\rangle$ and some simplifications so-called Andreev equation can be obtained [3, 97]:

$$\left[\varepsilon\hat{\tau}_3 - \widehat{\Delta}(\mathbf{p}, \mathbf{r}) \right] |\Psi_{\mathbf{p}}(\mathbf{r})\rangle + i\hbar\mathbf{v}_{\mathbf{p}} \cdot \left(\boldsymbol{\nabla} - i\frac{2e}{\hbar c}\mathbf{A}(\mathbf{r}) \right) |\Psi_{\mathbf{p}}(\mathbf{r})\rangle = 0. \tag{1.17}$$

11

Here $\mathbf{p}_F$ is the Fermi momenta, $\widehat{\tau}_3$ is the third Pauli's matrix, $\mathbf{p} = p_F\hat{\mathbf{p}}$ and $\mathbf{v_p} = v_F\hat{\mathbf{p}}$, $\mathbf{v_p}$ is a Fermi momenta and velocity at different unit directions $\hat{\mathbf{p}}$, and $\widehat{\Delta}$ is a matrix with Δ parameters (it is different for different parity of the Cooper pairs). Finally, $|\Psi_{\mathbf{p}}(\mathbf{r})\rangle$ should ba understood as the Andreev spinor $|\Psi_{\mathbf{p}}(\mathbf{r})\rangle := \mathrm{col}\left(u_{\mathbf{p}\uparrow}(\mathbf{r})\ u_{\mathbf{p}\downarrow}(\mathbf{r})\ v_{\mathbf{p}\uparrow}(\mathbf{r})\ v_{\mathbf{p}\downarrow}(\mathbf{r})\right)$.

The Andreev equations and formulas for the Andreev levels are exact in the so-called Andreev limit. In this limit, the chemical potential μ is considered to be the biggest parameter of the system. This step is often made in the calculations: the calculation of the GF model is followed by approximation, which is performed by setting non-leading by μ terms to zero [1].

This equation opens a window to analyzing of one the most famous phenomena in mesoscopic physics: Andreev reflection and Andreev bound states (ABS). There are two types of solutions: one for propagating particles (for $\varepsilon > |\Delta|$) and another for sub-gap states (for $\varepsilon < |\Delta|$). Knowing them, one can solve a problem of a contact between normal metal (N) and superconductor (S). It turns out that there is a probability for an electron from normal region to combine with electron from superconductive region and form a Cooper pair, while a hole will be created and reflected back. This is called "Andreev reflection", which is illustrated in the center of Fig. 2. The probability of this reflection is

$$|r_{\mathrm{A}}|^2 = \begin{cases} 1 & , \varepsilon \leq |\Delta|, \\ \dfrac{|\Delta|^2}{(\varepsilon + \sqrt{\varepsilon^2 - |\Delta|^2})^2} & , \varepsilon > |\Delta| . \end{cases} \qquad (1.18)$$

The electron is changed to hole with unit probability for energies $\varepsilon < \Delta$.
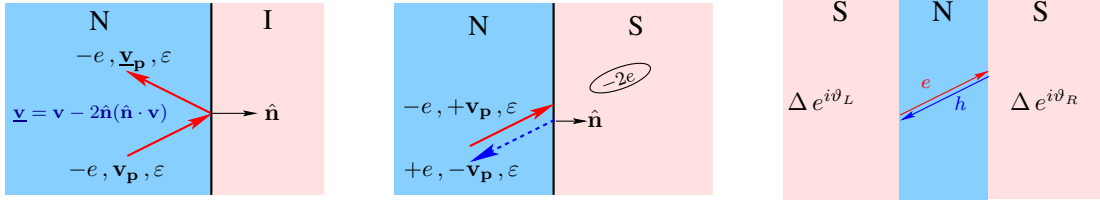

Figure 2: Left: "electron-electron" reflection at an N-I boundary. Center: "electron-hole" reflection at an N-S boundary. Right: Andreev bound state in SNS contact. Credit: [3].

If we combine two such NS interfaces into a SNS junction with normal length L_N, the following quantization condition for the discrete levels holds was first found by Kulik [44]:

$$\varphi - 2\arccos\left[\frac{E(\varphi)}{\Delta}\right] - 2\frac{E(\varphi)}{\Delta}\frac{L_N}{\xi} = 2\pi n, \qquad n \in \mathbb{Z}, \qquad (1.19)$$

where ξ is the superconducting coherence length. For short junction $L_N \ll \xi$ limit, this formula for a slightly general case is simplified as follows [63, 48, 105]:

$$E_i(\varphi) = \pm\Delta\sqrt{1 - T_N^i\sin^2\frac{\varphi}{2}}. \qquad (1.20)$$

Here we assume that there are several modes that are numerated by i and T_N^i is their transparency. The explicit form of ABS (Eq. (1.20)) is one of the best-known formula in mesoscopic physics and sometimes referred as "Beenakker's formula". The Eq. in

the form (1.19) is sometimes generalizes to other setups, for instance, to three-terminal junctions in [32].

Typical plots of Josephson currents and Andreev states for a point-contact junctions are shown in Fig. 3. The current resembles the first Josephson equation $I = I_c \sin \phi$, but for the point contact there is a sharp jump at $\phi = \pi$. The temperature effects can be taken into account by typical Matsubara summation methods and make the CPR flatter.
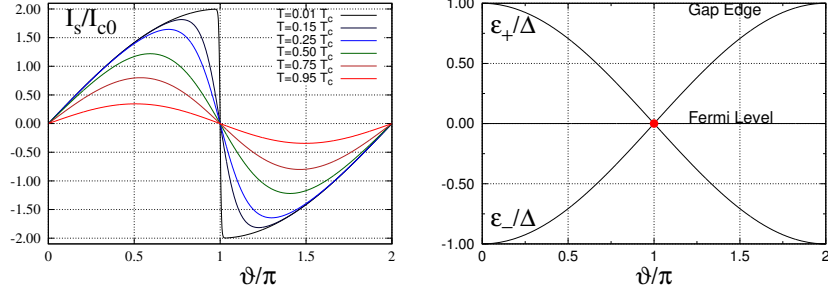

Figure 3: Left: Josephson current as a function of phase bias and temperature for a point contact. The current is normalized in units of the Ambegaokar-Baratoff critical current at $T = 0$, $I_{c_0} = \frac{\pi \Delta(0)}{2e\,R_N}$. Right: Branches of ABS of a point-contact JJ as a function of the phase ϑ. Credit: [3].

Finally, the informative comparison the effects of the Zeeman and SO interaction in on the SNS states and reflection is shown in Fig. 4. If both terms are present and the magnetic field is high, the bound states changes (this regime is called "topological"). Our main theory will also demonstrate how Zeeman term and change of other parameters influences the ABS. The detailed description of this effects can be found in [63].
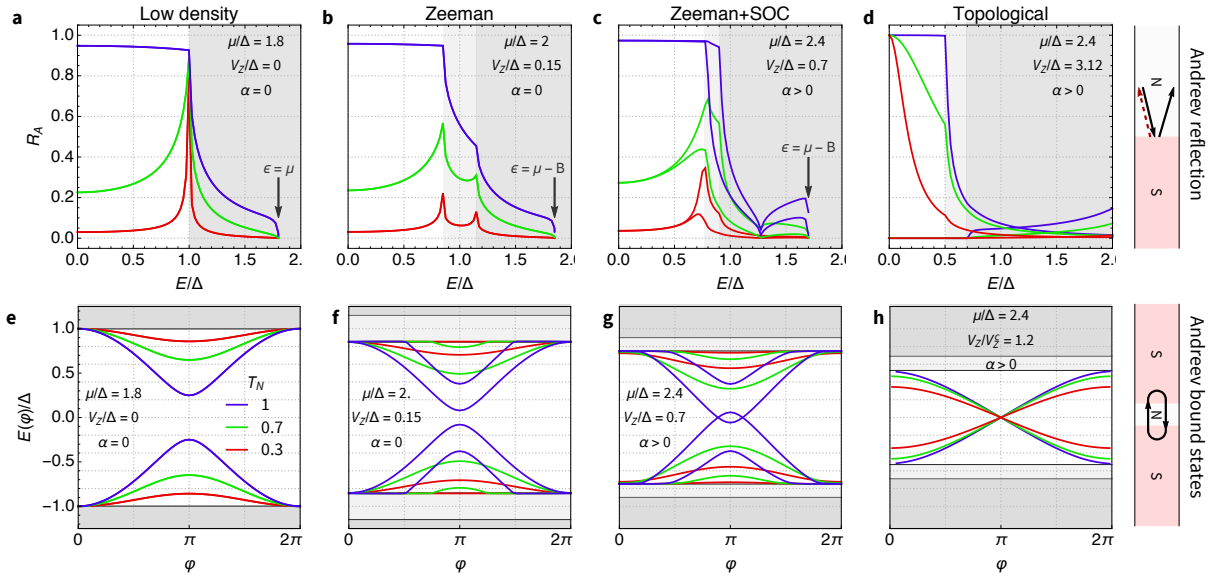
Figure 4: Andreev reflection probability R_A at low-density NS contact (top row) and ABS energy $E(\varphi)$ (bottom row) at short SNS contact with various parameters and varying normal-state transparency T_N (blue, green, red). Credit: [63].

Applications of ABS arise if a quantum point contact is embedded in an rf-SQUID: such configuration allows one to make an Andreev level qubit [50]. As a classical bit, it can be used to host information, but also more peculiar processes like interaction with

acoustic phonons can be taken into account for it [116]. Thus, Andreev states are a hot-studied topic for quantum computing applications [53, 56, 57]. We will discuss some of them below in the context of multiterminal junctions. Reviews of experimental techniques for the detection of ABS can be found in [103, 63].

The Josephson Current

Supercurrent through junctions is the main quality of interest; therefore, it is necessary to discuss the best-known and practical tools for analyzing it. It is connected to the junction's free energy F and the SC phase difference φ via the following fundamental relation

$$I = \frac{2e}{\hbar} \frac{\partial F}{\partial \varphi}. \tag{1.21}$$

Usually, the calculations start with this formula or some of its consequence (e.g. (2.51)). The energy of the junction can be thought about as usual energy of the wire $E = \int_0^t I_s V \, dt$. Here the electrostatic potential is related to the phase by the second Josephson eq. $\dot{\varphi} = \left(\frac{2\pi}{\Phi_0}\right) V$. After the generalization of E to the Gibbs free energy F, both these formulas give the (1.21).

Another way to see the current is to define it as an operator that acts on BdG Hamiltonian:

$$\hat{I}_\alpha = 2e \frac{\partial \hat{H}}{\partial \phi_\alpha}, \tag{1.22}$$

where α is the number of the lead in a multiterminal setup [33] and $\hbar \equiv 1$ is assumed. Then, by calculating the expectation value, and solving the time-dependent Schrödinger equation, one can get a more general expression, $I_\alpha(t) = \frac{2e}{\hbar} \frac{\partial E}{\partial \phi_\alpha} - 2e\dot{\phi}_\beta B^{\alpha\beta}$, where the last term contains the Berry curvature $B_k^{\alpha\beta} := -2 \operatorname{Im} \left[\partial_{\phi_\alpha} \langle \varphi_{k\sigma} | \partial_{\phi_\beta} | \varphi_{k\sigma} \rangle\right]$. This more general formula was used, for example, for multiterminal systems in [23], or it can be applied with Keldysh Green's function [16], but in our main theory we will use the consequences of (1.21). A more detailed proof can be found in sec. 2.2.3 of [10].

The free energy can be calculated using several approaches. For finite temperatures there is a useful general relation in terms of special Matsubara Green function, it can be expressed as [88]:

$$I = -\frac{e}{\hbar} \frac{\partial}{\partial \varphi} T \sum_{\omega = 2\pi T(n+1/2)} i\omega \int dx \, \operatorname{Tr} G_\omega(x, x). \tag{1.23}$$

Here T is the temperature and the Matsubara Green function is a matrix that satisfies the equation $(i\omega - H)G_\omega(x, x') = \delta(x - x')$. Another, closely related and fertile direction is to find the free energy by relating it to the density of states $\rho(\varepsilon)$:

$$F = -k_{\mathrm{B}}T \int_0^\infty d\varepsilon \rho(\varepsilon) \ln\left[2 \cosh\left(\varepsilon/2k_{\mathrm{B}}T\right)\right]. \tag{1.24}$$

Through this relation, the current is connected to the density of states. By expressing the latter in terms of energy levels, the Eq. (1.24) leads to a well-known formula for short

SNS junction with $\Delta_L = \Delta_R = \Delta$:

$$I = -\frac{e}{\hbar}\frac{\partial}{\partial\varphi}\sum_i E_i \tanh\frac{E_i}{2T},\qquad(1.25)$$

where $E_i = \Delta\sqrt{1 - T_i\sin^2\varphi/2}$ and T_i is a transmission probability of i-th channel [71, 88].

Another important related property - current noise - can be obtained by decomposing current into Fourier harmonics and then averaging exponents. It was analyzed in a context of creation topological mater by Riwar et al. [33]. More methods and formulas for obtaining current can be found in [68, 111, 105].

1.2 Overview of Mesoscopic SC Methods and Models

Well-known Methods and Models of Junctions with SC

To be fully prepared to study the properties of multiterminal transitions, it is important to have a broad picture of approaches, models and have references for their explanations. The most notable ones are summarized below.

For a numerical analysis within the tight-binding approximation, the lattice Green's function method was developed by Wimmer et al. [82]. Alternatively, the famous numerical methods are the numerical renormalization group (an example, of its application to junction through the quantum dot is presented in [98, 99]) or quantum Monte Carlo simulations (examples of applications to the similar systems can be found in [100, 101]).

The scattering matrix method is the best-known among the analytical methods, which was developed on basis of the BdG equations (1.15). It was first applied to the SC junctions in the celebrated work by Blonder, Tinkham, and Klapwijk [80], thus becoming known as "the BTK approach" [79]. Later, it was further generalized by C. Beenakker to the multichannel case in [71], which is currently known as the Beenakker's determinant method. Now this method is a classical approach in mesoscopic physics, theory of which is well-developed for semiconductor nanostructures [119], systems with disorder [118], or open systems [72]. An introduction, derivations, and examples of it can be found in [69] and the example of calculation of Andreev reflection can be found in [105]. There are many applications as well to junctions with semiconductive nanowires (which have SO and Zeeman terms in Hamiltonian) [102]. An example of analyzed semiconducting nanowire with scattering matrix can be found in [24]. A disadvantage of the scattering matrix approach is that it cannot take into account all inelastic processes.

The second popular type of approach, the Green's function method, plays an important role in condensed matter and is explained in numerous celebrated textbooks [106, 107, 111]. It is especially well-known for applications to superconductive systems by Gor'kov's formalism, which is widely recognized for its famous diagrammatic interpretation in condensed matter. In the 1970s and 1980s, it was also popular to be applied to SC contacts, which led to the first exact expressions of the current and bound states [44, 48]. Modern examples of calculation of the current through SN, SNS junction using Gor'kov's method can be found in [107]. For nonequilibrium problems and numerical calculations, the NEGF method is often used. It was pioneered in the 1960s by the classic work of Martin, Schwinger [47], Kadanoff, Baym [108], Keldysh [46], which is reviewed by Danielewicz [112] and Mahan [114]. An example of applications of NEGF to electronic transport can be found in [110]. The Keldysh formalism, which can also be considered

as part of NEGF methods, provides a famous and powerful tool for analytical calculations of the current [96]. See [6, 14, 15] for examples of its applications to multiterminal junctions. The overview would not be complete without mentioning the Eilenberger and Usadel equations, famous superconductivity frameworks that also rely on quasiclassical Green's function. Both are also traditionally used for describing disorder and proximity effects and are applied to tunneling problems, for example, for SFIFS, SNINS, and SIS contacts [95]. The GF methods for disorder and superconductive contacts are profoundly reviewed in [96]. Another typical generalization is the GF of the multilayered systems [1, 97]. Finally, from the tunneling Hamiltonian the transport properties can be obtained by using a special local representation and Keldysh's GF, which was found by Caroli et al. [92]. Within this method, a microscopic theory of Multiple Andreev reflections (MAR) has been developed by Cuevas et al. [91]. A closely related method for arbitrary heterostructures was proposed by Piasotski et al. [1], which had a strong influence on the present work. For special junctions with several channels and Majorana states, a generalized framework based on boundary Green's function (BGF) is developed in [21].

The basic SNS contact can be generalized in a variety of ways. For instance, there are numerous studies of a junction with various types of ferromagnets (SFS junctions) [89, 74]. The description of S-QD-S and N-QD-S systems with a variety of numerical and analytical methods is provided in [4, 104]. More details about the quantum dots that are coupled to superconductors can be found in [5]. A description of the mean-field methods for quantum dot can be learned from [75] and a discussion of the model, variation, and alternative approaches is in [76]. The Andreev states and reflection for ferromagnets, ferromagnetic insulators were fully investigated using the scattering matrix approach in [74].

One of the most profoundly studied models is the that of junctions with quantum dot (QD). Its applications range from the designing artificial atoms and molecules [8] to quantum-coherent nanoscience [9]. The theoretical approaches for such systems developed decades ago are still ongoing. The basic references for such models are works by Martín-Rodero and Levy Yeyati [4, 5], where numerous properties of different models with QD are examined. Another excellent description of the ABS with discussion diagrammatic approach can be found in [10][3]. An example of a modern research of a QD system that uses an approach similar to ours (Sec. 2), is presented in [11], but it is focused on the analysis of correlations.

Besides, in the last decades, the special direction blew up condensed matter physics. It was predicted that special superconductors or special configurations of junctions could host very stable (so-called "topologically protected") states. Such states would be constructed out of Majorana fermions - special construction of electron and hole excitations [63, 62]. A pair of Majorana has non-Abelian exchange statistics (rotate with neither with spin 1 of spin 1/2) and a state of them called "Majorana bound states" (MBS), occur at precisely zero energy. One of the requirements for such states to exist is that a strong Zeeman interaction should appear. In such regime, the matter changes to a so-called "topological state" (see Fig. 4, right panel). Such states are described by Majorana operators, which are self-conjugate, $\gamma = \gamma^\dagger$. This property means that 'particle-equals-antiparticle', is exactly the same as Majorana fermions in field theory. The great interest in them arose because of their potential role in quantum computation [59] as topological

---

[3]This paper is especially useful because of concise reviews of the methods and examples of derivations in appendix.

qubits. However, the process of their preparation is still a topic for debate, though several methods were proposed (like the Shockley mechanism, chiral p-wave superconductors, topological insulators, semiconductor heterostructures) [60]. Another challenge and a big debate is the method of detection of Majorana bound states, and again, there are several proposals (like nonlocal tunneling, celebrated 4π-periodic Josephson effect, thermal metal-insulator transition, etc.). Discussion of experimental results by Josephson spectroscopy, microwave spectroscopy, and tunneling spectroscopy can be found in an excellent review by Prada et al. [63]. Such materials are called "topological superconductors" (TS) and the junctions with them have already been studied theoretically (for instance, the current of the S-TS junction was analyzed in [88]).

Overview of Multiterminal Junctions

The scattering matrix approach is often used for the analysis of the multiterminal junctions [26]. It was proven that a special Kramers degeneracy of Andreev levels, which is connected to time reversal symmetry, can be broken in multiterminal Josephson junctions, which is a fundamental requirement for the creation of Majorana states [25]. Another direction is to consider the overlap of ABS of two parts of the system (Andreev molecule) [27, 29]. This approach was used in the data analysis of experiment [40]. Attempts of generalizing this method are ongoing, for example, a graph theory was used to prove that it is possible at all to obtain the ABS for any number of terminals [32]. For three-terminal Josephson junctions with the scattering matrix approach the ABS and current were calculated in [22], and Shapiro plateaus for case of time-dependent voltage were analyzed in [23]. Such devices have finite energy band crossings and host a diode effect (when current flows to one direction stronger than to another) with different phases [7].

There are several recognized Green's function methods for multiterminal junctions as well, which often differ from one model to another. The description of the S-QD-S-S junctions with a variety of methods is done in [5, 75]. For the S-N-S-S contact the density of states and proximity effect was analyzed in [13]. This model can be generalized by taking into account topological wires, for which low-energy Green's functions, as well as conductance, noise correlations, and the supercurrent-phase relation, are discussed in detail in [16]. The basic MTJJ with topological superconductors were first analyzed in [14] and later by a mean-field approach in [17] by Zazunov et. al. More general models that have also a quantum dot inside of a contact (like S-QD-TS-TS junction) were also discussed by the same authors a year later [19]. Another big direction is an analysis of the noise and correlations of the current in MTJJ with Green's functions, which is reviewed in [6]. Besides, MTJJ can be analyzed by the Usadel equation [30], which is a simplification of Eilenberger's equation and is used in the diffusive limit. With this method and by Keldysh Green's function pairing symmetry can be analyzed [31].

To imagine, how in experiments MTJJ looks like, let us look at one that was analyzed in 2020 by Pankratova et al. [39]. A four-terminal junction on which the experiment was conducted is shown in Fig. 5. On the left and central figures, the SEM images of the junction and bigger part of the circuit (which forms a multi-SQUID) are depicted and the right part illustrates the material components components. The normal two-dimensional electron gas (2DEG) is confined near the crystalline interface between InAs semiconductor (which is a typical 2DEG, that plays the role of N region) and a superconducting Al film (as a typical SC). The SC terminals are electrically isolated by mesa etching. The
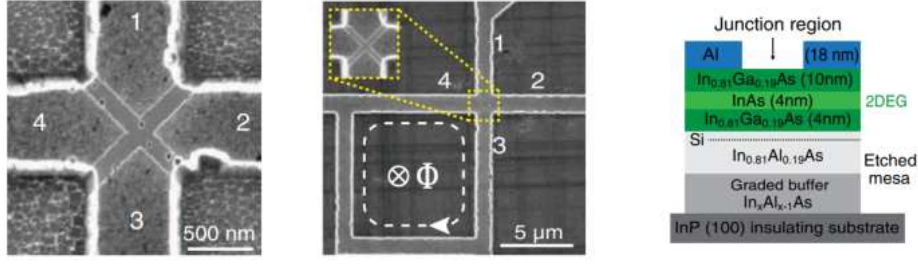
Figure 5: Four-terminal junctions analyzed in the experiment of [39]. On the right, we see the material components of the system.

junction's scattering region was created by removing the Al layer. Examples of 3TJJ that were analyzed by Matute-Cañadas et al. [2] are shown in Fig. 6. On the (a) a similar superconductor-semiconductor heterostructure is proposed with similar materials. Again, aluminium film is placed on InGaAs layer and induces SC by proximity. Along the 2DEG the Al strings were etched (depicted with red lines), allowing terminals to exchange Cooper pairs. Yellow elements indicate the gate electrodes, which control the couplings. Panels (b,c) of Fig. 6 show two types of models that describe a trijunction.
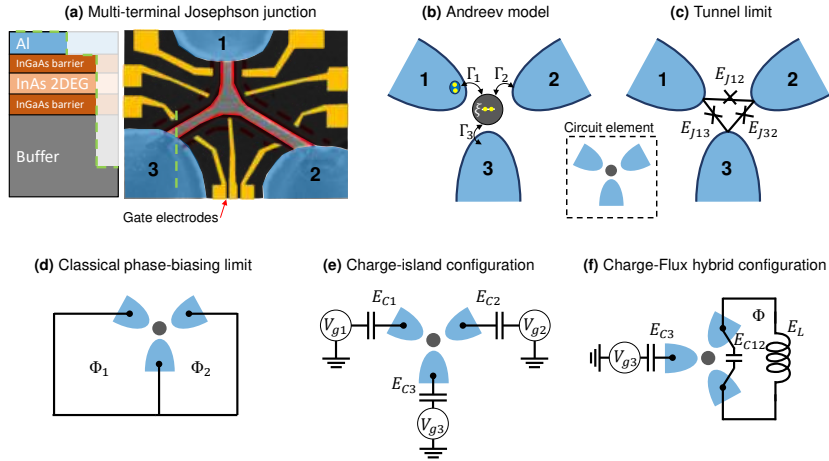

Figure 6: Different kinds of quantum circuits for multiterminal Josephson-Andreev junctions. Sub figure (a) shows material components along the green dashed line. Credit: [2].

In (b), traveling through the middle region is modeled by hopping amplitudes. In (c), the system is described by effective tunneling energies and is equivalent to 3-terminal-triangle-Josephson junctions. It is a limit of (b). Parts (d, e, f) show the different types of the rest of the circuit, that are used for manipulations of its dynamics. In (d), external fluxes $\Phi_{1,2}$ can be used to fix the phases. In (e), the charging energies $E_{C\nu}$ of SC parts are fixed by an applied voltage (so-called islands). In (f), two leads are connected in a loop with capacitive and inductive energy, and the third lead is a SC island. Recently ABS of 3TJJ was spectroscopically investigated by Coraiola et al. [40] and a broad review of the experimental methods and materials can be found in [38].

1.3 Green's Function Methods

Here we will review the GF methods that will be used in the main theory below.

Concept of Green's Function

Suppose we have a many-body system that is governed by Schrödinger equation and has a Hamiltonian of the form $\widehat{\mathcal{H}} = \widehat{\mathcal{H}}_0 + \widehat{\mathcal{H}}_{\text{int}}$, where second term is a perturbation to the first one. Each state can be described by a multi-particle wavefunction ψ_i, where i indicates, how many particles occupy the state. The set of all functions $\{\psi_i\}$ is an orthogonal one. We introduce the operators [107]

$$\widehat{\psi}(x) = \sum_i \widehat{a}_i \psi_i(x); \qquad \widehat{\psi}^+(x) = \sum_i \widehat{a}_i^+ \psi_i^*(x), \tag{1.26}$$

where $a, a^\dagger$ are the creation and annihilation operators. The particles can be bosons and fermions, and their operators satisfy commutation or anticommutation relations respectively. Usually, the GF is applied to electrons, which are fermions (have spin $1/2$), and have the following anticommutative relations of the operators by definition:

$$\left[a_i^+, a_j\right]_+ = a_i^+ a_j + a_j a_i^+ = \delta_{ij}, \quad \left[a_i, a_j\right]_+ = \left[a_i^+, a_j^+\right]_+ = 0. \tag{1.27}$$

$$\left[\widehat{\psi}(x), \widehat{\psi}^+(x')\right]_+ = \delta(x - x'), \quad \left[\widehat{\psi}(x), \widehat{\psi}(x')\right]_+ = \left[\widehat{\psi}^+(x), \widehat{\psi}^+(x')\right]_+ = 0. \tag{1.28}$$

Now, to work with Green's function, we need to go to the interaction picture, i.e. we transform:

$$\widehat{\mathcal{H}}_{\text{int}}(t) := e^{(i/\hbar)\widehat{\mathcal{H}}_0 t}\widehat{\mathcal{H}}_{\text{int}} e^{-(i/\hbar)\widehat{\mathcal{H}}_0 t} \qquad \tilde{\psi}_\alpha(x) = e^{i\widehat{\mathcal{H}}_0 t}\widehat{\psi}_\alpha(\mathbf{r})e^{-i\widehat{\mathcal{H}}_0 t}, \qquad \tilde{\psi}_\alpha^+(x) = e^{i\widehat{\mathcal{H}}_0 t}\widehat{\psi}_\alpha^+(\mathbf{r})e^{-i\widehat{\mathcal{H}}_0 t}.$$

Here $x \equiv (t, \mathbf{r})$ and we do it for both spin components α. The so-called causal Green's function is defined as the average of the chronological ordering of the ψ operators taken in the interaction picture:

$$G_{\alpha\beta}^c(x, x') = -i\left\langle \mathrm{T}\tilde{\psi}_\alpha(x)\tilde{\psi}_\beta^+(x')\right\rangle.$$

Here, the brackets $\langle \ldots \rangle$ mean that the matrix element $\left\langle \widehat{S}_0\right\rangle^{-1}\langle 0|\ldots|0\rangle$ is taken from the ground state of the system with the Hamiltonian $\widehat{\mathcal{H}}_0$, where the factor $\left\langle \widehat{S}_0\right\rangle = \langle 0|e^{-i\widehat{\mathcal{H}}_0 t}|0\rangle_{t\to\infty}$ is a usual normalization. The chronological ordering for Fermi-operators is defined as $\mathrm{T}\widehat{A}(x)\widehat{B}(x') := \begin{cases} \widehat{A}(x)\widehat{B}(x'), & t > t', \\ -\widehat{B}(x')\widehat{A}(x), & t < t' \end{cases}$. In the case of bosons the expressions are slightly different.

The causal GF is related to the retarded and advances GFs by

$$G^c(t, t') = \begin{cases} G^R(t, t'), & t > t', \\ G^A(t, t'), & t < t'. \end{cases}$$

If the temperature is finite, the Matsubara GF is used (which was seen in (1.23)), which is defined as

$$G(\mathbf{r}, \mathbf{r}', \tau, \tau') := -\left\langle \mathrm{T}_\tau \psi(\mathbf{r}, \tau)\psi^+(\mathbf{r}'\tau')\right\rangle_T.$$

Here the averaging is done over the thermodynamic ensemble:

$$\langle \widehat{A} \ldots \widehat{B} \rangle_T := \frac{\text{Tr}\left(\widehat{A} \ldots \widehat{B} e^{-\beta \widehat{\mathcal{H}}} \right)}{\text{Tr}\, e^{-\beta \widehat{\mathcal{H}}}} \equiv \sum_n w_n \langle n | \widehat{A} \ldots \widehat{B} | n \rangle, \qquad w_n := \frac{e^{-\beta E_n}}{Z}, \quad Z := \sum_n e^{-\beta E_n}.$$

As usual, $\beta = 1/kT$. Here instead of the chronological ordering, the definition of the Matsubara's GF has ordering w.r.t. imaginary time (so-called Matsubara time $\tau = it$, which ranges from $-\beta$ to $+\beta$). Examples of calculations with Matsubara GF and more details can be found in [107, 106, 111].

The GF of the system is closely related to the density matrix of the system by

$$\rho_{\alpha\beta}(\mathbf{r}, \mathbf{r}', t) = \pm i \lim_{t' \to t+0} G_{\alpha\beta}(x, x') \tag{1.29}$$

("+" corresponds for bosons, "-" for fermions.) Such relation allows one to write the particle and current density as

$$n(x) = \pm i \lim_{\substack{t' \to t+0 \\ \mathbf{r}' \to \mathbf{r}}} \text{Tr}\, G_{\alpha\beta}(x, x'); \qquad \mathbf{j}(x) = \pm \frac{\hbar}{2m} \lim_{\substack{t' \to t+0 \\ \mathbf{r}' \to \mathbf{r}}} (\nabla_{\mathbf{r}} - \nabla_{\mathbf{r}'}) \text{Tr}\, G_{\alpha\beta}(x, x'),$$

where Tr takes the trace by spin indices α, β. Taking the limit on $t' > t$ is necessary due to the ambiguity of the definition of the Green's function for $t = t'$. In our main theory we will use the formula for the density of states as

$$\rho(\omega) = -\frac{1}{\pi} \text{Im}\, \text{tr}\, G(\omega + i\eta), \tag{1.30}$$

where G is the full retarded GF of the system.

Most often GF are calculated by Fourier transformation,

$$G_{\alpha\beta}(x - x') = \iint G_{\alpha\beta}(\varepsilon, \mathbf{p}) e^{-i\varepsilon(t-t')+i\mathbf{p}(\mathbf{r}-\mathbf{r}')} \frac{d\varepsilon \, d^3 p}{(2\pi)^4}, \tag{1.31}$$

which is substituted into another definition of the GF:

$$(E - \hat{H}) G(\boldsymbol{r}, \boldsymbol{r}') = \delta(\boldsymbol{r} - \boldsymbol{r}'). \tag{1.32}$$

This is a well-known quantum mechanical approach, which, for instance, gives the free particle propagator $G(\boldsymbol{r}, \boldsymbol{r}') = \int \frac{d^3 k}{(2\pi)^3} \frac{e^{i\boldsymbol{k}(\boldsymbol{r}-\boldsymbol{r}')}}{E - \frac{k^2}{2m}}$. For our tunneling models, this approach will also be used, and instead of the free-particle Hamiltonian we will use the BCS Hamiltonian.

Another typical method is used in the systems with interactions (for example, if there in an interaction with phonons). Interactions can effectively be described by another operator, called self-energy Σ and the GF can be obtained from the so-called Dyson equation:

$$G = G_0 + G_0 \Sigma G. \tag{1.33}$$

Here G_0 is a GF of the system without interaction, which is often called "bare GF". This equation is obtained by decomposing G into a series of G_0, and then noting that some

terms with GF of the particle with which our particle interacts can be combined into Σ and the rest series can be reexpressed through the original G. The introduction of Σ is one of the most brilliant ideas in condensed matter, which allows one to describe numerous of models and make the GF method usable. The main feature of the Dyson equation is that the desired GF is on both sides.

Many other approaches for calculation of the GFs, self-energies and solving the Dyson equations can be found in [107], and an example will be presented in our main theory.

Idea of Boundary Green's Function and GF for Discrete Models

Finally, let us mention the idea of boundary Green's function (BGF). This is a powerful tool for many models of condensed matter (see, for example, other works by the authors of [1]) In simple words, by knowing the GF of one part of a system, one can establish the GF of the whole system by using some symmetric constructions. Often it is done in tight-binding models, but here we will show an example of a continuous one. For instance, for a 1D system with one barrier at the coordinate X, the GF can be expressed from the bare GF $G^{(0)}$ by

$$G_X(x,x') := G^{(0)}(x,x') - G^{(0)}(x,X)\big[G^{(0)}(X,X)\big]^{-1}G^{(0)}(X,x'). \tag{1.34}$$

One needs just to plug different coordinates in $G^{(0)}$ and use the simple formula with them. Now, suppose we have two barriers at the coordinates X,Y (for example, for Josephson junction). Now we will have:

$$G_{X,Y}(x,x') := G^{(0)}(x,x') -$$
$$- G^{(0)}(x,X)\big[G_Y(X,X)\big]^{-1}G_Y(X,x') - G^{(0)}(x,Y)\big[G_X(Y,Y)\big]^{-1}G_X(Y,x'). \tag{1.35}$$

Here the formula (1.34) is used (for coordinates X and Y). These formulas vividly illustrate what the BGF method looks like. The usage can be exemplified by derivations in Sec. B.6.1.

For the tight-binding models the GF methods are well-designed as well [82], which will be presented in the main theory. The GF of such models ar connected to the GF of continuous ones by limiting the distance between sites a to zero [1]:

$$x \equiv na, \qquad G\left(x, x'\right) = \lim_{a \to 0} \frac{1}{a} G_{n,n'}. \tag{1.36}$$

Here x is the continuous coordinate and the n is the atomic site. The GF of the discrete model (with Hamiltonian $h_{np''}$) is defined between two sites n and n' analogous to the continuous case:

$$\sum_{p''} \left(\omega \delta_{np''} - h_{np''}\right) G_{p''n'} = \delta_{nn'}, \tag{1.37}$$

whith a Kronecker-δ function at the r.h.s. More details can be found in the original article by Caroli et al. [92], where tunneling through a barrier was analyzed and further generalizations are discussed in [93, 1].

Green's Function of BCS Superconductors

Since superconductive GFs are indispensable for many solutions, we deem necessary to consider at least one textbook example of such GF . In the Nambu notation, in which the Hamiltonian is $H_{\text{BCS}} = \sum_{\boldsymbol{k}} \psi_{\boldsymbol{k}}^\dagger h(\boldsymbol{k}) \psi_{\boldsymbol{k}}$, where $\psi_{\boldsymbol{k}} := \left(c_{\boldsymbol{k}\uparrow}, c_{-\boldsymbol{k}\downarrow}^\dagger \right)$, and $h(\boldsymbol{k}) := \epsilon_{\boldsymbol{k}} \sigma^3 + \Delta \sigma^1$, the Green's function is obtained just by inverting matrix:

$$G(\omega, \boldsymbol{k}) = (\omega - h(\boldsymbol{k}))^{-1} = \frac{\omega \sigma^0 + \epsilon_k \sigma^3 + \Delta \sigma^1}{\omega^2 - \epsilon_k^2 - \Delta^2}.$$

This nice, compact expression can be often seen in a slightly different form or as its variations. For instance,

$$\widehat{G}_0 = -\frac{1}{\omega_n^2 + \xi^2 + \Delta^2} \begin{pmatrix} (i\omega_n + \xi_{\mathbf{p}}) \delta_{\alpha\beta} & -\Delta_{\alpha\beta} \\ -\Delta_{\alpha\beta}^+ & (i\omega_n - \xi_{\mathbf{p}}) \delta_{\alpha\beta} \end{pmatrix}; \qquad \Delta_{\alpha\beta} = i\Delta \sigma_{\alpha\beta}^y. \tag{1.38}$$

This is a Matsubara GF, where $\omega \to i\omega$ was changed, and it is written in the extended Nambu space. The $\xi_{\mathbf{p}} = v_F (|\mathbf{p}| - p_0)$ is the electron spectrum linearized near the Fermi level, which is a common approximation. Another frequently published expression takes the form of

$$g(\omega) = -\frac{i\omega \tau_0 + \Delta \tau_x}{\sqrt{\omega^2 + \Delta^2}}. \tag{1.39}$$

One can think that this is a purely different GF, however, it is not. The integration (1.38) over the momenta p gives this expression (we will see this explicitly in the main theory). Finally, there is a third famous formula for the GF of the BCS with a different sing under the square root. For example, for the transport properties of superconducting contacts [91] the GF can be written as

$$\hat{g}_{LL}^{r,a}(\omega) = \hat{g}_{RR}^{r,a}(\omega) = \frac{1}{W \sqrt{\Delta^2 - (\omega \pm i\eta)^2}} \begin{pmatrix} -\omega \pm i\eta & \Delta \\ \Delta & -\omega \pm i\eta \end{pmatrix}. \tag{1.40}$$

Here W is connected to normal density of states at the Fermi level by $\rho(\epsilon_F) \sim 1/(\pi W)$, parameter $\eta \to 0$. This formula is for ordinary (non-Matsubara) and $\pm$ indicates where the poles in the complex plane should be bypassed.

Finally, there is a simple trick for calculation of GF of SC with different phases [1]: one can neglect them, and then restore by the transformation:

$$G(x, x') = U G^{(0)}(x, x') U^\dagger, \qquad U := e^{\frac{i}{4} \tau_z \varphi}. \tag{1.41}$$

More practice can be found in such popular textbooks as [111, 107], or see the derivation of the GF without linearizing approximation in the Appendix F. of [1], and for the topological SC in the Appendix of [16].

Green's Function Method by Piasotski et al.

Recently the Green's function formalism for continuous multi-layered quasi-onedimensional junctions has been developed by Piasotski, Pletyukhov, Shnirman [1]. This method takes into account several transport channels and allows one to analyze transport balistically (more exact that in scattering matrix approach, beyond Andreev limit), account for the effects of static disorder and local Coulomb interaction. Our final results of the DOS and the current are similar to the ones reviewed below.

Algorithm by Piasotski et al.

Suppose we have a 1D system with a several regions (which are numerated by $m = 1, .., M$), and in each of which there are several channels of propagation[4]. Then the density of bound states (with energy ω) can be obtained by the formula

$$\rho(\omega) = \sum_{m=0}^{M} \rho^m(\omega) - \underbrace{\frac{1}{\pi} \operatorname{Im} \frac{\partial}{\partial \omega} \ln \det d\,(\omega + i\eta)}_{\equiv \delta\rho}. \tag{1.42}$$

In other words, the DOS is a sum of a contribution from each region, plus the overlap that is evaluated from the special d matrix, This is a $N_c M \times N_c M$ matrix, which is the biggest challenge for calculation. Let us consider a double-barrier case, which corresponds for example to Josephson junction. We will denote the coordinate of the barriers as 0 and W. Here the d matrix is obtained from the Green's functions from the central region $G^{(C,0)}$ (which is obtained directly from the central region's Hamiltonian h_c by $G^{(C,0)}(x, x'; z) = \int_{-\infty}^{\infty} \frac{dk}{2\pi} \frac{e^{ik(x-x')}}{z - h_c(k)}$) and special p_0, p_W matrices that are calculated from strengths of barriers $\mathcal{U}(x) \equiv \sum_m \mathcal{U}_m \delta(x - x_m)$, and functions $\mathcal{L}_L, \mathcal{L}_R, \mathcal{L}_{L \to C}, \mathcal{L}_{R \to C}$. In turn the $\mathcal{L}_L, \mathcal{L}_R$ are calculated from terms form the left and right region's Hamiltonian, Greens' functions and its derivatives respectively. The functions $\mathcal{L}_{L \to C}, \mathcal{L}_{R \to C}$ are obtained from the same approach, but from the central region. This is a relatively complicated algorithm, however the alternative approaches for multilayered systems are also quite substantial. Let us state the formulas for reference.

$$d = \begin{pmatrix} G^{(C,0)}(0,0) & G^{(C,0)}(0,W) \\ G^{(C,0)}(W,0) & G^{(C,0)}(W,W) \end{pmatrix}^{-1} - \begin{pmatrix} p_0 & 0 \\ 0 & p_W \end{pmatrix}; \qquad \begin{aligned} p_0 &= \mathcal{U}_1 + \mathcal{L}_L - \mathcal{L}_{L \to C}, \\ p_W &= \mathcal{U}_2 - \mathcal{L}_R + \mathcal{L}_{R \to C}, \end{aligned}$$

$$\mathcal{L}_{L \to C} := \frac{\mathcal{A}_C}{2} G_1^{(0,C)}(0^-,0)[G^{(0,C)}(0,0)]^{-1} + \frac{i}{2}\mathcal{B}_C; \qquad \mathcal{L}_R := \frac{\mathcal{A}_R}{2} G_1^{(0,R)}(0^+,0)\left[G^{(0,R)}(0,0)\right]^{-1} + \frac{i}{2}\mathcal{B}_R;$$

$$\mathcal{L}_{R \to C} := \frac{\mathcal{A}_C}{2} G_1^{(0,C)}(0^+,0)[G^{(0,C)}(0,0)]^{-1} + \frac{i}{2}\mathcal{B}_C; \qquad \mathcal{L}_L := \frac{\mathcal{A}_L}{2} G_1^{(0,L)}(0^-,0)\left[G^{(0,L)}(0,0)\right]^{-1} + \frac{i}{2}\mathcal{B}_L.$$

Here $\mathcal{A}, \mathcal{B}, \mathcal{B}$ are the terms from the Hamiltonian $H_m \equiv \frac{1}{2}\mathcal{A}_m p^2 + \mathcal{B}_m p + \mathcal{C}_m$ and index "1" (in, for example, $G_1^{(0,C)}(0,0)$) means the derivative w.r.t. first argument. The derivation is discussed in [1].

More importantly, for the SNS junction, the left and right parts have SC phases, so we can introduce phase difference φ and δ will be also a function of it: $\delta\rho(\omega,\varphi)$. Thus we can use it to obtain the Josephson current from the Gibbs free energy by $J(\varphi) := \frac{2e}{\hbar} \frac{dF}{d\varphi}$ and get the formula for Josephson current:

$$\delta\rho(\omega,\varphi) = -\frac{1}{\pi}\operatorname{Im}\frac{\partial}{\partial\omega} \ln \det d(\omega + i0^+, \varphi), \tag{1.43}$$

$$J(\varphi) = -\frac{2e}{\hbar\beta} \int_0^{\infty} d\omega \ln\left(2\cosh\frac{\beta\omega}{2}\right) \frac{\partial}{\partial\varphi}\delta\rho(\omega,\varphi) = -\frac{1}{\Phi_0}\operatorname{Im}\int_0^{\infty} d\omega \operatorname{th}\frac{\beta\omega}{2}\frac{\partial}{\partial\varphi}\ln\det d(\omega + i0^+, \varphi), \tag{1.44}$$

where $\Phi_0 := \frac{h}{2e}$ (SC magnetic flux quantum) and we have integrated by parts to get rid of $\frac{\partial}{\partial\omega}$. Now we are left only with the calculation of d. The same setup is applicable for junctions with Majorana wires, for tight-binding models.

---

[4]In another words, if there are N_c channels, the Hamiltonian of the separate region is $N_c \times N_c$ matrix.

Josephson Junction by Piasotski's et al. Method

To exemplify the use of this approach an example of Josephson Junction is presented. We will start with writing the Hamiltonian for the left and right regions ($\lambda = R, L,$) and the delta-potential in the center in the reduced Nambu formalism:

$$\mathcal{H} = \frac{1}{2} \int_{-\infty}^{\infty} dx \hat{\Psi}^{\dagger}(x) H \hat{\Psi}(x) + \mathcal{U}(x),$$

$$\hat{\Psi}(x) = \left(\hat{\psi}_{\uparrow}(x), \hat{\psi}_{\downarrow}^{\dagger}(x) \right)^{T}, \qquad H_{\lambda} = \begin{pmatrix} \frac{p^2}{2m} - \mu & \Delta_{\lambda} \\ \Delta_{\lambda}^{*} & -\frac{p^2}{2m} + \mu \end{pmatrix}, \qquad \begin{array}{l} \Delta_{\lambda} := \Delta_0 e^{i\varphi_{\lambda}}, \\ \varphi_{\lambda} := \lambda \frac{\varphi}{2}, \\ \mathcal{U}(x) := \delta(x) V_0 \tau_z. \end{array}$$

The normal (central) region will be modeled the same way, but with $\Delta = 0$. The key d matrix after a long computations (where the first challenge is to obtain Green's functions for left, central and right region, ans the second is to substitute it into the d-matrix setup) gives

$$d(z, \varphi) = -V_0 \tau_z + i \frac{k^{(+)}}{m} \tau_z + i \frac{k^{(-)}}{m} \frac{z - \Delta_0 \cos \frac{\varphi}{2} \tau_x}{z \sqrt{1 - \left(\frac{\Delta_0}{z} \right)^2}}, \tag{1.45}$$

where $k^{(\pm)} := \frac{k_F}{2} \left(\sqrt{1 + \frac{z}{\mu} \sqrt{1 - \left(\frac{\Delta_0}{z} \right)^2}} \mp \sqrt{1 - \frac{z}{\mu} \sqrt{1 - \left(\frac{\Delta_0}{z} \right)^2}} \right)$ and $k_F := \sqrt{2m\mu}$. Fortunately, we can approximate this expression: in the Andreev limit $\mu \gg \Delta$ we have

$$d_{\mathrm{A}}(z, \varphi) \approx -V_0 \tau_z + \frac{i k_F}{m} \frac{z - \Delta_0 \cos \frac{\varphi}{2} \tau_x}{z \sqrt{1 - \left(\frac{\Delta_0}{z} \right)^2}}.$$

Now, from $\det d = 0$ we get the known ABS expression:

$$\omega_A(\varphi) = \Delta_0 \sqrt{1 - D \sin^2 \frac{\varphi}{2}}, \qquad D := 1 / \left[1 + (m V_0 / k_F)^2 \right]; \tag{1.46}$$

For the Josephson junction the important simplification can be done to the general formula (1.44) (using the residue theorem), and the current can by a much simpler formula just from Andreev levels:

$$J = -\frac{2\pi}{\Phi_0} \tanh \frac{\beta \omega_A(\varphi)}{2} \frac{d\omega_A(\varphi)}{d\varphi}.$$

This formula underlines the connection of the ABS and the current. With this equation we understand the final analytical expression of the current:

$$J_{\mathrm{ABS}}(\varphi) = \frac{\pi \Delta_0}{2\Phi_0} \frac{D \tanh \left[\frac{\beta \Delta_0 \sqrt{1 - D \sin^2 \frac{\varphi}{2}}}{2} \right]}{\sqrt{1 - D \sin^2 \frac{\varphi}{2}}} \sin \varphi. \tag{1.47}$$

These are the most important properties of the most typical SC junctions.

1.4 Some Methods for Multiterminal Junctions

Now we will review two famous theoretical works regarding multiterminal junctions. The first one is an example of a currently popular direction, for which our method can potentially be used: analysis of topological multiterminal systems, and the other is closely related to our main model.

Review of Multiterminal Topological Junctions

Let us show, how the formalism discussed in Sec. 1.3 can be applied to the models with Majorana properties (see Sec. B.5), following Zazunov et al. [17]. We will briefly review the model of topological SC - conventional SC -topological SC (TS-S-TS) junctions. These models illustrate what the field of multiterminal junctions looks like currently and can be used for applications of our main theory, which is a topic for future work. Let us consider a general three-terminal junction, that is shown in Fig. 7. Here all superconductors have
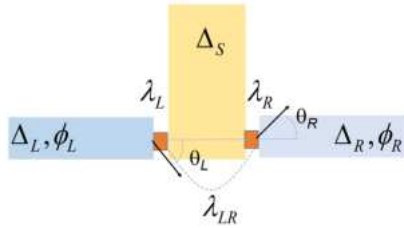

Figure 7: TS-S-TS junction setup. $\lambda_L, \lambda_r, \lambda_{LR}$ are the coupling strengths. Credit: [17].

different gap and order parameters and the couplings are denoted as $\lambda \geq 0$. We have seen recently the Hamiltonians of uncoupled parts. The TS wires spin polarization axes θ_L, θ_R, however, all processes depend only on the relative angle $\theta = \theta_L - \theta_R$. The coupling of the parts of the system can be described in Nambu notation as

$$H_t = \frac{1}{2}\Phi_L^\dagger W_{LR}\Phi_R + \sum_{j=L/R} \Psi^\dagger W_j \Phi_j + \text{h.c.}, \qquad \begin{aligned} W_{LR} &:= \lambda_{LR} e^{-i\sigma_z \phi/2}\sigma_z, \\ W_j &:= \lambda_j e^{i\sigma_z \phi_j/2}\text{diag}(\alpha_j, -\beta_j^*) \\ \alpha_j &:= \cos(\theta_j/2) \\ \beta_j &:= \sin(\theta_j/2). \end{aligned}$$

Here parameters $\lambda_{L/R} \geq 0$, and the prefactors α_j and β_j determine the weight of each spin component through the angles $\theta_{L/R}$. Φ is a Nambu wave function of a topological superconductor (see Eq. (B.71)), and Ψ is of an ordinary one (see Eq. (1.8)). The meaning of the tunneling Hamiltonian is simple: it destroys an excitation in on TS or S part and creates an excitation in another part with different probability. The exact form on the Hamiltonian is a result of non-trivial construction of it in ordinary (not Nambu) space and can be found in [17, 18].

The full bGF, $\mathcal{G}(\omega)$, follows from the uncoupled bGFs as a solution of the Dyson equation,

$$\mathcal{G}^{-1}(\omega) = G^{-1}(\omega) - \Sigma(\omega), \qquad (1.48)$$

where $G := \text{diag}(G_L, G_R)$ acts in TS lead space and the self-energy $\Sigma(\omega)$ captures the effects of interactions of TS and S. It can be obtained by integrating out the S lead. All terms here are 4×4 matrices in lead-Nambu space. For applications of the model we

review the result:

$$\Sigma_{LL/RR}(\omega) = -\frac{i\omega\lambda_{L/R}^2}{\sqrt{\omega^2 + \Delta_S^2}}\,\sigma_0,$$

$$\Sigma_{LR}(\omega) = W_{LR} - \frac{\lambda_L\lambda_R}{\sqrt{\omega^2 + \Delta_S^2}}\begin{pmatrix} i\omega\cos(\theta/2)e^{-i\tilde{\phi}/2} & \sin(\theta/2)\Delta_S e^{-i\tilde{\phi}/2} \\ -\sin(\theta/2)\Delta_S e^{i\tilde{\phi}/2} & i\omega\cos(\theta/2)e^{i\phi/2} \end{pmatrix},$$

With them the Josephson current is obtained by Matsubara summation:

$$I_j = -iT\,\mathrm{tr}\sum_\omega \sigma_z\left[\Sigma(\omega)\mathcal{G}(\omega)\right]_{jj}. \tag{1.49}$$

Here the trace operation goes in Nambu space.

For example, for S-TS-S junction with fixed $\phi_L = \phi_R$ the current-phase relation obtained numerically from (1.49) is shown in Fig. 8. There are different plots for different spin angles $4\theta/\pi = 4, 3, 2, 1, 0$ (from top to bottom). Besides, the values $\lambda_L = \lambda_R = 1$, $\Delta_S = \Delta_{TS}$, $T = 0.02\Delta_{TS}$ are assumed. The analytical expression can be obtained in the limit $\Delta_S \to \infty$ and $\theta = \pi$. It is given by $I_{L/R}^{(\Delta_S\to\infty)}(\tilde{\phi}) = -\frac{\partial E_A}{\partial\tilde{\phi}}\tanh(E_A/2T)$ (where $E_A(\tilde{\phi}) := \sqrt{\tau(\theta)}\Delta_{TS}\cos(\tilde{\phi}/2)$) and depicted aa a red dashed curve.
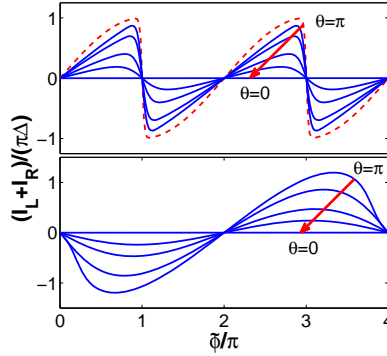

Figure 8: Current-phase relation of a TS-S-TS junction with fixed $\phi_L = \phi_R$ from [17]. The upper panel corresponds $\lambda_{LR} = 0$, the lower panel corresponds $\lambda_{LR} = 1$.

Besides, this method allows one to find the current for the case $\phi_L = \phi_R$ in different limits ($\Delta_S = 0, \Delta_S \to \infty, \Delta \to \infty$), find the spin structure of Majorana states in the TSs and analyze current-phase relation at topoligical transition (where $V \approx V_c$) [17], but these results are beyond this review.

Review of Analysis of Multiterminal Josephson Junctions by Matute-Cañadas, et al.

The last method that we will review is a method from work by Matute-Cañadas, Tosi, Levy Yeyati [2]. To our best knowledge, is the closest to our main theory.

The model is as follows. We have three leads with one channel per each, that are connected to one two-level system. We denote by $d_\sigma^\dagger$ the operator creating an electron with spin σ in that level, so its Hamiltonian is $\sum_\sigma \epsilon d_\sigma^\dagger d_\sigma$. The full Hamiltonian will be

$$H = \sum_\sigma \epsilon d_\sigma^\dagger d_\sigma + H_T + \sum_\nu H_\nu\,, \qquad H_T = \sum_{\nu,\sigma,k} t_\nu e^{-i\phi_\nu/2}d_\sigma^\dagger c_{\nu,k\sigma} + \text{h.c..} \tag{1.50}$$

Here H_ν is the BCS-type Hamiltonian for each $\nu = 1,2,3$ terminal; ϕ_ν is the supercon-ducting phase on each lead. This model can be simplified by "integrating out" the leads, so the effective action can be expressed in terms of a dot Hamiltonian and a self-energy that is responsible for the interaction between the dot and leads.

$$H^{\text{eff}} = \sum_\sigma \epsilon n_\sigma + U n_\uparrow n_\downarrow + \sum_{\nu=1}^{3} \left[\Gamma_\nu e^{-i\phi_\nu} d_\uparrow^\dagger d_\downarrow^\dagger + \text{h.c.} \right] . \quad (1.51)$$

Here ϵ is the position of the central level referred to the leads chemical potential, U is its charging energy, and Γ_ν is the tunneling rate to the lead ν, which has a phase ϕ_ν. This model is further simplified in the limit where $\Delta \gg \omega$ (Andreev limit), and for significant
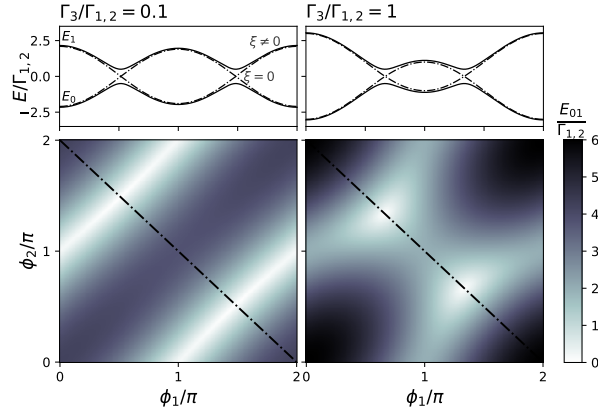

Figure 9: Top: transition energies $E_{0,1} := E_1 - E_0$ (up to a shift) of the Andreev states along the lines in the bottom diagrams, with solid (dash-dotted) lines; solid lines: $\epsilon + U/2 = 0.5\Gamma_{1,2}$; dot-dashed lines: $\epsilon = -U/2$. Bottom: E_{01} versus the phase differences $\phi_{1,2}$ for $\Gamma_1 = \Gamma_2$ and different Γ_3. Left: $\Gamma_3 \ll \Gamma_{1,2}$; right: $\Gamma_3 = \Gamma_1 = \Gamma_2$. Phase ϕ_3 is assumed equal to zero. Credit: [2].

Josephson couplings, when

$$H^{\text{eff}}_{\text{even}} \approx -(\epsilon + U/2)\tau_z + (\epsilon + U/2) + \sum_\nu \Gamma_\nu(\cos\phi_\nu \tau_x - \sin\phi_\nu \tau_y), \quad (1.52)$$

τ_i the Pauli matrices acting on the space $\{|0\rangle_d, |\uparrow\downarrow\rangle_d\}$. From it the spectrum has a form:

$$E_{0,1}(\{\phi_\nu\}) = -(\epsilon + U/2) \mp \sqrt{(\epsilon + U/2)^2 + \left| \sum_\nu \Gamma_\nu e^{-i\phi_\nu} \right|^2} . \quad (1.53)$$

This formula can be understood as follows. Let us assume that phase $\phi_3 = 0$ (we will count other phases from it). In the limit $\Gamma_3 = 0$ and for $\Gamma_1 = \Gamma_2$ the states are known Andreev states (1.20) $E_{0,1}(\phi_{12}) + \xi = \mp\sqrt{\xi^2 + \Gamma^2}\sqrt{1 - T\sin^2(\phi_{12}/2)}$ and $T := (\Gamma^2 - \delta\Gamma^2)/(\xi^2 + \Gamma^2)$, where $\delta\Gamma := \Gamma_1 \pm \Gamma_2$. For this case the transition energies $E_{01} = E_1 - E_0$ are shown on the left in Fig. 9. The system, as expected, behaves as a junction between the first and second SC, and depends on their phase difference $\phi_1 - \phi_2$. The case of $\Gamma_3 = \Gamma_1 = \Gamma_2$ is shown on the right in the same figure.

This method can be applied to all three-junction models from Fig. 6 and noise in the external flux can be taken into account [2]. The "perfect phase bias" configuration
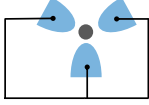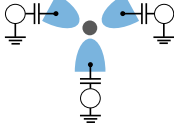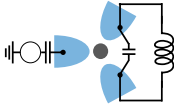
Configuration	Control parameters	Features
Perfect phase bias	ϕ_{1e}, ϕ_{2e} ξ, Γ_ν	- Sensitivity of relaxation to phase drop distribution - Appearance of Weyl points - Connection with Bi-SQUID
Charge islands	n_{g_ν} ξ, Γ_ν	- Mapping to a discrete lattice: platform for topology - Controllable disjointness
Hybrid charge/flux	ϕ_e, n_{g_3} ξ, Γ_ν	- 0-π and bifluxon in the tunnel limit $\Updownarrow$ - Simultaneous noise protection to relaxation and n_g, ϕ_e-dephasing

Table 1: Typical circuit configurations of possible three-terminal junctions. Here $\xi := \epsilon + U/2$ from the model in Eq. (1.51). Credit: [2].

was briefly discussed above. For charge islands' configuration, the total number of paired electrons $N_T = \sum_\nu N_\nu + n_d$ is conserved (where N_ν is the number of Cooper pairs in each island, n_d can be 1 or 2). The charge that is held because of finite capacitance can be taken into account by several numbers $\vec{n}_g$, which enter the island's Hamiltonian directly. The hybrid charge/flux configuration is a more general model of the previous ones, where there is an inductance energy, which also depends on the phases. Charging effects for Josephson junction with inductance are reviewed in [90]. The features of the junctions are summarized in Table 1.

Now, having reviewed the methods and a few examples, we are prepared to delve into the main theory.

2 Multiterminal Junction: The Quantum Dot Model

2.1 Model and Bound States

The Hamiltonian of the Model

This part offers our analysis of a quantum dot (QD) that is coupled to N leads of one-dimensional superconductors (SC). The geometry of the setup is illustrated in Fig. 10 and all SC are not coupled directly one with another. We will show how the bound states and the currents in such system can be obtained. The total Hamiltonian of the system has a form:

$$H_{\text{tot}} = H_D + H_{SC} + H_T, \tag{2.1}$$

where the H_D is the Hamiltonian of the dot, H_{SC} is one of the all superconductors, H_T is one that couples the dot and superconductors.
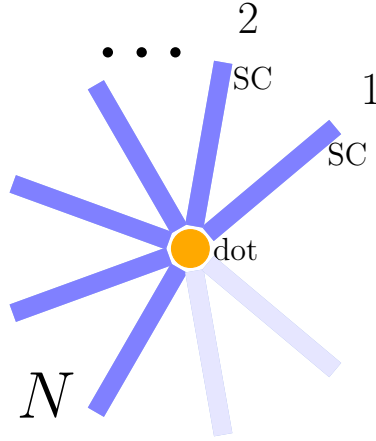

Figure 10: Illustration of a quantum dot, coupled to N one-dimensional SC leads.

The quantum dot will be described by

$$H_D := \sum_{\sigma=\pm} (V + \sigma \Delta_Z) d_\sigma^\dagger d_\sigma, \tag{2.2}$$

where $d_\sigma^\dagger$ and d_σ are the creation and annihilation operators of fermions ($\sigma = +, -$ is spin) on the quantum dot. The term $\sigma \Delta_Z$ takes into account the Zeeman splitting, V, Δ_Z are real parameters and non-indexed σ is $+1$ or -1. The fermion operators by definition satisfy

$$\{d_\sigma, d_{\sigma'}\} = \{d_\sigma^\dagger, d_{\sigma'}^\dagger\} = 0, \qquad \{d_\sigma, d_{\sigma'}^\dagger\} = \delta_{\sigma,\sigma'}. \tag{2.3}$$

Let us introduce a generalized Nambu spinor

$$D := \begin{pmatrix} d_+ & d_- & d_-^\dagger & -d_+^\dagger \end{pmatrix}^T, \tag{2.4}$$

which satisfies

$$\{D_a, D_b\} = \{D_a^\dagger, D_b^\dagger\} = P_{ab}, \quad \{D_a, D_b^\dagger\} = \delta_{ab}, \quad P := \tau_y \sigma_y = \begin{pmatrix} 0 & 0 & 0 & -1 \\ 0 & 0 & 1 & 0 \\ 0 & 1 & 0 & 0 \\ -1 & 0 & 0 & 0 \end{pmatrix}.$$
$$(2.5)$$

This is evident from an examination of the components[5]. In terms of D we have

$$H_D = \frac{1}{2} D^\dagger \left[V \tau_z + \Delta_Z \sigma_z \right] D + \text{const.} \tag{2.6}$$

The proof is straightforward and can be found in Sec. B.6.1. As it was explained in 1.1, here a matrix product between Nambu spinors and a tensor product between τ and σ-matrices is assumed. This Hamiltonian takes the symmetric form after introduction of h_D:

$$H_D = \frac{1}{2} D^\dagger h_D D + \text{const}, \qquad h_D := V \tau_z + \Delta_Z \sigma_z. \tag{2.7}$$

All N one-dimensional semi-infinite s-wave superconductors will be described by the tight-binding case of the BCS model (see review in Sec. 1.1):

$$H_{SC} := \sum_{j=1}^{N} \left(-t_j \sum_{n=1}^{\infty} \sum_{\sigma=\pm} (c_{n,\sigma,j}^\dagger c_{n+1,\sigma,j} + c_{n+1,\sigma,j}^\dagger c_{n,\sigma,j}) + \Delta_j \sum_{n=1}^{\infty} (e^{i\varphi_j} c_{n,+,j}^\dagger c_{n,-,j}^\dagger + \text{h.c.}) - \right.$$
$$\left. - \mu \sum_{\sigma=\pm} \sum_{n=1}^{\infty} c_{n,\sigma,j}^\dagger c_{n,\sigma,j} \right). \tag{2.8}$$

Here index j tells us the number of the SC lead; term with Δ_j is the usual BCS term that generates the gap and Cooper pairs, and μ is the energy of the wire. The t_j is the hopping matrix element between the nearest-neighbor sites in the jth lead (it is responsible for the traveling of excitations in the SC), the $\Delta_j e^{i\varphi_j}$ is the order parameter in the jth SC terminal, and $\mu \sim t \gg \Delta$ is the filling factor that tells how many states are occupied[6]. Note that at this stage we assume that $j \neq 0$ (later we will associate $j = 0$ with the dot). The fermionic operators $c_{n,\sigma,j}$, as usual, satisfy

$$\{c_{n,\sigma,j}, c_{n',\sigma',j'}\} = \{c_{n,\sigma,j}^\dagger, c_{n',\sigma',j'}^\dagger\} = 0, \qquad \{c_{n,\sigma,j}, c_{n',\sigma',j'}^\dagger\} = \delta_{n,n'} \delta_{\sigma,\sigma'} \delta_{j,j'}. \tag{2.9}$$

The only difference between them, compared to the usual ones, is the two indexes n and j, which determine the position of the point: the j terminal and the n site on it.

We will define the Nambu fermion for superconductor:

$$C_{n,j} := \begin{pmatrix} c_{n,+,j} & c_{n,-,j} & c_{n,-,j}^\dagger & -c_{n,+,j}^\dagger \end{pmatrix}^T. \tag{2.10}$$

It satisfies

$$\{C_{n,j,a}, C_{n',j',b}\} = P_{a,b} \delta_{n,n'} \delta_{j,j'}, \quad \{C_{n,j,a}, C_{n',j',b}^\dagger\} = \delta_{a,b} \delta_{n,n'} \delta_{j,j'}, \quad P := \tau_y \sigma_y = \begin{pmatrix} 0 & 0 & 0 & -1 \\ 0 & 0 & 1 & 0 \\ 0 & 1 & 0 & 0 \\ -1 & 0 & 0 & 0 \end{pmatrix}.$$
$$(2.11)$$

---

[5]Note that index allows us not to bother about transforming the first D into a row to be multiplicable to second D, which is a column.

[6]The real chemical potential corresponding to the continuous model can be obtained by adding and subtracting $2t$, then defining $\mu_{\text{real}} := 2t + \mu$. This will be important for understanding the Andreev limit, since soon in calculations we will set $\mu_{\text{real}} \to \infty$, and not $\mu \to \infty$.

These are the same as for D spinors, but with the obvious factors $\delta_{n,n'}\delta_{j,j'}$. In Nambu notation, we will have

$$H_{SC} = \frac{1}{2}\sum_{j=1}^{N}\left(-t_j\sum_{n=1}^{\infty}(C_{n,j}^{\dagger}\tau_z C_{n+1,j} + C_{n+1,j}^{\dagger}\tau_z C_{n,j}) + \Delta_j\sum_{n=1}^{\infty}(e^{i\varphi_j}C_{n,j}^{\dagger}\tau_+ C_{n,j} + \text{h.c.})-\right.$$

$$\tag{2.12}$$

$$\left.-\mu\sum_{n=1}^{\infty}C_{n,j}^{\dagger}\tau_z C_{n,j}\right) + \text{const.}$$

The proof is again straightforward and is presented in Sec. B.6.1. We can introduce an operator similar to h_D, but with three indexes $h_{SC,j}^{n,n'}$:

$$H_{SC} = \frac{1}{2}\sum_{j=1}^{N}\sum_{n=1,n'=1}^{\infty} C_{n,j}^{\dagger}\, h_{SC,j}^{n,n'}\, C_{n',j}, \tag{2.13}$$

$$h_{SC,j}^{n,n'} := -\tau_z(t_j\delta_{n',n+1} + t_j\delta_{n',n-1} + \mu\delta_{n',n}) + (\Delta_j e^{i\varphi_j}\tau_+ + \Delta_j e^{-i\varphi_j}\tau_-)\delta_{n',n}. \tag{2.14}$$

This formula can be understood as follows: the δ-functions select from the sum over n only the needed[7] terms for the sum over n'. Such a new double summation of $C_{n,j}$ and $C_{n',j}$ is equivalent to the single summation of $C_{n,j}$ and $C_{n+1,j}$.

Finally, the tunneling will be described by the following hopping Hamiltonian

$$H_T := -\sum_{j=1}^{N}t_j'\sum_{\sigma=\pm}(c_{1,\sigma,j}^{\dagger}d_{\sigma} + d_{\sigma}^{\dagger}c_{1,\sigma,j}). \tag{2.15}$$

The term for some j in all N superconducting leads is the usual hermitian term of the coupled systems. It tells us that in one part of the system an excitation is annihilated (by operators d_{σ} and $c_{1,\sigma,j}$) and created in another part (by operators $d_{\sigma}^{\dagger}$ and $c_{1,\sigma,j}^{\dagger}$). The parameter t_j' is responsible for the strength of the coupling. As above, index j is numerating the SC leads. We assume the sign of the coupling constant t_j' to be positive to make gain in energy without interaction, though another sign works as well, as will be shown below. Obviously, we impose anticommutative properties for the interchange of fermions of different types (c and d). The coupling can also be rewritten in the Nambu notation as

$$H_T = -\frac{1}{2}\sum_{j=1}^{N}t_j'(C_{1,j}^{\dagger}\tau_z D + \text{h.c.}). \tag{2.16}$$

The proof is also straightforward and can be found in Sec. B.6.1.

Finally, it is easy to see by matrix multiplication that

$$\begin{aligned} PD^{\dagger T} = D, \quad PC_{nj}^{\dagger T} = C_{nj}, \\ D^T P = D^{\dagger}, \quad C_{nj}^T P = C_{nj}^{\dagger}, \end{aligned} \qquad P := \tau_y\sigma_y = \begin{pmatrix} 0 & 0 & 0 & -1 \\ 0 & 0 & 1 & 0 \\ 0 & 1 & 0 & 0 \\ -1 & 0 & 0 & 0 \end{pmatrix}. \tag{2.17}$$

---

[7]To be more precise, we also need to agree that $\delta_{n'0}$ for all n' gives zero, since here for $n=1$ we have $\delta_{n'(1-1)}$ which gives from $\sum_{n'}$ the term $n'=0$, which we don't have. We assume that this is obvious.

These identities allow us to replace daggered spinors with non-daggered, which is essential derivations of formulas. If these formulas are written without indices, it is assumed that we can take components from l.h.s. and r.h.s.[8]

$$Ph_D P = -h_D^*, \qquad Ph_{SC,p}^{k,l} P = -h_{SC,p}^{k,l*}, \qquad P\tau_z P = -\tau_z.$$

Now, we will change our picture from Schrödinger to Heisenberg one by usual change of all operators $A \to A_H(t) \equiv A(t) = e^{\frac{i}{\hbar}tH} A e^{-\frac{i}{\hbar}tH}$. We will omit index and understand that we work in Heisenberg's picture by time-dependence "(t)" of the operators. The Nambu fields satisfy the following Heisenberg equation:

$$i\frac{d}{dt}C_{nj}(t) = \sum_l h_{SC,j}^{n,l} C_{l,j}(t) - \delta_{n,1} t_j' \tau_z D(t), \tag{2.18}$$

$$i\frac{d}{dt}D(t) = h_D D(t) - \sum_{j=1} t_j' \tau_z C_{1,j}(t). \tag{2.19}$$

The derivation is shown in Sec. B.6.1.

The Green's Functions

To see which transport properties follow from this model, we introduce the position space retarded Green's functions[9] of the combined system as multi-index function $G_{n,n'}^{j,j'}$. It will have for all $j = 0$ spinors of a dot and for $j \neq 0$ the SC spinors:

$$[G_{0,0}^{0,0}(t)]_{a,b} := -i\Theta(t)\langle\{D_a(t),\ D_b^\dagger(0)\}\rangle, \tag{2.20}$$

$$[G_{n,n'}^{j,j'}(t)]_{a,b} := -i\Theta(t)\langle\{C_{n,j,a}(t),\ C_{n',j',b}^\dagger(0)\}\rangle, \tag{2.21}$$

$$[G_{0,n}^{0,j}(t)]_{a,b} := -i\Theta(t)\langle\{D_a(t),\ C_{n,j,b}^\dagger(0)\}\rangle, \tag{2.22}$$

$$[G_{n,0}^{j,0}(t)]_{a,b} := -i\Theta(t)\langle\{C_{n,j,a}(t),\ D_b^\dagger(0)\}\rangle. \tag{2.23}$$

Here, the lower index zero corresponds to an upper index zero and we have a 4×4 G matrix for each fixed combination n, j, n', j'. One can access its components by setting indices a, b, thus all GF of non-Nambu fields are the elements of the matrix-GF G. Such definitions allow us to see correlations between the dot and each point in every superconductor.

---

[8]However, if we have rows and columns, the understanding of positions of indices becomes important. In some literature of field theory it is proposed to change the position of index by shifting $x_a \to x_{\bullet a}$, where $\bullet$ fixes the empty position of column index (for example, $(dx')^{\alpha\bullet} = \Lambda_{\bullet\beta}^\alpha dx^{\beta\bullet}$, see [115]). We will avoid using this notation, as it would unnecessarily complicate the formulas and is not particularly necessary. We assume the reader understands the context, and we have already agreed on the positioning: the first index always means the n-th site, the second index means j-th lead, and the last index tells us which of four components of the Nambu field we take.

[9]Sometimes they referred to as "Gorkov/Nambu Green's functions", but in our model they are only similar to well-known Gorkov's GF (see, for example, §17 of [117])

These GF satisfy the following Dyson equations:

$$\left[i\frac{d}{dt} - h_D\right]G_{0,0}^{0,0}(t) + \sum_{j=1}^{N} t_j' \tau_z G_{1,0}^{j,0}(t) = \delta(t), \tag{2.24}$$

$$\sum_{n''}\left[i\frac{d}{dt}\delta_{n,n''} - h_{SC,j}^{n,n''}\right]G_{n'',n'}^{j,j'}(t) + \delta_{n,1}t_j'\tau_z G_{0,n'}^{0,j'}(t) = \delta_{n,n'}\delta_{j,j'}\delta(t), \quad j, \, j' \neq 0, \tag{2.25}$$

$$\left[i\frac{d}{dt} - h_D\right]G_{0,n'}^{0,j'}(t) + \sum_{j''=1}^{N} t_{j''}' \tau_z G_{1,n'}^{j'',j'}(t) = 0, \quad j' \neq 0, \tag{2.26}$$

$$\sum_{n''}\left[i\frac{d}{dt}\delta_{n,n''} - h_{SC,j}^{n,n''}\right]G_{n'',0}^{j,0}(t) + \delta_{n,1}t_j'\tau_z G_{0,0}^{0,0}(t) = 0, \quad j \neq 0, \tag{2.27}$$

which can be seen by straightforward transformations (see proof in Sec. B.6.1). As usual using GF, we will transform to Fourier space by

$$G_{n,n'}^{j,j'}(\omega) = \int d\omega e^{i(\omega+i\eta)t} G_{n,n'}^{j,j'}(t). \tag{2.28}$$

Here η is a cut-off parameter that we will later set to zero $\eta \to 0$. Now, we have obtained a set of four Dyson equations:

$$[z - h_D]G_{0,0}^{0,0}(\omega) + \sum_{j=1}^{N} t_j' \tau_z G_{1,0}^{j,0}(\omega) = 1, \tag{2.29}$$

$$\sum_{n''}[z\delta_{n,n''} - h_{SC,j}^{n,n''}]G_{n'',n'}^{j,j'}(\omega) + \delta_{n,1}t_j'\tau_z G_{0,n'}^{0,j'}(\omega) = \delta_{n,n'}\delta_{j,j'}, \quad j, \, j' \neq 0, \tag{2.30}$$

$$[z - h_D]G_{0,n'}^{0,j'}(\omega) + \sum_{j''=1}^{N} t_{j''}' \tau_z G_{1,n'}^{j'',j'}(\omega) = 0, \quad j' \neq 0, \tag{2.31}$$

$$\sum_{n''}[z\delta_{n,n''} - h_{SC,j}^{n,n''}]G_{n'',0}^{j,0}(\omega) + \delta_{n,1}t_j'\tau_z G_{0,0}^{0,0}(\omega) = 0, \quad j \neq 0, \tag{2.32}$$

where we defined $z := \omega + i\eta$. These equations can be understood as follows. In the first equation, the dot's system is described by the first term, and the coupling from each lead gives contribution from each term in the sum. The index "1" means that SC is coupled at its first site. In the second equation, two leads j, j' and two points n, n' on them are chosen. It tells us how such points are correlated. The first sum runs over all points of j-th superconductor and collects correlations, the second term is a manifestation of the coupling at the point $n = 0$ (which is the location of the dot). The latter two equations are understood in the same way. Note that in Eq. (2.30) and (2.32), there is no sum over repeated j, since the j-th lead is fixed.

Now we will introduce a Green's function of an uncoupled[10] SC $g_{n'',n'}^{j}$ (if $t_j' = 0$ for all j), as a solution of

$$\sum_{n''}[z\delta_{n,n''} - h_{SC,j}^{n,n''}]g_{n'',n'}^{j}(\omega) = \delta_{n,n'}. \tag{2.33}$$

---

[10]This quite nontrivial though a natural approach was first introduced by Caroli et al. [92].

We can view this equation as a product of two matrices. Thus, by multiplying by the inverse to the first one we can obtain the $g^j_{n'',n'}(\omega)$. By doing the same transformation for Eq. (2.32), the relation between the two GF in terms of bare GF is obtained:

$$G^{j,0}_{n,0}(\omega) = -g^j_{n,1}(\omega)t'_j\tau_z G^{0,0}_{0,0}(\omega), \quad j \neq 0. \tag{2.34}$$

More detailed proof can be found in Sec. B.6.1.

Now, we can plug $G^{j,0}_{n,0}(\omega)$ into Eq. (2.29) and rewrite it with the following self-energy $\Sigma(\omega)$:

$$[z - h_D - \Sigma(\omega)]G^{0,0}_{0,0}(\omega) = 1, \qquad \Sigma(\omega) := \sum_{j=1}^{N} (t'_j)^2 \tau_z g^j_{1,1}(\omega)\tau_z. \tag{2.35}$$

It should be kept in mind that this formula is written in the Nambu notation and $\Sigma(\omega)$ is a 4×4 matrix (the tensor product to σ_0 is omitted). We have transformed the Dyson equation (2.29) to a form, where a dot's GF is expressed from an effective function $\Sigma(\omega)$ that takes into account the contribution from all superconductors.

The Description of the coupled dot requires an expression for $\Sigma(\omega)$, for which the formula for $g^j_{n,n'}(\omega)$ is needed. As a standard approach, we can use Lehmann representation $g_{n,n'} = \int_0^\pi dk \frac{\psi_k(n)\psi_k(n')}{z-h_k}$, where we have a basis functions $\psi_k(n) = \sqrt{\frac{2}{\pi}}\sin(kn)$ for a model with a wall (since the SC leads are modeled in such way). In (2.14) the terms $\delta_{n',n+1}$ and $\delta_{n',n-1}$ will give the $2\cos(k)$ in the spectrum[11]:

$$h^j_k := -\tau_z\left(2t_j\cos(k) + \mu\right) + \left(\Delta_j e^{i\varphi_j}\tau_+ + \Delta_j e^{-i\varphi_j}\tau_-\right). \tag{2.36}$$

The calculation of $\Sigma(\omega)$ requires the evaluation of the integral

$$g^j_{n,n'}(\omega) = \frac{2}{\pi}\int_0^\pi dk \frac{\sin(kn)\sin(kn')}{z + \tau_z\left(2t_j\cos(k) + \mu\right) - \Delta_j\left[e^{i\varphi_j}\tau_+ + e^{-i\varphi_j}\tau_-\right]}. \tag{2.37}$$

First, we approximate it in the wide-band limit $t_j \to \infty$. As shown in Fig. 11, in this limit the integral is obtained near Fermi points $\pm\frac{\pi}{2}$ and the spectrum is linear. We set $\mu \ll t_j$ and $k \approx \frac{\pi}{2} + q$, then $\sin(k) \approx 1$; $\cos(k) \approx q$. The wide-band limit corresponds to $\mu_{\text{real}} \to \infty$, where $\mu_{\text{real}} := \mu + 2t$ (see the description of the model) and thus we have an Andreev limit. We will have:

$$g^j_{1,1}(\omega) \approx \frac{2}{\pi}\int_{-\pi/2}^{\pi/2} \frac{dq}{z + \tau_z 2t_j q - \Delta_j\left[e^{i\varphi_j}\tau_+ + e^{-i\varphi_j}\tau_-\right]}. \tag{2.38}$$

Here the inverse matrix can be evaluated by $M^{-1} = \text{Adj}(M)/\det M$ and by introduction $\bar{q} := 2t_j q_j$ the following formula can be obtained:

$$g^j_{1,1}(\omega) = \frac{1}{\pi t_j}\int_{-\infty}^{\infty} \frac{d\bar{q}\left(z - \tau_z\bar{q} + \Delta_j\left[e^{i\varphi_j}\tau_+ + e^{-i\varphi_j}\tau_-\right]\right)}{z^2 - \bar{q}^2 - \Delta_j^2}. \tag{2.39}$$

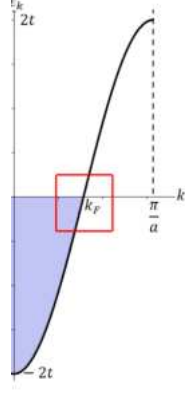[11]More details about this step can be found in Sec. B.6.1.

Figure 11: The spectrum (2.36) and its linearization near Fermi points. μ shows how many of the states are filled. In our model lattice constant $a=1$. Credit: [113]

Now, we investigate the poles of the denominator:

$$z^2 - \bar{q}^2 - \Delta_j^2 = -(\bar{q} - k_+)(\bar{q} - k_-); \qquad k_\pm := \pm\sqrt{z^2 - \Delta_j^2}.$$

Since $z := \omega + i\eta^+$, we have $\operatorname{Im} k_+ > 0$ and $\operatorname{Im} k_- < 0$. Explicitly, we have

$$k_+(\omega + i\eta^+) = \begin{cases} \sqrt{(\omega + i\eta^+)^2 - \Delta_j^2}, & \omega > \Delta_j, \\ i\sqrt{\Delta_j^2 - \omega^2}, & |\omega| < \Delta_j, \\ -\sqrt{(\omega + i\eta^+)^2 - \Delta_j^2}, & \omega < -\Delta_j. \end{cases} \qquad (2.40)$$

Also, the term in the integral with $\bar{q}$ in the numerator after integration will vanish, since the integral is odd[12]. Finally, we close the integration contour in the upper half-plane (where there is only k_+), and by the residue theorem obtain

$$g_{1,1}^j(\omega) = -\frac{2\pi i}{\pi t_j}\frac{\left(z + \Delta_j\left[e^{i\varphi_j}\tau_+ + e^{-i\varphi_j}\tau_-\right]\right)}{2i\sqrt{\Delta_j^2 - \omega^2}} = -\frac{1}{t_j}\frac{z + \Delta_j\left[e^{i\varphi_j}\tau_+ + e^{-i\varphi_j}\tau_-\right]}{\sqrt{\Delta_j^2 - \omega^2}}. \qquad (2.41)$$

Another derivation, which shows the methods of boundary Green's function can be found in Sec. B.6.1.

We return to the definition of Σ in Eq. (2.35) and obtain its approximation:

$$\Sigma(\omega) \simeq -\sum_{j=1}^{N}\Gamma_j\frac{z - \Delta_j[e^{i\varphi_j}\tau_+ + e^{-i\varphi_j}\tau_-]}{\sqrt{\Delta_j^2 - z^2}}, \qquad \Gamma_j := \frac{(t_j')^2}{t_j}, \qquad z := \omega + i\eta^+, \qquad (2.42)$$

since $\tau_z\tau_+\tau_z = -\tau_+$; $\tau_z\tau_-\tau_z = -\tau_-$. We see that only combination of $\frac{(t_j')^2}{t_j}$ influences the physics, not the t_j' and t_j separately.

---

[12]There are mathematical subtleties, which we will omit, since the argument of the odd integral still holds. Another proof can be found in Sec. B.6.1

The Spectrum

Now, having Σ, we can obtain the full GF of the superconductors to plug it into the DOS formula (1.30). This is a long and beautiful computation, which can be seen in Sec. B.6.1. As a result, the dispersion of Andreev bound states is given by

$$\rho(\omega) = \underbrace{\rho_{SC}^{(0)}(\omega) + \rho_D^{(0)}(\omega)}_{\text{bare DOS}} + \underbrace{\left(-\frac{1}{\pi}\text{Im}\,\frac{\partial}{\partial\omega}\log\det\left[1 - g_D(\omega)\Sigma(\omega)\right]\right)}_{\text{tunneling contribution}}. \qquad (2.43)$$

This is the main formula in our formalism. Here Σ is given by (2.35) and dot's GF is defined as a solution of $[z - h_D]g_D(\omega) = 1$. There is a peculiar similarity between the DOS for heterostructures (1.42) and the DOS in the scattering matrix formalism (B.61), though the expression under the determinant is different. A significant contribution to tunneling arises from those ω that satisfy the expression

$$\det\left(\omega - h_D - \Sigma(\omega)\right) = 0. \qquad (2.44)$$

This formula is used to obtain bound states numerically, as shown below. It is a similar expression to a junctions with multilayered systems, which was reviewed in Sec. 1.3. An analytical solution from this formula can be obtained only by assumptions.

Approximation of the Spectrum

An analytical solution can be obtained if we approximate the system: we linearize the local dot's Green's function near the Fermi energy, in other words, we approximate as follows:

$$\Sigma(\omega) \simeq \Sigma(0) + \omega\,\frac{d\Sigma(\omega)}{d\omega}\bigg|_{\omega=0}, \qquad (2.45)$$

where

$$\Sigma(0) = \sum_{j=1}^N \Gamma_j[e^{i\varphi_j}\tau_+ + e^{-i\varphi_j}\tau_-]; \qquad \frac{d\Sigma(\omega)}{d\omega}\bigg|_{\omega=0} = \sum_{j=1}^N \frac{\Gamma_j}{\Delta_j}. \qquad (2.46)$$

After the introduction of Z, which is proportional to unit 4×4 matrix,

$$Z := 1 - \frac{d\Sigma(0)}{d\omega} = 1 + \sum_{j=1}^N \frac{\Gamma_j}{\Delta_j}, \qquad (2.47)$$

we obtain:

$$\omega - h_D - \Sigma(\omega) \simeq \omega - h_D - \Sigma(0) - \omega\frac{d\Sigma(0)}{d\omega} = Z\omega - h_D - \Sigma(0) = Z(\omega - h_{\text{eff}}); \qquad (2.48)$$

$$h_{\text{eff}} := Z^{-1}\big(h_D + \Sigma(0)\big) = Z^{-1}\left(V\tau_z + \Delta_Z\sigma_z + \sum_{j=1}^N \Gamma_j[e^{i\varphi_j}\tau_+ + e^{-i\varphi_j}\tau_-]\right). \qquad (2.49)$$

36

Eq. (2.44) tells us that we need to find eigenvalues of h_{eff}. This can be achieved, for example, straightforwardly by writing 4×4 matrix[13]. We will parameterize the four eigenvalues by indices $\tau = 0, 1$ and $\sigma = 0, 1$ and write the analytical formula for the bound states as follows:

$$E_{\tau,\sigma} = \tau \left[1 + \sum_{j=1}^{N} \frac{\Gamma_j}{\Delta_j} \right]^{-1} \left(\sqrt{V^2 + |\sum_{j=1}^{N} \Gamma_j e^{i\varphi_j}|^2} + \sigma \Delta_Z \right). \tag{2.50}$$

Now the dependence of our system's Andreev levels on the initial parameters of the model $\Gamma_j, \Delta_j, \varphi_j, V, \Delta_Z, t'_j, t_j$ (for each wire) by the combination $\Gamma_j := (t'_j)^2/t_j$ plays role. The simplification of this formula for the case of $N = 2$ and $N = 3$ will be presented shortly.

2.2 Josephson Current

The current can be determined from the Gibbs free energy, which, in its turn, is derived from the density of states ρ (see review in Sec. 1.3). More precisely, ρ is obtained from d matrix by $\rho(\omega, \varphi) = -\frac{1}{\pi} \text{Im} \frac{\partial}{\partial \omega} \ln \det d(\omega, \varphi)$, and the d matrix is obtained from GF of the model by (2.43). Thus, the current in the jth lead can be determined by some careful transformations:

$$J_j(\varphi) = -\frac{2e}{\hbar\beta} \int_0^\infty d\omega \ln\left(2\cosh\frac{\beta\omega}{2}\right) \frac{\partial}{\partial\varphi} \delta\rho(\omega, \varphi) \overset{\text{i b p}}{\underset{\Phi_0 = \frac{\hbar}{2e} \equiv \frac{\pi\hbar}{e}}{=}} \tag{2.51}$$

$$= -\frac{1}{\Phi_0} \text{Im} \int_0^\infty d\omega \tanh\frac{\beta\omega}{2} \frac{\partial}{\partial\varphi} \ln\det d(\omega + i\eta, \varphi) \overset{f(\omega) = \frac{1}{e^{\beta\omega}+1}}{=} \tag{2.52}$$

$$= \frac{1}{\Phi_0} \text{Im} \int_{-\infty}^{+\infty} d\omega f(\omega) \text{tr} \frac{\partial}{\partial\varphi} \ln\det(\omega + i\eta - h_D - \Sigma(\omega + i\eta)) = \tag{2.53}$$

$$= \frac{1}{\Phi_0} \text{Im} \int_{-\infty}^{+\infty} d\omega f(\omega) \text{tr} \frac{1}{\omega + i\eta - h_D - \Sigma(\omega + i\eta)} \frac{\partial\Sigma(\omega + i\eta)}{\partial\varphi_j} = \tag{2.54}$$

$$= \frac{1}{2i\Phi_0} \int d\omega f(\omega) \text{tr} \frac{1}{\omega + i\eta - h_D - \Sigma(\omega + i\eta)} \frac{\partial\Sigma(\omega + i\eta)}{\partial\varphi_j} - \tag{2.55}$$

$$- \frac{1}{2i\Phi_0} \int d\omega f(\omega) \text{tr} \frac{1}{\omega - i\eta - h_D - \Sigma(\omega - i\eta)} \frac{\partial\Sigma(\omega - i\eta)}{\partial\varphi_j}. \tag{2.56}$$

The poles of the integrand allows one to make a simplification. The Fermi function produces fermionic poles. The first integral because of $\omega + i\eta$ has poles from the propagator in the lower-half of the complex plane, thus we need to close the contour to the upper-half. In this region we have only poles from Fermi's function (when $e^{\beta\omega} = -1$). It means, $\beta\omega = \pi + 2\pi n, n = 0, 1, 2, 3...$ The second integral should be closed in the lower part of the plane, where the poles are $\beta\omega = \pi + 2\pi n, n = -1, -2, -3..$, because of $\omega - i\eta$ in it.

---

[13] Or by using Wolfram Mathematica, or by solving for $\Delta_Z = 0$ and then add the Zeeman splitting Δ_Z like in quantum mechanics.

As a result,

$$J_j(\varphi) = \frac{1}{2i\Phi_0} \cdot 2\pi i \sum_{\omega_n \geq 0} \underbrace{\text{res}(f(\omega))}_{-1/\beta} \text{tr} \frac{1}{\omega + i\eta - h_D - \Sigma(\omega + i\eta)} \frac{\partial \Sigma(\omega + i\eta)}{\partial \varphi_j} - \tag{2.57}$$

$$- \frac{1}{2i\Phi_0} \cdot (-2\pi i) \sum_{\omega_n < 0} \underbrace{\text{res}(f(\omega))}_{-1/\beta} \text{tr} \frac{1}{\omega - i\eta - h_D - \Sigma(\omega - i\eta)} \frac{\partial \Sigma(\omega - i\eta)}{\partial \varphi_j} = \tag{2.58}$$

$$= -\frac{\pi}{\Phi_0} \frac{1}{\beta} \sum_{\omega_n} \text{tr} \frac{1}{i\omega_n - h_D - \Sigma(i\omega_n)} \frac{\partial \Sigma(i\omega_n)}{\partial \varphi_j}. \tag{2.59}$$

At $T = 0$ the sum is changed to the integral[14]:

$$J_j(\varphi, T = 0) = -\frac{1}{2\Phi_0} \int d\omega \, \text{tr} \frac{1}{i\omega - h_D - \Sigma(i\omega)} \frac{\partial \Sigma(i\omega)}{\partial \varphi_j}. \tag{2.60}$$

From this equation, the Ambegoakar-Baratoff's formula can be obtained if one neglects $\Sigma(i\omega)$ in the denominator (this is the tunneling limit). This is because $\Sigma \sim \Gamma$, so after decomposition of the denominator into series, the terms from Σ from the denominator will be of the highest order in Γ.

To compute currents from j-th contact to j'-th we need to compute $J_j - J_{j'}$. Soon the results of this formula will be presented.

2.3 Two-Terminal Junction Revisited

Bound states of two terminal junction

Let us consider the special case of $N = 2$. The first step is to obtain the Andreev levels of S-QD-S contact. We expect the same relation as (1.20), since short normal region is similar to the quantum dot, at least to some limit. We define $\varphi := \varphi_2 - \varphi_1$ and the formula (2.50) gives[15]:

$$E_{\tau,\sigma} = \tau E_J \underbrace{\sqrt{1 - D \sin^2 \frac{\varphi}{2}}}_{\equiv \omega_A} + \sigma E_Z, \tag{2.61}$$

where

$$E_J := \frac{\sqrt{V^2 + (\Gamma_1 + \Gamma_2)^2}}{1 + \frac{\Gamma_1}{\Delta_1} + \frac{\Gamma_2}{\Delta_2}}, \qquad D := \frac{4\Gamma_2\Gamma_1}{V^2 + (\Gamma_1 + \Gamma_2)^2}, \qquad E_Z := \frac{\Delta_Z}{1 + \frac{\Gamma_1}{\Delta_1} + \frac{\Gamma_2}{\Delta_2}}. \tag{2.62}$$

Yes, this are precisely the Andreev levels, as was expected. And now we clearly see the connection between the macroscopic E_J and D and the microscopic V, Δ Γ (based on t'_j and t_j) parameter of our theory. Such formulas are referred as "tunneling limit" for the case of $D \sim 1$

---

[14]See, for example, Eq. (89) in [1]

[15]The proof is straightforward, and is provided in Sec. B.6.1

In the simplest symmetric case $\Gamma_1 = \Gamma_2 \equiv \Gamma$; $\Delta_1 = \Delta_2 \equiv \Delta$; $\Delta_Z = 0$ the coefficients are

$$E_J = \Delta \frac{\sqrt{V^2 + 4\Gamma^2}}{\Delta + 2\Gamma} \quad \approx \begin{cases} V, & \Gamma \ll \max\{\Delta, V\}, \\ \Delta, & \Gamma \gg \max\{\Delta, V\}; \end{cases}$$

$$D = \frac{4\Gamma^2}{(V^2 + 4\Gamma^2)} \quad \approx \begin{cases} \frac{4\Gamma^2}{V^2}, & \Gamma \ll \max\{\Delta, V\}; \\ 1, & \Gamma \gg \max\{\Delta, V\}, \end{cases} \qquad (2.63)$$

$$E_Z = \Delta_Z \frac{\Delta}{\Delta + 2\Gamma} \quad \approx \begin{cases} \Delta_Z, & \Gamma \ll \max\{\Delta, V\}, \\ \frac{\Delta_Z}{2\Gamma}, & \Gamma \gg \max\{\Delta, V\}. \end{cases}$$

Let us show that our approximation is indeed valid. We can plot the levels from the Eq. (2.61) and from the determinant (Eq. (2.44)) for some parameters. To show this we plot two configurations in Fig. 12. We see that the energy levels from both formulas are very similar.

$$V = 1.4, \ \Delta_Z = 0.3, \quad \Gamma_1 = 1.3, \ \Delta_1 = 1.4, \quad \Gamma_2 = 1.4, \ \Delta_2 = 1.4 \qquad\qquad V = 0.5, \ \Delta_Z = 0.2, \quad \Gamma_1 = 1.0, \ \Delta_1 = 1.0, \quad \Gamma_2 = 1.0, \ \Delta_2 = 3.0$$
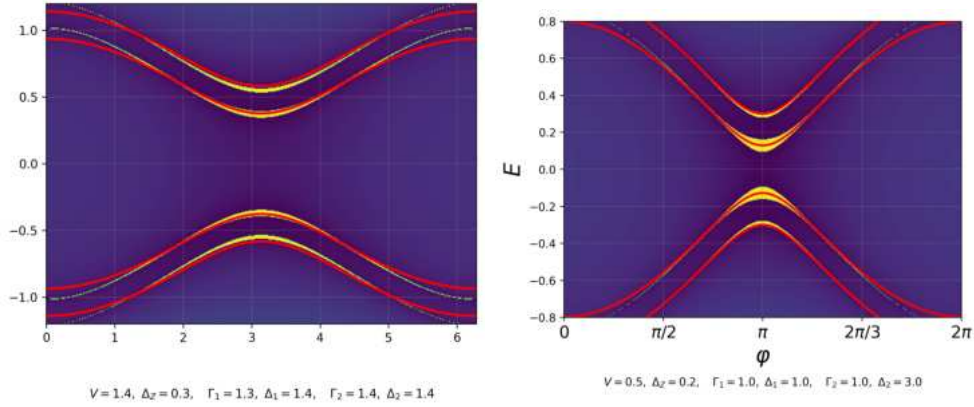
Figure 12: Comparison of ABS of the analytical (2.61) (red lines) and general (2.44) (yellow lines) formulas.

Now we can demonstrate how the ABS changes as we vary parameters of our model. First of all, if we set $\Delta_Z = 0, V = 0$, we will get a spectrum in Fig. 13. It crosses zero as it was known [4].
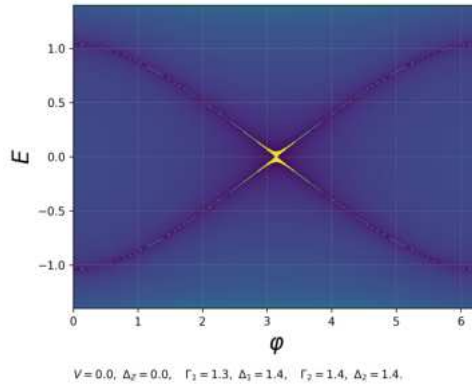

$$V = 0.0, \ \Delta_Z = 0.0, \quad \Gamma_1 = 1.3, \ \Delta_1 = 1.4, \quad \Gamma_2 = 1.4, \ \Delta_2 = 1.4.$$

Figure 13: Case of zero on-site energy of the dot V and zero Zeeman interaction.

Here we have only one level with positive energy, since the Zeeman splitting is absent. Next, we will consider cases of $\Delta_Z \neq 0$, so we will have a two levels (for each sign of

energy): one with spin-up and one with spin-down. By varying the on-site energy V, the bound states will slightly diverge, as shown in Fig. 14.
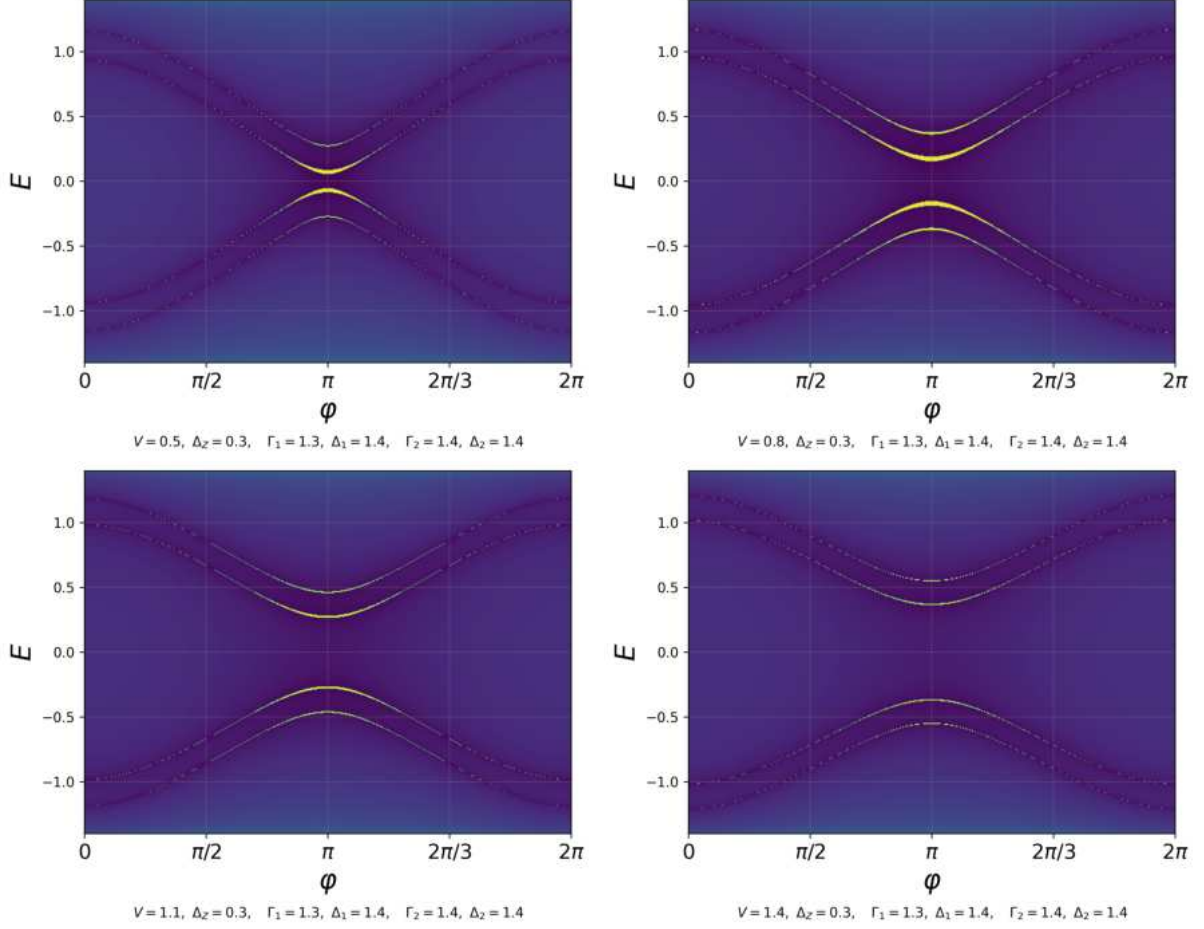

Figure 14: Changing of ABS by varying on-site energy of the dot V.

Fig. 15 shows the dependence of ABS on the superconductive gap Δ of the one of the terminals. The first two plots limit the levels to the lowest gap (which is Δ_2). The next plots are for $\Delta_2 > \Delta_1$ are levels between $\Delta_1 = 1$ are shown. The levels are slightly narrow as the gap increases.
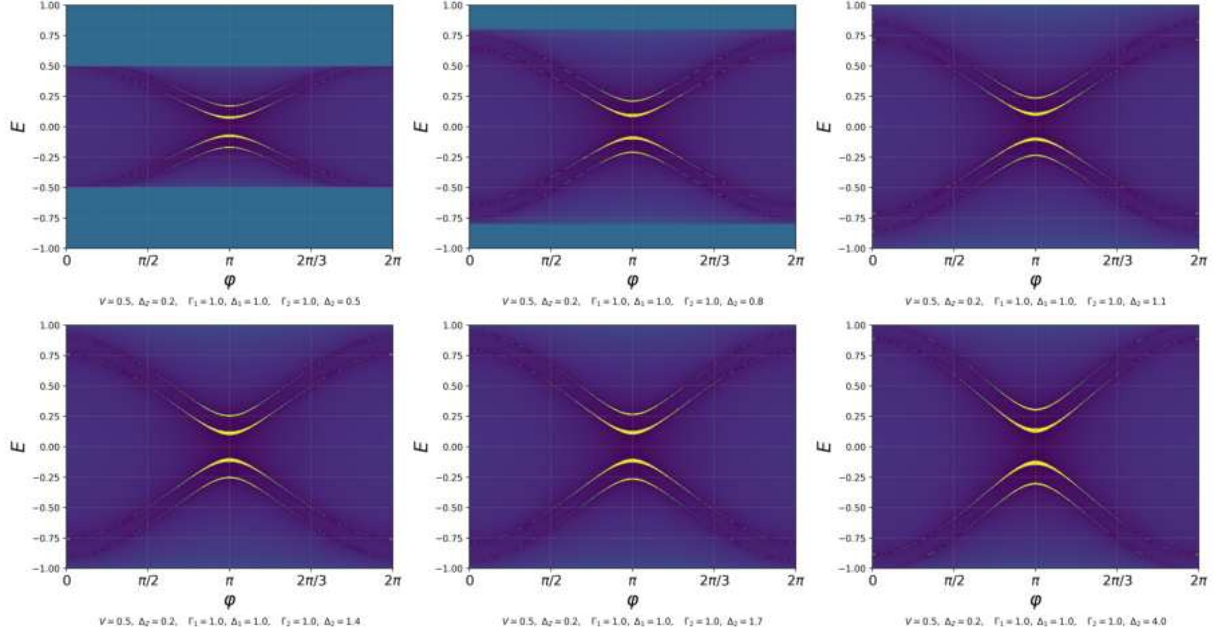
Figure 15: Changing of ABS by varying the gap Δ_2 of the second SC.

Finally, the effect of the change of couplings between a SC and QD on the levels is shown in Fig. 16. We have chosen the second SC and varied its Γ_2. We se the divergence of the levels from the central region. The big difference between two positive and two negative energy levels is a result of a strong Zeeman energy (Δ_Z).
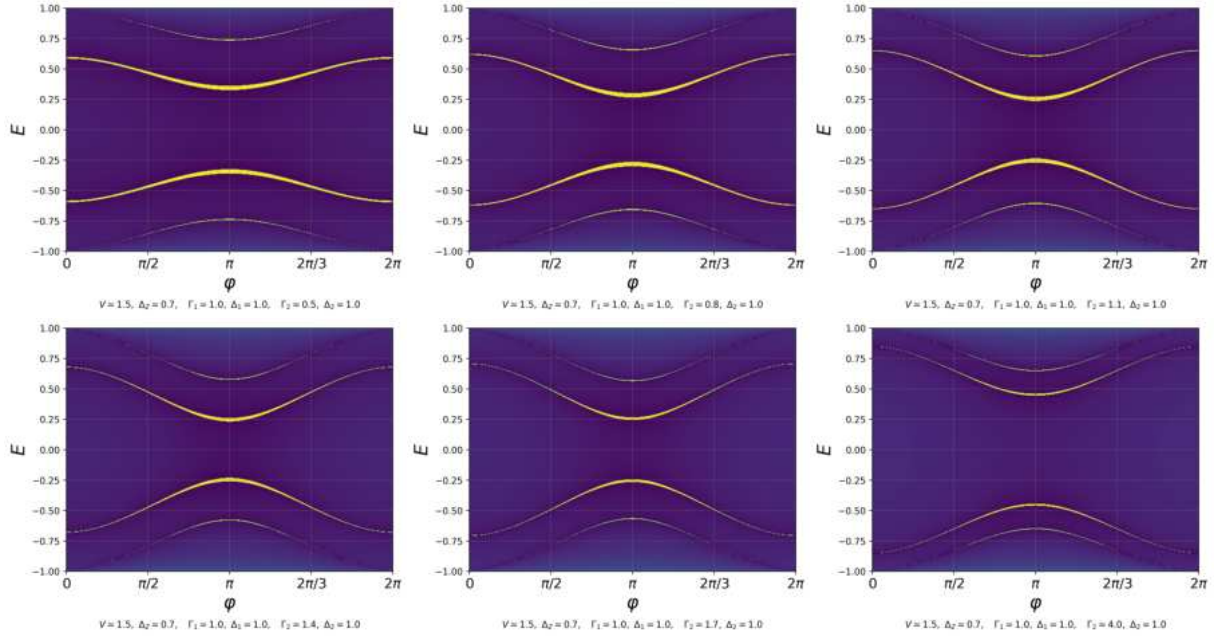

Figure 16: Changing of ABS by varying the coupling to the second SC Γ_2.

Current of Two-terminal Junction

The general expression for the Josephson current (2.54) is allows one to determine the current numerically. In case of $D \sim 1$ and for not high temperatures $\beta \gg 1$ the current

can be expressed analytically by

$$J_1(\varphi) = = \frac{DE_J\pi}{2\Phi_0} \frac{\sinh\left(\beta E_J\sqrt{1 - D\sin^2\frac{\varphi}{2}}\right)}{\cosh(\beta E_Z) + \cosh\left(\beta E_J\sqrt{1 - D\sin^2\frac{\varphi}{2}}\right)} \frac{\sin\varphi}{\sqrt{1 - D\sin^2\frac{\varphi}{2}}}. \tag{2.64}$$

The index 1 means that this current is passing through the first (left) terminal, and, obviously, the opposite one goes through the second one $J_2(\varphi) = -J_1(\varphi)$. The proof is done by transforming (2.54) with the help of (2.61) and can be found in B.6.1. This formula for $E_Z = 0$, is the Beenaker's formula for Josephson current (1.47), but for the QD instead of N region:

$$J_1(\varphi) = \frac{DE_J\pi}{2\Phi_0} \tanh\left(\beta E_J\sqrt{1 - D\sin^2\frac{\varphi}{2}}/2\right) \frac{\sin\varphi}{\sqrt{1 - D\sin^2\frac{\varphi}{2}}}. \tag{2.65}$$

For the tunneling regime $\Gamma \ll \max\{\Delta, V\}$, the parameter $D \ll 1$ and

$$J_1(\varphi) \approx I_c\sin\varphi, \quad I_c = \frac{DE_J\pi}{2\Phi_0} \frac{\sinh(\beta E_J)}{\cosh(\beta E_Z) + \cosh(\beta E_J)}. \tag{2.66}$$

Fig. 17 shows the comparison of the currents. The applicability of this formula depends strongly on the regime. For low D the differences in currents are distinguishable.
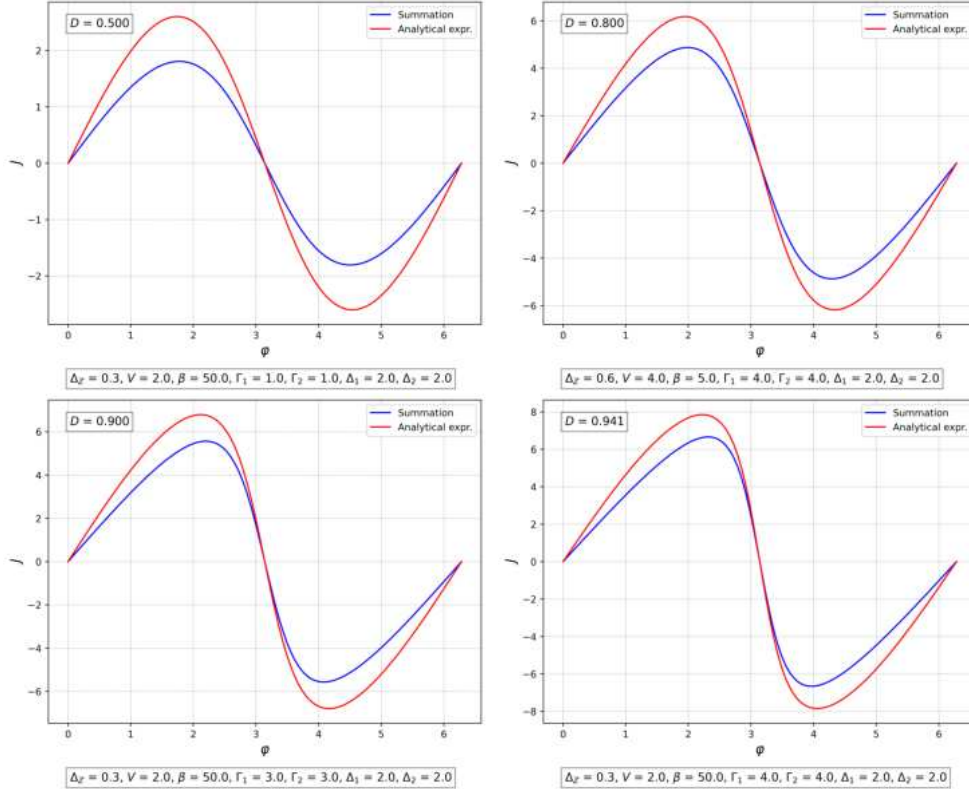

Figure 17: Comparison of numerical and analytical currents of two-terminal junctions. Several parameters, including β, were varied.

More details about bound states and current of the S-QD-S model and calculation for the continuum contribution can be found in [10].

2.4 Three-Terminal Josephson Junction

Bound States of 3TJJ

The applications of the formalism presented above to the three-terminal Josephson junctions is as follows. First of all, the phase differences between junctions will be denoted by $\varphi := \varphi_1 - \varphi_3$ and $\chi := \varphi_2 - \varphi_3$. For simplicity we consider the symmetric setup, where $\Gamma_1 = \Gamma_2 = \Gamma_3$; $\Delta_1 = \Delta_2 = \Delta_3$. The general formula (2.50) gives

$$E_{\tau,\sigma} = \tau E_J \sqrt{1 - D\Phi(\varphi, \chi)} + \sigma \tilde{\Delta}_Z, \tag{2.67}$$

where

$$E_J := \left[1 + 3\frac{\Gamma}{\Delta}\right]^{-1} \sqrt{V^2 + 9\Gamma^2}, \qquad D := \frac{9\Gamma^2}{V^2 + 9\Gamma^2},$$

$$\Phi(\varphi, \chi) := \frac{4}{9}\left(\sin^2\varphi/2 + \sin^2\chi/2 + \sin^2(\varphi/2 - \chi/2)\right), \qquad \tilde{\Delta}_Z := \frac{\Delta_Z}{1 + 3\frac{\Gamma}{\Delta}}. \tag{2.68}$$

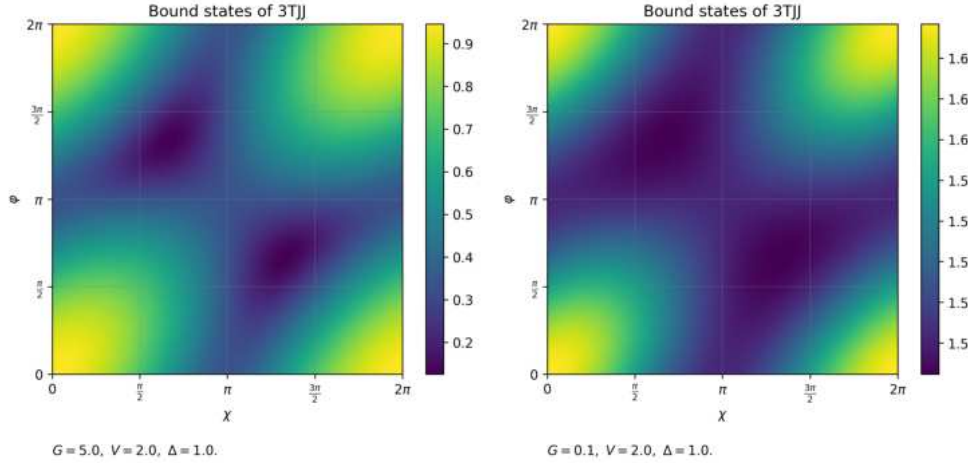An easy calculation can be found in Sec. B.6.1.

Figure 18: Change of the ABS of symmetric 3TJJ for two values of couplings Γ, calculated from Eq. (2.67).

Further this model will be analyzed in $\varphi_1 = \varphi/3$; $\varphi_2 = -2\varphi/3$; $\varphi_3 = \varphi/3$. This is the symmetric situation, since $\varphi_1 - \varphi_2 = \varphi$ and $\varphi_3 - \varphi_2 = \varphi$. The ABS from Eq. (2.68) are depicted in Fig. 18. For this plot, the Δ_Z was set to zero, since it trivially adds a constant splitting. We have seen this plot before (see Fig. 9). Similarly, one can imagine a line in the plane of phases in Fig. 18 and obtain CPR in a form as in a previous section. Now we clearly see that the levels become flatter if couplings between terminals are increased.

A similar situation is shown in Fig. 19, but by numerical computation. Now we increase the coupling only to the third terminal, Γ_3. In this case the levels from above and below zero slightly diverge.
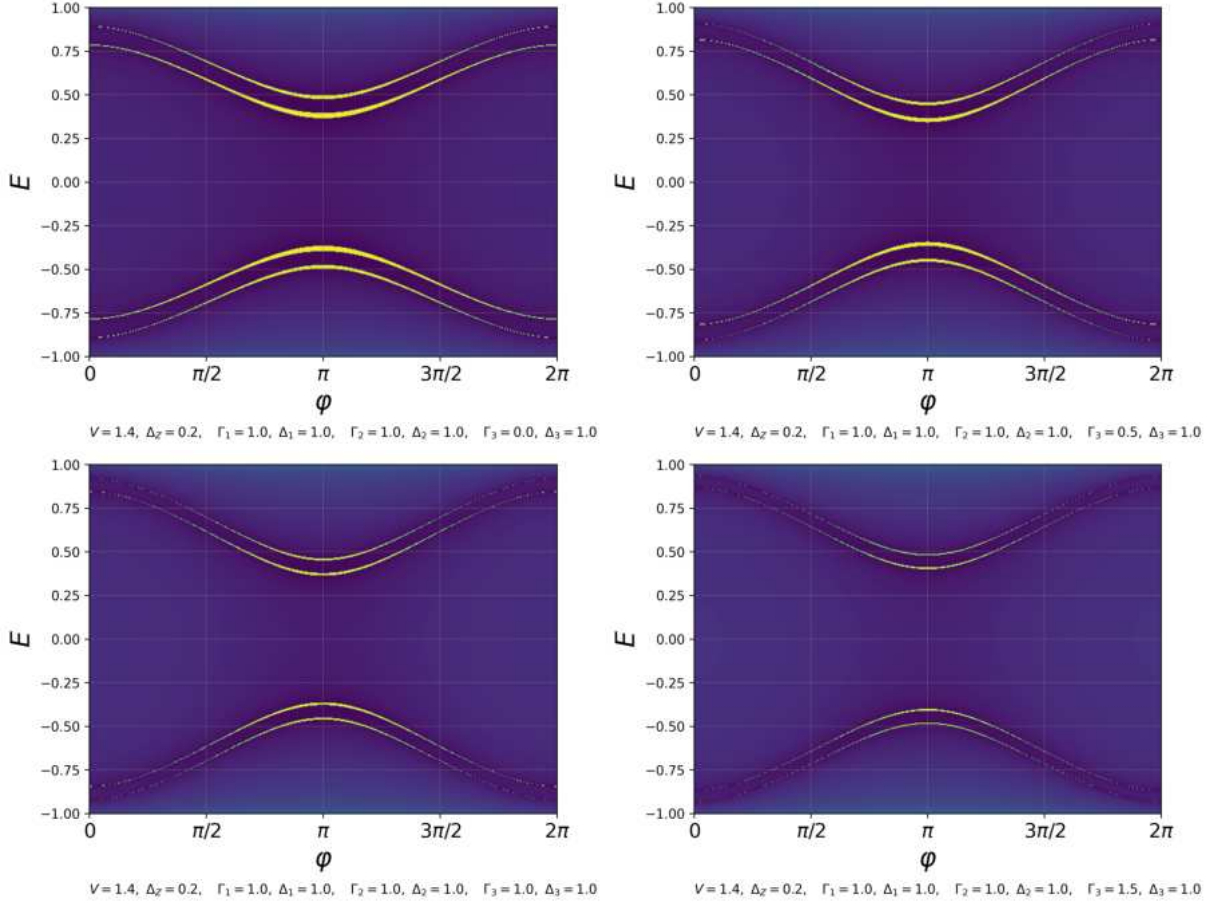
Figure 19: Dependence of $E(\varphi)$ for different strength of coupling to the third SC Γ_3 (from 0 to 1.5). Here $\varphi_1 = \varphi/3$; $\varphi_2 = -2\varphi/3$; $\varphi_3 = \varphi/3$

Let us investigate the dependence on the gap Δ_3. In this case the $E(\varphi)$ will be symmetric. The change of spectrum with increased Δ_3 is shown in Fig. 20. After passing the value $\Delta_{\max}$, the increase of the Δ_3 has no influence on the levels.
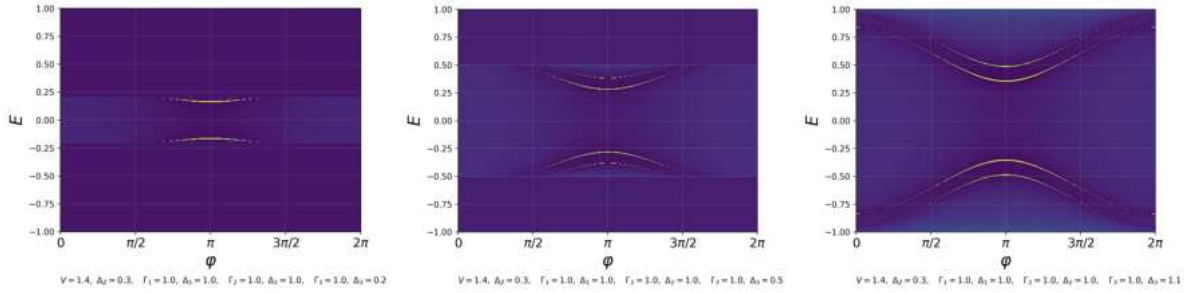

Figure 20: Dependence of $E(\varphi)$ for different gaps of the third SC Δ_3 (from 0 to 2). Here $\varphi_1 = \varphi/3$, $\varphi_2 = -2\varphi/3$, $\varphi_1 = \varphi/3$.

Current of 3TJJ

Following the example of two-terminal junction, the current of 3TJJ are obtained the same way. There in no need to re-derive again the analytical expression, since the spectral equation for 2TJJ (2.61) and for 3TJJ (2.67) have the same form. One needs to

just substitute at the last stage of the derivation $\sin \to \Phi$. Thus, the following formula for the critical current is obtained:

$$I_c(\varphi, \chi) := \frac{4}{9} \frac{DE_J \pi}{2\Phi_0} \frac{\sinh(\beta E_J \sqrt{1 - D\Phi(\varphi, \chi)})}{\cosh(\beta \tilde{\Delta}_Z) + \cosh(\beta E_J \sqrt{1 - D\Phi(\varphi, \chi)})} \frac{1}{\sqrt{1 - D\Phi(\varphi, \chi)}}. \quad (2.69)$$

The most tricky part is to understand, w.r.t. which phase differences take the derivative in the step (B.121), since in many terminals there are different phases and we usually define some "effective combination of phases" to decrease the number of parameters. First, let us set $\varphi_3 = 0$, since there is a gauge possibility: we can count phases from any value. Now, to get the current through the first terminal $J_1(\varphi, \chi)$, we take the derivative w.r.t φ (the definitions were $\varphi := \varphi_1 - \varphi_3$ and $\chi := \varphi_2 - \varphi_3$). The expressions for $J_2(\varphi, \chi)$ and $J_3(\varphi, \chi)$ are obtained in a similar way. The result is

$$J_1(\varphi, \chi) = I_c(\varphi, \chi)[\sin(\varphi) + \sin(\varphi - \chi)], \quad (2.70)$$

$$J_2(\varphi, \chi) = I_c(\varphi, \chi)[\sin(\chi) - \sin(\varphi - \chi)], \quad (2.71)$$

$$J_3(\varphi, \chi) = -I_c(\varphi, \chi)[\sin(\varphi) + \sin(\chi)]. \quad (2.72)$$

These are the final formulas for the current in the three-terminal junction. The currents obey the Kirchoff's law

$$J_1(\varphi, \chi) + J_2(\varphi, \chi) + J_3(\varphi, \chi) = 0, \quad (2.73)$$

which is intuitive: no parts of the current disappears. Fig. 21 shows the current J_1 as functions of phase differences for the symmetric 3TJJ. The plots are quite similar[16] The
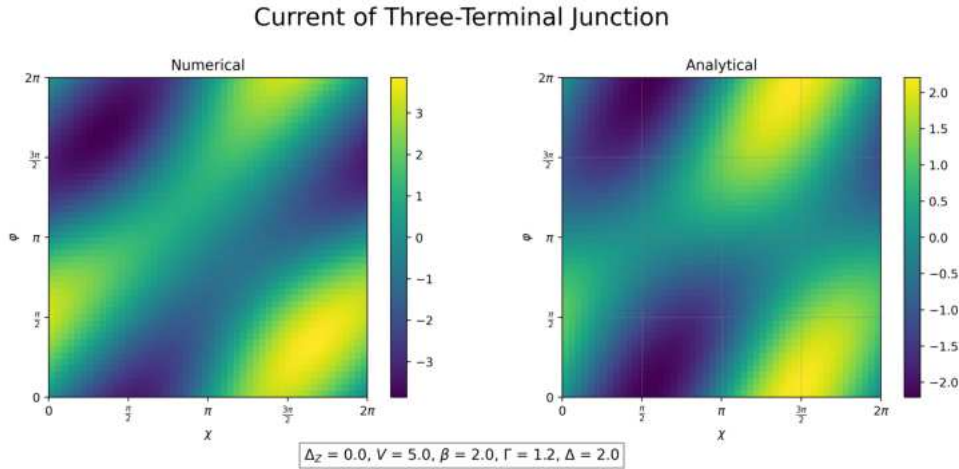

Figure 21: Comparison of numerical (from (2.59)) and analytical (from (2.70)) expressions of current in 3TJJ.

equation (2.69) allows one to see the effective dependence on the Δ-s and Γ-s through just one parameter D.

For the case $T = 0$ and $E_J > \tilde{\Delta}_z$, second fraction in (2.69) disappears and the current has a much simpler form:

$$I_c(\varphi, \chi, T \to 0) \to \frac{E_J \pi}{2\Phi_0} \frac{D}{\sqrt{1 - D\Phi(\varphi, \chi)}}. \quad (2.74)$$

We see a non-trivial dependence only on the transparency D.

---

[16]The plot for analytical expressions was multiplied by (-1). We relate it to the choice of phases.

Diode Efficiency for 3TJJ

The diode effect, which consists of stronger current to one direction than to another (see e.g. [7], is described by the diode efficiency. To obtain it, the critical currents in the first and second leads should be introduced as

$$I^{c+}(\chi) := \max_{\varphi} \left(J_1(\varphi, \chi) - J_2(\varphi, \chi) \right), \tag{2.75}$$

$$I^{c-}(\chi) := \min_{\varphi} \left(J_1(\varphi, \chi) - J_2(\varphi, \chi) \right). \tag{2.76}$$

Whichever χ is chosen, the system by design cannot have current higher than $I^{c+}(\chi)$ and lower than $I^{c-}(\chi)$ for some phase difference $\varphi(I_{\max})$ and $\varphi(I_{\min})$ respectively. Thus, the diode efficiency can be defined as a difference between currents in

$$\eta_{1,2}(\chi) := \frac{|I^{c+}(\chi)| - |I^{c-}(\chi)|}{|I^{c+}(\chi)| + |I^{c-}(\chi)|}. \tag{2.77}$$

Here labels 1,2 indicate the first and the second terminal. The $\eta_{1,2}(\chi)$ reflects the relative difference between maximal and minimal possible current (analogous to interferometric visibility in optics). If there were no dependence on φ, the $\eta_{1,2}(\chi)$ would be 0, which means that it is not possible manipulate the system (if the device is created). The $\eta_{1,2}(\chi) = 1$ means that we can tune the system in a way that no current flows (set $\varphi(I_{\max})$) or, opposite, allow the system to have the maximal possible current that can be achieved with such materials and design (by setting $\varphi(I_{\max})$).

The properties of η for case $T = 0$, in which the formula (2.74) is applicable, are as follows. In this limit, η is dependent only on $D := 9\Gamma^2/(V^2 + 9\Gamma^2)$ (not on E_J and Δ_Z). This can be seen in Fig. 22. We see that only for D around 1 the diode efficiency is distinguishable from sine.
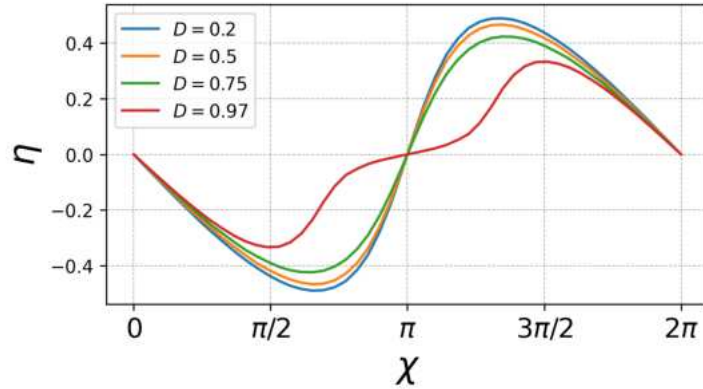

Figure 22: Diode efficiency as a function of phase difference $\chi := \varphi_2 - \varphi_3$. The transparency is defined as $D := 9\Gamma^2/(V^2 + 9\Gamma^2)$.

We can also find the dependence of the maximum value of $\eta_{1,2}(\chi)$ for all χ on D. Thus, we can see how the possibility of tuning the setup is dependent on the input parameters (coupling constants Γ-s and gaps Δ-s). This is shown in Fig. 23. We see that the η vanishes if D goes to the maximal value.
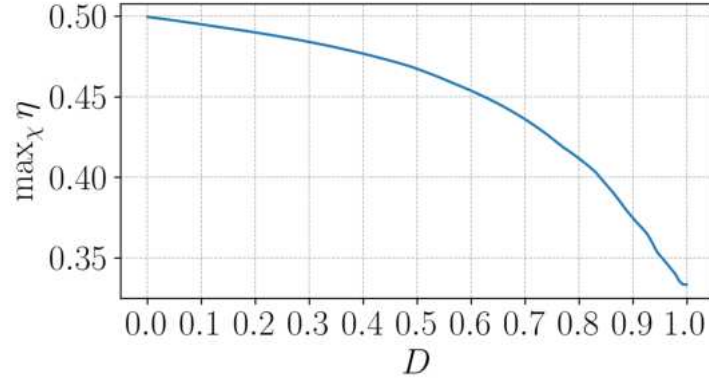
Figure 23: Maximal value of the diode efficiency for all φ, η as a function of $D := 9\Gamma^2/(V^2 + 9\Gamma^2)$.

The interpretation of it in terms of microscopic parameters of model is as follows. By decreasing the on-site energy of the dot V, the D increases and the "diode" becomes less effective. For the case $V \gtrsim \Gamma$, if the couplings between terminals and the dot Γ are increased, the diode loses its efficiency. However, if $V \ll \Gamma$, the efficiency is no longer lost (since D$\sim$const if the Γ increases).

2.5   Other Results

Many Junctions Example

Our model in Sec. 2.1 and our code in Sec. B.7 allows one to find the Andreev levels for arbitrary parameters and arbitrary numbers of junctions. To show it ones more, the ABS of seven junctions with parameters are shown in Fig. 24. This model incorporates seven different phases, different gaps Δ and different couplings Γ. Here, the code that displays energy levels is not able to distinguish levels around $2\pi/3$, as this is not a property of the levels. Now we are the first in the world to see how the bound states for the seven terminal JJ look for such the configuration in Fig. 24.
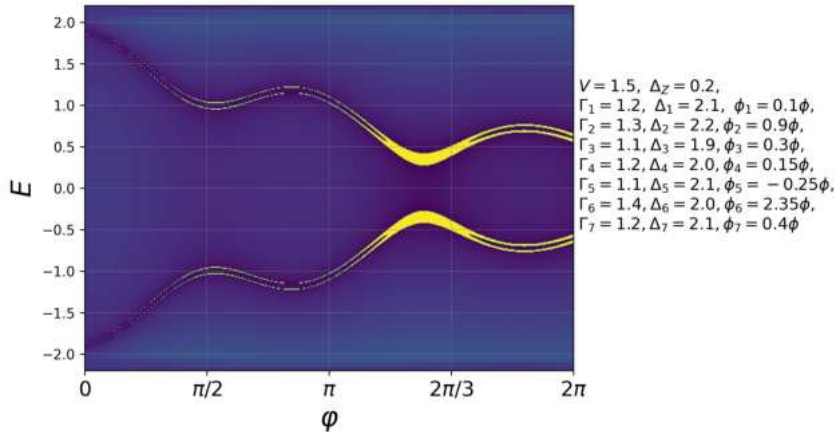

Figure 24: Seven-terminal junction with different parameters.

Of course, such model is not physically motivated and provides only an illustration of our method.

47

Conclusion and Future Work

This study has presented the promising Green's function formalism for the description of multiterminal Josephson junctions. The fundamental concepts of superconductivity have been reviewed: the BCS model, BdG equations, Andreev states and reflection. We introduced methods that were used as the building blocks for our research: ways of calculating current, Nambu notation, and definitions of Green's functions. We have developed a GF theory for the model of a quantum dot that is coupled to an arbitrary number of superconductive leads. Additionally, the dependence of the bound states and the supercurrent on phases of superconductors for a general number of terminals has been provided. For the tree-terminal system the diode efficiency has been established.

Several directions for future research and applications emerge from this work. Within the analyzed models the exact dependence of the levels splitting parameters is yet to be explored. Such dependence can play a crucial role in the spin-qubit applications, as the ability to manipulate spin splitting opens the way to decoding and reading the information contained in them. The calculations of the diode efficiency at the finite temperature and for more realistic configurations are still the next steps in the creation of the superconductive diode. Moreover, the diode efficiency in analogous models can be analyzed and ways of its improvement by changing parameters can be established.

Another promising direction lies in refining the methodology. Additional effort is required to make the method more accessible and applicable to a broader range of models. Currently, the introduction to the method requires further elaboration and applications without strong background in condensed matter physics are problematic. Such work will systematize the analyzed models, popularize the essential methods of mathematical transformations.

The extension of the formalism to the continuous systems opens a window to a broad range of models. The general formulas for the bound states in terms of microscopic parameters for such systems are nearly ready to be used. The remaining inputs for computation are the Green's functions of the uncoupled systems, the coupling strengths, and the positions of the contacts. The hardest part of applying the method is the calculation of the full Green's function for a non-superconductive central region. However, for some systems these functions have already been published in books and articles. Further development of the formalism will allow one to calculate the current and its noise correlations for more complicated, continuous models.

We hope that these ideas will inspire future studies and lead to their successful implementation.

A Formalism for Multiterminal Continuous Junctions

A.1 General Formalism for Many Terminals, Simplified Version

This section provides a simplified version of a real formalism from Sec. A.2, which is created with a purpose of making understanding it better. It is more complicated than main theory in Sec. 2.1, since we now consider continuous models and we do not specify the non-SC Hamiltonian, but easier than Sec. A.2, since the SC are 1D, not 3D and the terminal is only one.

The Model

We consider a one-dimensional system, which is coupled to one one-dimensional superconductive leads. The biggest disadvantage of this model is that the lead is just one, however, adding another lead is straightforward and only make proofs bigger in length. Besides, this model provides a simplification compared to the model in the main part 2.1, since in formulas there will be no sum over all leads (for example, $\sum_j$), so it will help in understanding. We model the system by the following Hamiltonian:

$$H_{\text{tot}} = H_{\text{n}} + H_{\text{SC}} + H_{\text{T}}, \tag{A.1}$$

where H_{n} - a term for a normal system, H_{SC} - a term for a superconductive leads, H_{T} - a term for coupling. By "normal system" we mean not superconductive system; it can be, for example, a metal, semiconductor, Majorana wire, insulator.

The local quantum system described by a set of fermion fields $\{\hat{\psi}_\sigma(x)\}$, where $x \in \Omega \subset \mathbb{R}$ is the position-space quantum number, $\sigma = \pm$ is the spin projection, and Ω is the volume occupied by the system. Here we assume Schrödinger picture, however, we later will transform it into Heisenberg one. By fields we mean an operators that annihilate or create (if $\hat{\psi}_\sigma^\dagger(x)$) an excitation with a quantum number x. Fermionic fields satisfy the following anticommutative algebra:

$$\{\hat{\psi}_\sigma(x), \hat{\psi}_{\sigma'}(x')\} = 0, \quad \{\hat{\psi}_\sigma(x), \hat{\psi}_{\sigma'}^\dagger(x')\} = \delta_{\sigma,\sigma'}\delta(x - x'). \tag{A.2}$$

We assume that such fields evolve under the following effective single-particle Hamiltonian

$$H_{\text{n}} = \sum_{\sigma,\sigma'=\pm} \int_\Omega dx \ \hat{\psi}_\sigma^\dagger(x) \ h_{\sigma,\sigma'}(p, x) \ \hat{\psi}_{\sigma'}(x). \tag{A.3}$$

Here $h_{\sigma,\sigma'}(p, x)$ for each index is a hermitian complex operator (for example, in trivial case it is a Hamiltonian of a free fermion). The first-quantized momentum operator p has the usual form: $p = -i\nabla$. We require for all Fermi fields $\hat{\psi}_\sigma(x)$ to respect the open boundary conditions at the system's surface, which have the form:

$$\hat{\psi}_\sigma(x)\big|_{x \in \partial\Omega} = 0. \tag{A.4}$$

This means that all fields propagate only inside of our material, but don't leave it. The normal system in the extended Nambu basis looks like:

$$H_{\text{n}} \equiv \frac{1}{2} \int_{\Omega} dx \hat{\Psi}^{\dagger}(x) \mathcal{H}_{\text{n}}(p, x) \hat{\Psi}(x), \tag{A.5}$$

$$\tag{A.6}$$

$$\mathcal{H}_{\text{n}}(p, x) := \begin{pmatrix} h(p, x) & 0 \\ 0 & -\sigma_y h^*(p, x) \sigma_y \end{pmatrix}, \qquad h(p, x) := \sum_{\sigma, \sigma' = \pm} h_{\sigma, \sigma'}(p, x) \ket{\sigma} \bra{\sigma'} ;$$

$$\hat{\Psi}(x) := \begin{pmatrix} \hat{\psi}(x) \\ i\sigma_y \left[\hat{\psi}^{\dagger}(x) \right]^T \end{pmatrix}, \qquad \hat{\psi}(x) := \sum_{\sigma = \pm} \hat{\psi}_{\sigma}(x) \ket{\sigma} . \tag{A.7}$$

The proof is straightforward and can be found in App. B.6.2.

The electrodes will be modeled as one-dimensional semi-infinite s-wave superconductors, described by the following set of Fermi field operators $\{\chi_{\sigma}(x)\}$ governed by the BCS-type Hamilton operator:

$$H_{\text{SC}} := \sum_{\sigma = \pm} \int_0^{\infty} dx \hat{\chi}_{\sigma}^{\dagger}(x) \left[\frac{p^2}{2m} - \mu \right] \hat{\chi}_{\sigma}(x) + \int_0^{\infty} dx \left[\Delta \hat{\chi}_+^{\dagger}(x) \hat{\chi}_-^{\dagger}(x) + \Delta^* \hat{\chi}_-(x) \hat{\chi}_+(x) \right] .$$

$$\tag{A.8}$$

Note that here Δ is a complex function and SC phase is assumed in it. Here the superconductive fields χ are fermions, they obey anticommutative relations:

$$\{\hat{\chi}_{\sigma}(x), \hat{\chi}_{\sigma'}(x')\} = 0, \qquad \{\hat{\chi}_{\sigma}(x), \hat{\chi}_{\sigma'}^{\dagger}(x')\} = \delta_{\sigma, \sigma'} \delta(x - x').$$

In the Nambu basis we will have:

$$H_{\text{SC}} = \frac{1}{2} \int_0^{\infty} dx \hat{\Upsilon}^{\dagger}(x) \mathcal{H}_{\text{SC}}(p, x) \hat{\Upsilon}(x), \quad \mathcal{H}_{\text{SC}}(p, x) = \begin{pmatrix} \left[\frac{p^2}{2m} - \mu \right] & \Delta \\ \Delta^* & - \left[\frac{p^2}{2m} - \mu \right] \end{pmatrix}, \tag{A.9}$$

$$\hat{\Upsilon}(x) = \begin{pmatrix} \hat{\chi}(x) \\ i\sigma_y \left[\hat{\chi}^{\dagger}(x) \right]^T \end{pmatrix}, \quad \hat{\chi}(x) = \sum_{\sigma = \pm} \hat{\chi}_{\sigma}(x) \ket{\sigma} , \tag{A.10}$$

and $\sigma_y = -i \left(\ket{+} \bra{-} - \text{h.c.} \right)$ is an ordinary Pauli matrix (for several channels it will be a generalization of a Pauli matrix, as we will see in the next section). The proof is straightforward and can be found in App. B.6.2

To describe the particle tunneling between them, we propose the following "point-hopping" Hamiltonian

$$H_T = \sum_{\sigma, \sigma' = \pm} W_{\sigma, \sigma'} \hat{\chi}_{\sigma}^{\dagger}(a) \hat{\psi}_{\sigma'}(\tilde{R}) + \text{h.c.}, \qquad \tilde{R} := \begin{cases} R, & R \notin \partial\Omega, \\ R - a, & R \in \partial\Omega. \end{cases} \tag{A.11}$$

The coordinate $\tilde{R}$ is the fixed point of the contact. We can have any points, where we can connect the SC and normal electrodes (inside the latter), but if we connect at the boundary $\partial\Omega$, the are no non-SC fermions, so to make sense, we shift it back by the

introduced distance a. The a (so-called "short-distance cut-off") is the outward-pointing normal to the surface $\partial\Omega$ at the point R. The $\hat{\chi}_\sigma^\dagger(a)$ means that the SC lead is coupled at distance $a \to 0$ at its end. The $W_{\sigma,\sigma'}$ is a phenomenological numerical constant of dimensions [Energy] $\times$ [Length]$^{-1}$, describing the tunneling rate of quasi-particles. It can be obtain by a first-principles microscopic study by, for example, analyzing the Wannier-function overlap integral of the Coulomb interaction vertex, but for our formalism this is an input-constant of the model.

And for their tunneling we have:

$$H_T = \frac{1}{2}\hat{\Upsilon}^\dagger(a)\mathcal{W}\hat{\Psi}(\tilde{R}) + \text{h.c.}, \qquad \mathcal{W} := \begin{pmatrix} W & 0 \\ 0 & -W^* \end{pmatrix}, \qquad W := \sum_{\sigma,\sigma'=\pm} W_{\sigma,\sigma'}\,|\sigma\rangle\,\langle\sigma'|\,. \tag{A.12}$$

Let us emphasis again, that here $\hat{\Upsilon}^\dagger(a)$ means creating an excitation in SC electrode at a distance to its end and $\hat{\Psi}(\tilde{R})$ means annihilating excitation at the normal material at coordinate R inside it. At the last stage of our transformations we will take the limit $a \to 0$.

Symmetries, Commutators, Equations of Motion

There are some properties of the introduced formalism. The extended Nambu fields have a charge conjugation constraint

$$\mathcal{C}\left[\Psi^\dagger(x)\right]^T = \Psi(x), \quad \mathcal{C}\left[\Upsilon^\dagger(x)\right]^T = \Upsilon(x), \quad \mathcal{C} := \tau_y\sigma_y = \begin{pmatrix} 0 & 0 & 0 & -1 \\ 0 & 0 & 1 & 0 \\ 0 & 1 & 0 & 0 \\ -1 & 0 & 0 & 0 \end{pmatrix}. \tag{A.13}$$

Field operators have the following commutation relations:

$$\{\Psi_a(x),\ \Psi_b(x')\} = \mathcal{C}_{ab}\delta(x - x'), \qquad \{\Psi_a(x),\ \Psi_b^\dagger(x')\} = \delta_{ab}\delta(x - x'), \tag{A.14}$$

$$\{\Upsilon_a(x),\ \Upsilon_b(x')\} = \mathcal{C}_{ab}\delta(x - x'), \qquad \{\Upsilon_a(x),\ \Upsilon_b^\dagger(x')\} = \delta_{ab}\delta(x - x'). \tag{A.15}$$

and the Hamiltonian possesses chiral symmetry:

$$\mathcal{C}\mathcal{H}_\text{n}(p,x)\mathcal{C} = -\mathcal{H}_\text{n}^*(p,x), \qquad \mathcal{C}\mathcal{H}_\text{SC}(p,x)\mathcal{C} = -\mathcal{H}_\text{SC}^*(p,x), \quad \mathcal{C}\mathcal{W}\mathcal{C} = -\mathcal{W}^*, \tag{A.16}$$

as was reviewed before. All this is obviously seen by do matrix multiplications.

Now, we will transform to Heisenberg's picture and for new field we will have t-dependence. The Heisenberg equations of motion for the Nambu field operators are:

$$\begin{cases} i\dfrac{d}{dt}\hat{\Upsilon}(x,t) = \mathcal{H}_\text{SC}(p,x)\hat{\Upsilon}(x,t) + \delta(x - a)\mathcal{W}\hat{\Psi}(\tilde{R},t), & \tag{A.17} \\[2mm] i\dfrac{d}{dt}\hat{\Psi}(x,t) = \mathcal{H}_\text{n}(p,x)\hat{\Psi}(x,t) + \delta(x - \tilde{R})\mathcal{W}^\dagger\hat{\Upsilon}(a,t). & \tag{A.18} \end{cases}$$

Note that in the rhs. in the second term we have a value of the field at a fixed point (the contact), and is not a function of coordinates. The derivation is done in Sec. B.6.2.

Green's Functions, Dyson Equations

Now we define the following set of Green's functions

$$[G_{\text{NN}}(x, x'|t)]_{ab} := - i\Theta(t) \langle\{\hat{\Psi}_a(x, t), \hat{\Psi}_b^\dagger(x', 0)\}\rangle, \tag{A.19}$$

$$[G_{\text{SS}}(x, x'|t)]_{ab} := - i\Theta(t) \langle\{\hat{\Upsilon}_a(x, t), \hat{\Upsilon}_b^\dagger(x', 0)\}\rangle, \tag{A.20}$$

$$[G_{\text{NS}}(x, x'|t)]_{ab} := - i\Theta(t) \langle\{\hat{\Psi}_a(x, t), \hat{\Upsilon}_b^\dagger(x', 0)\}\rangle, \tag{A.21}$$

$$]G_{\text{SN}}(x, x'|t)]_{ab} := - i\Theta(t) \langle\{\hat{\Upsilon}_a(x, t), \hat{\Psi}_b^\dagger(x', 0)\}\rangle. \tag{A.22}$$

By taking the derivative $\frac{d}{dt}$ from them and using the Heisenberg equations (A.18), one can show that they satisfy the following set of Dyson's equations:

$$\left(i\frac{d}{dt} - \mathcal{H}_{\text{n}}(p, x)\right) G_{\text{NN}}(x, x'|t) = \delta(x - \tilde{R})\mathcal{W}^\dagger G_{SN}(a, x'|t) + \delta(t)\delta(x - x'), \tag{A.23}$$

$$\left(i\frac{d}{dt} - \mathcal{H}_{\text{SC}}(p, x)\right) G_{\text{SS}}(x, x'|t) = \delta(x - a)\mathcal{W} G_{\text{NS}}(\tilde{R}, x'|t) + \delta(t)\delta(x - x'), \tag{A.24}$$

$$\left(i\frac{d}{dt} - \mathcal{H}_{\text{SC}}(p, x)\right) G_{\text{SN}}(x, x'|t) = \delta(x - a)\mathcal{W} G_{\text{NN}}(\tilde{R}, x'|t), \tag{A.25}$$

$$\left(i\frac{d}{dt} - \mathcal{H}_{\text{n}}(p, x)\right) G_{\text{NS}}(x, x'|t) = \delta(x - \tilde{R})\mathcal{W}^\dagger G_{\text{SS}}(a, x'|t). \tag{A.26}$$

Now, by Fourier transforming $\tilde{F}(z) = \int_0^\infty dt e^{izt} f(t)$ we find

$$(z - \mathcal{H}_{\text{n}}(p, x)) G_{\text{NN}}(x, x') = \delta(x - \tilde{R}) \, \mathcal{W}^\dagger \, G_{\text{SN}}(a, x') + \delta(x - x'), \tag{A.27}$$

$$(z - \mathcal{H}_{\text{SC}}(p, x)) G_{\text{SS}}(x, x') = \delta(x - a) \, \mathcal{W} \, G_{NS}(\tilde{R}, x') + \delta(x - x'), \tag{A.28}$$

$$(z - \mathcal{H}_{\text{SC}}(p, x)) G_{\text{SN}}(x, x') = \delta(x - a) \, \mathcal{W} \, G_{\text{NN}}(\tilde{R}, x'), \tag{A.29}$$

$$(z - \mathcal{H}_{\text{n}}(p, x)) G_{\text{NS}}(x, x') = \delta(x - \tilde{R}) \, \mathcal{W}^\dagger \, G_{SS}(a, x'). \tag{A.30}$$

The derivation can be found in App. B.6.2.

Bare GF-s g and m and Expression of Coupled GF-s in Terms of D and $\mathcal{M}$

We got the set of equation that describe the system with coupling. To move forward we can notice, that we know everything for uncoupled systems, so we know Green's function for uncoupled Hamiltonians. Let us denote them as g for superconductor and m for normal metal:

$$\left[z - \mathcal{H}_{\text{n}}(p, x)\right] m(x, x') = \delta(x - x'). \tag{A.31}$$

$$\left[z - \mathcal{H}_{SC}(p, x)\right] g(x, x') = \delta(x - x'). \tag{A.32}$$

We assume that g and m are also z-dependent, but for compactness we don't write it[17]. From them by multiplying on the inverse operators we get the following system of

---

[17]Note that functions m, g are in general not symmetric by interchange x and x', since only one argument in the Hamiltonian.

equations:

$$\begin{cases} G_{\text{NN}}(x, x') = m(x, x') + m(x, \tilde{R}) \, \mathcal{W}^\dagger \, G_{\text{SN}}(a, x'), & \text{(A.33)} \\ G_{\text{SS}}(x, x') = g(x, x') + g(x, a) \, \mathcal{W} \, G_{\text{NS}}(\tilde{R}, x'), & \text{(A.34)} \\ G_{\text{SN}}(a, x') = g(a, a) \, \mathcal{W} \, G_{\text{NN}}(\tilde{R}, x'), & \text{(A.35)} \\ G_{\text{NS}}(\tilde{R}, x') = m(\tilde{R}, \tilde{R}) \, \mathcal{W}^\dagger \, G_{\text{SS}}(a, x'). & \text{(A.36)} \end{cases}$$

This is done by rewriting terms as ones that are expressed in terms of m and g[18].

From it we get

$$\begin{cases} G_{\text{NN}}(x, x') = m(x, x') + m(x, \tilde{R}) \, \mathcal{W}^\dagger \, g(a, a) \, \mathcal{W} \, G_{\text{NN}}(\tilde{R}, x'), & \text{(A.37)} \\ G_{\text{SS}}(x, x') = g(x, x') + g(x, a) \, \mathcal{W} \, m(\tilde{R}, \tilde{R}) \, \mathcal{W}^\dagger \, G_{\text{SS}}(a, x'). & \text{(A.38)} \end{cases}$$

Now we are one step before the final formula. We will introduce two 4×4 matrices D and $\mathcal{M}$:

$$D := 1 - m(\tilde{R}, \tilde{R})\mathcal{W}^\dagger g(a, a)\mathcal{W}, \tag{A.39}$$

$$\mathcal{M} := \mathcal{W}m(\tilde{R}, \tilde{R})\mathcal{W}^\dagger, \tag{A.40}$$

with which we will find the final expression of a spectral density. Since all bare GF here depend only on the point of contact, these matrices are matrices of constants that are calculated from the construction of the model (positions of contacts, types of subsystems and coupling strengths).

The first equation (A.37) after plugging $x = \tilde{R}$ will give us

$$DG_{\text{NN}}(\tilde{R}, x') = m(\tilde{R}, x'), \tag{A.41}$$

then

$$G_{\text{NN}}(\tilde{R}, x') = D^{-1}m(\tilde{R}, x'), \tag{A.42}$$

and by plugging it back in (A.37) we get

$$G_{\text{NN}}(x, x') = m(x, x') + m(x, \tilde{R})\mathcal{W}^\dagger g(a, a)\mathcal{W}D^{-1}m(\tilde{R}, x'). \tag{A.43}$$

Now, the second equation (A.38) can be rewritten as:

$$G_{\text{SS}}(x, x') = g(x, x') + g(x, a)\mathcal{M}G_{\text{SS}}(a, x'), \tag{A.44}$$

From it by plugging $x = a$ we get

$$G_{\text{SS}}(a, x') = [1 - g(a, a)\mathcal{M}]^{-1}g(a, x'), \tag{A.45}$$

thus by plugging it in (A.38) we get

$$G_{\text{SS}}(x, x') = g(x, x') + g(x, a)\mathcal{M}[1 - g(a, a)\mathcal{M}]^{-1}g(a, x'). \tag{A.46}$$

To conclude, we have obtained the exact equations for full Green's functions of the normal part and the electrode by Eq. (A.43) and (A.46). The D and $\mathcal{M}$ matrices are determined by a setup (the coordinates of a point of a contact, types of uncoupled systems, coupling strength). The Green's function of the system will give us information about its properties (density of states, current), as we will se below.

---

[18]In the Eq. (A.35) we also set $x = \tilde{R}$ in Eq.(A.32) to plug g, then set $x = \tilde{R}$ to get the final expression. Analogously was done in the Eq. (A.36)

Spectral Density

The spectral density of the non-SC $\rho_{\mathrm{n}}(\omega)$ ans SC system $\rho_{\mathrm{SC}}(\omega)$ can be obtained with a help of (A.43) and (A.46):

$$\rho_{\mathrm{n}}(\omega) := -\frac{1}{\pi}\mathrm{Im}\int_\Omega dx \mathrm{tr} G_{\mathrm{NN}}(x,x) = \rho_{\mathrm{n}}^{(0)}(\omega) + \frac{1}{\pi}\mathrm{Im}\ \mathrm{tr}\mathcal{W}^\dagger g(a,a)\mathcal{W}D^{-1}\frac{\partial m(\tilde{R},\tilde{R})}{\partial\omega},$$
(A.47)

$$\rho_{\mathrm{SC}}(\omega) := -\frac{1}{\pi}\mathrm{Im}\int_0^\infty dx \mathrm{tr} G_{\mathrm{SS}}(x,x) = \rho_{\mathrm{SC}}^{(0)}(\omega) + \frac{1}{\pi}\mathrm{Im}\ \mathrm{tr}D^{-1}m(\tilde{R},\tilde{R})\frac{\partial\mathcal{W}^\dagger g(a,a)\mathcal{W}}{\partial\omega}.$$
(A.48)

The derivation is in Sec. B.6.2.

Finally, the total spectral density is a sum of two contributions above:

$$\rho(\omega) = \rho_{\mathrm{SC}}^{(0)}(\omega) + \rho_{\mathrm{n}}^{(0)}(\omega) + \tfrac{1}{\pi}\mathrm{Im}\ \mathrm{tr}\mathcal{W}^\dagger g(a,a)\mathcal{W}D^{-1}\tfrac{\partial m(\tilde{R},\tilde{R})}{\partial\omega} + \tfrac{1}{\pi}\mathrm{Im}\ \mathrm{tr}D^{-1}m(\tilde{R},\tilde{R})\tfrac{\partial\mathcal{W}^\dagger g(a,a)\mathcal{W}}{\partial\omega} =$$

$$= \rho_{\mathrm{SC}}^{(0)}(\omega) + \rho_{\mathrm{n}}^{(0)}(\omega) + \frac{1}{\pi}\mathrm{Im}\ \mathrm{tr}D^{-1}\frac{\partial\left(\mathcal{W}^\dagger g(a,a)\mathcal{W}m(\tilde{R},\tilde{R})\right)}{\partial\omega} = \tag{A.49}$$

$$= \rho_{\mathrm{n}}^{(0)}(\omega) + \rho_{\mathrm{SC}}^{(0)}(\omega) - \frac{1}{\pi}\mathrm{Im}\ \mathrm{tr}D^{-1}\frac{\partial D}{\partial\omega}. \tag{A.50}$$

Finally, using the identity[19] $\frac{\partial}{\partial\omega}\ln\det d = \mathrm{tr}\left\{d^{-1}\frac{\partial d}{\partial\omega}\right\}$, we have:

$$\rho(\omega) = \rho_{\mathrm{n}}^{(0)}(\omega) + \rho_{\mathrm{SC}}^{(0)}(\omega) - \frac{1}{\pi}\mathrm{Im}\frac{\partial}{\partial\varphi}\ln\det D. \tag{A.51}$$

This is our final formula for the spectral density. It tells us that $\rho(\omega)$ gets big contributions from tunneling for regimes, where D is close to zero and changes significantly, since there $-\log D$ is enormous. One can see that this expression is similar to (2.43).

A.2 General Formalism for Many Terminals

Here we will discuss the general model of multiterminal contacts with 3D superconductors and many channels for tunneling. If something is not clear, one can see Sec. A.1, which is a simplified version of this framework that is created to make understanding easier. The derivations here are also similar to the Sec. A.1, thus they will not be discussed much.

Model

We consider a d-dimensional local quantum system described by a set of fermion fields $\{\hat{\psi}_{\alpha,\sigma}(\boldsymbol{x})\}$, where $\boldsymbol{x} \in \Omega \subset \mathbb{R}^d$ is the position-space quantum number, $\alpha \in \{1,\ \ldots,\ N_c\}$ is the channel[20] (N_c - number of channels), $\sigma = \pm$ is the spin projection, and Ω is the volume occupied by the system. The N_e superconducting electrodes attached to N_e points $\boldsymbol{R}_j \in \Omega$, inside the normal region Ω (here $j = 1, \ldots, N_e$). This is illustrated in Fig. 25.

---

[19]This was used, for example, in [1], Eq. (89).
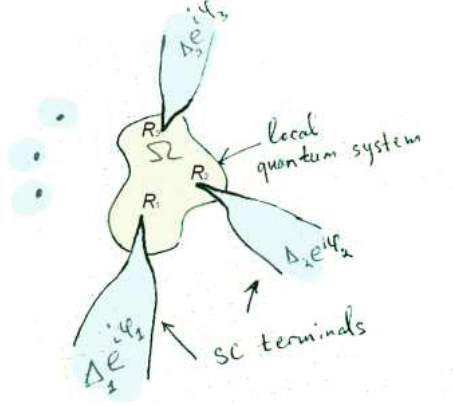[20]One can see discussion of channels on the example in [88].

Figure 25: Illustration of a multiterminal model.

As always, these satisfy the following Fermion algebra:

$$\{\hat{\psi}_{\alpha\sigma}(\boldsymbol{x}), \hat{\psi}_{\alpha'\sigma'}(\boldsymbol{x}')\} = 0, \quad \{\hat{\psi}_{\alpha\sigma}(\boldsymbol{x}), \hat{\psi}^\dagger_{\alpha'\sigma'}(\boldsymbol{x}')\} = \delta_{\alpha,\alpha'}\delta_{\sigma,\sigma'}\delta^{(d)}(\boldsymbol{x} - \boldsymbol{x}'). \quad \text{(A.52)}$$

We assume that such fields evolve under the following effective single-particle Hamiltonian

$$H_n = \sum_{\alpha,\alpha'=1}^{N_c} \sum_{\sigma,\sigma'=\pm} \int_\Omega d^{(d)}\boldsymbol{x}\, \hat{\psi}^\dagger_{\alpha\sigma}(\boldsymbol{x}) h_{\alpha\sigma,\alpha'\sigma'}(\boldsymbol{p},\ \boldsymbol{x}) \hat{\psi}_{\alpha'\sigma'}(\boldsymbol{x}). \quad \text{(A.53)}$$

For each set of indices $h_{\alpha\sigma,\alpha'\sigma'}(\boldsymbol{p},\ \boldsymbol{x})$ is a function, such that the total matrix-Hamiltonian is hermitian. As before, index n means non-SC, and exact model we do not specify, the formalism is applicable for any of it. Here the Fermi fields $\hat{\psi}_{\alpha\sigma}(\boldsymbol{x})$ respect the open boundary conditions

$$\hat{\psi}_{\alpha\sigma}(\boldsymbol{x})\big|_{\boldsymbol{x}\in\partial\Omega} = 0, \quad \text{(A.54)}$$

at the system's surface. Depending on the structure of $h_{\alpha\sigma,\alpha'\sigma'}(\boldsymbol{p},\ \boldsymbol{x})$, we may need to further specify the conditions on higher-order derivatives as well, but this goes beyond this thesis. As usual, $\boldsymbol{p} := -i\nabla$ is a first-quantized momentum operator.

As before, we model the electrodes as one-dimensional semi-infinite s-wave superconductors, described by the following set of Fermi field operators $\{\chi_{\alpha\sigma,j}(x)\}$ governed by the BCS-type Hamilton operator:

$$H_E = \sum_{j=1}^{N_e} \sum_{\alpha=1}^{N_c} \sum_{\sigma=\pm} \int_0^\infty dx\, \hat{\chi}^\dagger_{\alpha\sigma,j}(x) \left[\frac{p^2}{2m_j} - \mu_j\right] \hat{\chi}_{\alpha\sigma,j}(x) +$$

$$+ \sum_{j=1}^{N_e} \sum_{\alpha=1}^{N_c} \int_0^\infty dx \left[\Delta_j \hat{\chi}^\dagger_{\alpha+,j}(x)\hat{\chi}^\dagger_{\alpha-,j}(x) + \Delta_j^* \hat{\chi}_{\alpha-,j}(x)\hat{\chi}_{\alpha+,j}(x)\right],$$

where the SC operators satisfy

$$\{\hat{\chi}_{\alpha\sigma,j}(x), \hat{\chi}_{\alpha'\sigma',j'}(x')\} = 0, \quad \{\hat{\chi}_{\alpha\sigma,j}(x), \hat{\chi}^\dagger_{\alpha'\sigma',j'}(x')\} = \delta_{\alpha,\alpha'}\delta_{\sigma,\sigma'}\delta_{j,j'}\delta(x - x').$$

Each channel from all N_c channels just adds another BCS term to the Hamiltonian. Let us emphasis again, the the electrodes (as follows from the name) are a wires, they are effectively one dimensional, thus always the argument is non-bold.

The tunneling will be described in the point of the contact with the following "point-hopping" Hamiltonian

$$H_T = \sum_{\alpha,\alpha'=1}^{N_c} \sum_{\sigma,\sigma'=\pm} \sum_{j=1}^{N_e} W^{(j)}_{\alpha\sigma,\alpha'\sigma'} \hat{\chi}^{\dagger}_{\alpha\sigma,j}(a)\hat{\psi}_{\alpha'\sigma'}(\tilde{\boldsymbol{R}}_j) + \text{h.c.}. \tag{A.55}$$

Here a is the short-distance cut-off (real little constant), which penetrates the SC and $\tilde{\boldsymbol{R}}_j$ is just $\boldsymbol{R}_j$ the point of the contact, but in the case of the contact on the boundary, it is shifted:

$$\tilde{\boldsymbol{R}}_j = \begin{cases} \boldsymbol{R}_j, & \boldsymbol{R}_j \notin \partial\Omega, \\ \boldsymbol{R}_j - a\boldsymbol{n}_j, & \boldsymbol{R}_j \in \partial\Omega, \end{cases} \tag{A.56}$$

with $\boldsymbol{n}_j$ being the outward-pointing normal to the surface $\partial\Omega$ at the point $\boldsymbol{R}_j$. The $W^{(j)}_{\alpha\sigma,\alpha'\sigma'}$ is a phenomenological numerical constant of dimensions [Energy] × [Length]$^{-d/2-1/2}$, describing the tunneling rate of quasi-particles.

Now we rewrite the Hamiltonian in the extended Nambu basis. We hope that by this point the reader have seen it several times, so the generalization for a 3D model and several channels of expressions from Sec. A.1 is obvious. Now the size of the Nambu field is N_c times bigger. The normal part looks as follows:

$$H_n = \frac{1}{2} \int_{\Omega} d^{(d)}\boldsymbol{x}\,\hat{\Psi}^{\dagger}(\boldsymbol{x})\mathcal{H}_n(\boldsymbol{p},\,\boldsymbol{x})\hat{\Psi}(\boldsymbol{x}), \quad \mathcal{H}_n(\boldsymbol{p},\,\boldsymbol{x}) = \begin{pmatrix} h(\boldsymbol{p},\,\boldsymbol{x}) & 0 \\ 0 & -h^*(\boldsymbol{p},\,\boldsymbol{x}) \end{pmatrix}, \tag{A.57}$$

$$\hat{\Psi}(\boldsymbol{x}) = \begin{pmatrix} \hat{\psi}(\boldsymbol{x}) \\ i\sigma_y\left[\hat{\psi}^{\dagger}(\boldsymbol{x})\right]^T \end{pmatrix}, \quad \hat{\psi}(\boldsymbol{x}) = \sum_{\alpha=1}^{N_c} \sum_{\sigma=\pm} \hat{\psi}_{\alpha\sigma}(\boldsymbol{x})\,|\alpha\sigma\rangle, \tag{A.58}$$

$$h(\boldsymbol{p},\,\boldsymbol{x}) = \sum_{\alpha,\alpha'=1}^{N_c} \sum_{\sigma,\sigma'=\pm} h_{\alpha\sigma,\alpha'\sigma'}(\boldsymbol{p},\,\boldsymbol{x})\,|\alpha\sigma\rangle\,\langle\alpha'\sigma'|, \tag{A.59}$$

For superconductors we have:

$$H_E = \frac{1}{2} \sum_{j=1}^{N_e} \int_0^{\infty} dx\,\hat{\Upsilon}_j^{\dagger}(x)\mathcal{H}_j(p,x)\hat{\Upsilon}_j(x), \quad \mathcal{H}_j(p,x) := \begin{pmatrix} \left[\frac{p^2}{2m_j} - \mu_j\right] & \Delta_j \\ \Delta_j^* & -\left[\frac{p^2}{2m_j} - \mu_j\right] \end{pmatrix}, \tag{A.60}$$

$$\hat{\Upsilon}_j(x) = \begin{pmatrix} \hat{\chi}_j(x) \\ i\sigma_y\left[\hat{\chi}_j^{\dagger}(x)\right]^T \end{pmatrix}, \quad \hat{\chi}_j(x) = \sum_{\alpha=1}^{N_c} \sum_{\sigma=\pm} \hat{\chi}_{\alpha\sigma,j}(x)\,|\alpha\sigma\rangle, \quad \sigma_y = -i\sum_{\alpha=1}^{N_c}\left(|\alpha+\rangle\,\langle\alpha-| - \text{h.c.}\right), \tag{A.61}$$

Here we will use index j for j-th superconducting electrode, since this is the only index that numerates them. Same is true for fields Υ_j, with fixed index j we mean the field-operator of the j-th superconductor. The SCs are differ with the effective mass and chemical potential.

The tunneling will be as:

$$H_T = \frac{1}{2} \sum_{j=1}^{N_e} \hat{\Upsilon}_j^\dagger(a) \mathcal{W}^{(j)} \hat{\Psi}(\tilde{\boldsymbol{R}}_j) + \text{h.c.}, \quad \mathcal{W}^{(j)} = \begin{pmatrix} W^{(j)} & 0 \\ 0 & -W^{(j)*} \end{pmatrix}, \tag{A.62}$$

$$W^{(j)} = \sum_{\alpha,\alpha'=1}^{N_c} \sum_{\sigma,\sigma'=\pm} W^{(j)}_{\alpha\sigma,\alpha'\sigma'} |\alpha\sigma\rangle \langle\alpha'\sigma'|. \tag{A.63}$$

We again see that adding the channels increases the dimension of a coupling matrix, since in general it is possible for a particle to hop from one to any channel with any spin value. There are as many coupling matrices as many SC terminals (they are numerated by j).

We note that extended Nambu fields satisfy the following charge conjugation constraint

$$\mathcal{C}_{2N_c} \left[\Psi^\dagger(\boldsymbol{x}) \right]^T = \Psi(\boldsymbol{x}), \quad \mathcal{C}_{2N_c} \left[\Upsilon_j^\dagger(x) \right]^T = \Upsilon_j(x), \quad \mathcal{C}_{2N_c} = [\tau_y \sigma_y]_{2N_c}. \tag{A.64}$$

Here $\mathcal{C}_{2N_c}$ is a straightforward generalization of $\mathcal{C}$ for one channel. Furthermore, the following commutation relations are in due

$$\{\Psi_a(\boldsymbol{x}), \ \Psi_b(\boldsymbol{x}')\} = \mathcal{C}_{a,b} \ \delta^{(d)}(\boldsymbol{x} - \boldsymbol{x}'), \quad \{\Psi_a(\boldsymbol{x}), \ \Psi_b^\dagger(\boldsymbol{x}')\} = \delta_{a,b}\delta^{(d)}(\boldsymbol{x} - \boldsymbol{x}'), \tag{A.65}$$

$$\{\Upsilon_{a,j}(x), \ \Upsilon_{b,j'}(x')\} = \mathcal{C}_{a,b} \ \delta_{j,j'}\delta(x - x'), \quad \{\Upsilon_{a,j}(x), \ \Upsilon_{b,j'}^\dagger(x')\} = \delta_{a,b}\delta_{j,j'}\delta(x - x'). \tag{A.66}$$

Here a, b indicate different components of the Nambu fields, and j, j' indicate different superconductors.

We note that the Hamiltonian possesses chiral symmetry

$$\mathcal{C}_{2N_c}\mathcal{H}_n(\boldsymbol{p}, \ \boldsymbol{x})\mathcal{C}_{2N_c} = -\mathcal{H}_n^*(\boldsymbol{p}, \ \boldsymbol{x}), \quad \mathcal{C}_{2N_c}\mathcal{H}_j(p, \ x)\mathcal{C}_{2N_c} = -\mathcal{H}_j^*(p, \ x), \quad \mathcal{C}_{2N_c}\mathcal{W}^{(j)}\mathcal{C}_{2N_c} = -\mathcal{W}^{(j)*}. \tag{A.67}$$

Now, we go to Heisenberg's representation and consider the Heisenberg equations of motion for the Nambu field operators

$$i\frac{d}{dt}\hat{\Upsilon}_j(x, t) = \mathcal{H}_j(p, \ x)\hat{\Upsilon}_j(x, t) + \delta(x - a)\mathcal{W}^{(j)}\hat{\Psi}(\tilde{\boldsymbol{R}}_j, t), \tag{A.68}$$

$$i\frac{d}{dt}\hat{\Psi}(\boldsymbol{x}, t) = \mathcal{H}_n(\boldsymbol{p}, \ \boldsymbol{x})\hat{\Psi}(\boldsymbol{x}, t) + \sum_{j=1}^{N_e} \delta^{(d)}(\boldsymbol{x} - \tilde{\boldsymbol{R}}_j)\mathcal{W}^{(j)\dagger}\hat{\Upsilon}_j(a, t). \tag{A.69}$$

Green's functions and their properties

We define the following set of Gorkov/Nambu Green's functions

$$[G_{SS}(\boldsymbol{x}, \boldsymbol{x}'|t)]_{ab} := -i\Theta(t) \langle \{\hat{\Psi}_a(\boldsymbol{x}, t), \hat{\Psi}_b^\dagger(\boldsymbol{x}', 0)\} \rangle, \tag{A.70}$$

$$[G_{j,j'}(x, x'|t)]_{ab} := -i\Theta(t) \langle \{\hat{\Upsilon}_{a,j}(x, t), \hat{\Upsilon}_{b,j'}^\dagger(x', 0)\} \rangle, \tag{A.71}$$

$$[G_{S,j'}(\boldsymbol{x}, x'|t)]_{ab} := -i\Theta(t) \langle \{\hat{\Psi}_a(\boldsymbol{x}, t), \hat{\Upsilon}_{b,j'}^\dagger(x', 0)\} \rangle, \tag{A.72}$$

$$[G_{j,S}(x, \boldsymbol{x}'|t)]_{ab} := -i\Theta(t) \langle \{\hat{\Upsilon}_{a,j}(x, t), \hat{\Psi}_b^\dagger(\boldsymbol{x}', 0)\} \rangle. \tag{A.73}$$

The definition is the same as for the simplified case, but now a, b have much more values, since the dimension of the spinors is bigger. We see again that there are 3D arguments

and 1D, since the non-SC part is 3D and the SC leads are 1D. Also, the the total number of the GFs is much bigger, singe there is an each GF for each two SC, etc. We want to emphasis that S means non-SC system, and the SC-s are numerated by j.

These satisfy the following set of Dyson's equations

$$\left(i\frac{d}{dt} - \mathcal{H}_n(\boldsymbol{p},\ \boldsymbol{x})\right) G_{SS}(\boldsymbol{x},\boldsymbol{x}'|t) = \sum_{j=1}^{N_e} \delta^{(d)}(\boldsymbol{x} - \tilde{\boldsymbol{R}}_j)\mathcal{W}^{(j)\dagger} G_{j,S}(a,\boldsymbol{x}'|t) + \delta(t)\delta^{(d)}(\boldsymbol{x} - \boldsymbol{x}'),$$
(A.74)

$$\left(i\frac{d}{dt} - \mathcal{H}_j(p,\ x)\right) G_{j,j'}(x,x'|t) = \delta(x - a)\mathcal{W}^{(j)} G_{S,j'}(\tilde{\boldsymbol{R}}_j,x'|t) + \delta(t)\delta(\boldsymbol{x} - \boldsymbol{x}')\delta_{j,j'},$$
(A.75)

$$\left(i\frac{d}{dt} - \mathcal{H}_j(p,\ x)\right) G_{j,S}(x,\boldsymbol{x}'|t) = \delta(x - a)\mathcal{W}^{(j)} G_{SS}(\tilde{\boldsymbol{R}}_j,\boldsymbol{x}'|t),$$
(A.76)

$$\left(i\frac{d}{dt} - \mathcal{H}_n(\boldsymbol{p},\ \boldsymbol{x})\right) G_{S,j'}(\boldsymbol{x},x'|t) = \sum_{j=1}^{N_e} \delta^{(d)}(\boldsymbol{x} - \tilde{\boldsymbol{R}}_j)\mathcal{W}^{(j)\dagger} G_{j,j'}(a,x'|t).$$
(A.77)

These are exactly the same equations as before, but with some bold arguments ans sum over SC electrodes. By Fourier transforming the equations we find

$$(z - \mathcal{H}_n(\boldsymbol{p},\ \boldsymbol{x})) G_{SS}(\boldsymbol{x},\boldsymbol{x}') = \sum_{j=1}^{N_e} \delta^{(d)}(\boldsymbol{x} - \tilde{\boldsymbol{R}}_j)\mathcal{W}^{(j)\dagger} G_{j,S}(a,\boldsymbol{x}') + \delta^{(d)}(\boldsymbol{x} - \boldsymbol{x}'),$$
(A.78)

$$(z - \mathcal{H}_j(p,\ x)) G_{j,j'}(x,x') = \delta(x - a)\mathcal{W}^{(j)} G_{S,j'}(\tilde{\boldsymbol{R}}_j,x') + \delta(\boldsymbol{x} - \boldsymbol{x}')\delta_{j,j'},$$
(A.79)

$$(z - \mathcal{H}_j(p,\ x)) G_{j,S}(x,\boldsymbol{x}') = \delta(x - a)\mathcal{W}^{(j)} G_{SS}(\tilde{\boldsymbol{R}}_j,\boldsymbol{x}'),$$
(A.80)

$$(z - \mathcal{H}_n(\boldsymbol{p},\ \boldsymbol{x})) G_{S,j'}(\boldsymbol{x},x') = \sum_{j=1}^{N_e} \delta^{(d)}(\boldsymbol{x} - \tilde{\boldsymbol{R}}_j)\mathcal{W}^{(j)\dagger} G_{j,j'}(a,x').$$
(A.81)

Bare Green's functions g and m and the matrix form by D and $\mathcal{M}$ matrices

The bare GF will help. We define the following Green's functions

$$[z - \mathcal{H}_j(p,\ x)]g_j(x,x') = \delta(\boldsymbol{x} - \boldsymbol{x}'),$$
(A.82)

$$(z - \mathcal{H}_n(\boldsymbol{p},\ \boldsymbol{x})) m(\boldsymbol{x},\boldsymbol{x}') = \delta^{(d)}(\boldsymbol{x} - \boldsymbol{x}').$$
(A.83)

For each SC there is an each g_j. Now, we can rewrite

$$G_{SS}(\boldsymbol{x},\boldsymbol{x}') = m(\boldsymbol{x},\boldsymbol{x}') + \sum_{j=1}^{N_e} m(\boldsymbol{x},\tilde{\boldsymbol{R}}_j)\mathcal{W}^{(j)\dagger} g_j(a,a)\mathcal{W}^{(j)} G_{SS}(\tilde{\boldsymbol{R}}_j,\boldsymbol{x}'),$$
(A.84)

$$G_{j,j'}(x,x') = \delta_{j,j'} g_j(x,x') + g_j(x,a) \sum_{j''=1}^{N_e} \mathcal{W}^{(j)} m(\tilde{\boldsymbol{R}}_j,\tilde{\boldsymbol{R}}_{j''})\mathcal{W}^{(j'')\dagger} G_{j'',j'}(a,x'),$$
(A.85)

$$G_{j,S}(a,\boldsymbol{x}') = g_j(a,a)\mathcal{W}^{(j)} G_{SS}(\tilde{\boldsymbol{R}}_j,\boldsymbol{x}'),$$
(A.86)

$$G_{S,j'}(\tilde{\boldsymbol{R}}_j,x') = \sum_{j''=1}^{N_e} m(\tilde{\boldsymbol{R}}_j,\tilde{\boldsymbol{R}}_{j''})\mathcal{W}^{(j'')\dagger} G_{j'',j'}(a,x').$$
(A.87)

We can introduce a matrix $D_{j,j'}$, which has for fixed j, j' a size of the introduced Green's functions:

$$D_{j,j'} := \delta_{j,j'} - m(\tilde{\boldsymbol{R}}_j, \tilde{\boldsymbol{R}}_{j'})\mathcal{W}^{(j')\dagger}g_{j'}(a,a)\mathcal{W}^{(j')}. \tag{A.88}$$

Now, from the first equation (A.84) we have

$$\sum_{j'=1}^{N_e} D_{j,j'}G_{SS}(\tilde{\boldsymbol{R}}_{j'}, \boldsymbol{x}') = m(\tilde{\boldsymbol{R}}_j, \boldsymbol{x}'). \tag{A.89}$$

One hence has

$$G_{SS}(\tilde{\boldsymbol{R}}_j, \boldsymbol{x}') = \sum_{j'=1}^{N_e}[D^{-1}]_{j,j'}m(\tilde{\boldsymbol{R}}_{j'}, \boldsymbol{x}'), \tag{A.90}$$

and

$$G_{SS}(\boldsymbol{x}, \boldsymbol{x}') = m(\boldsymbol{x}, \boldsymbol{x}') + \sum_{j,j'=1}^{N_e} m(\boldsymbol{x}, \tilde{\boldsymbol{R}}_j)\mathcal{W}^{(j)\dagger}g_j(a,a)\mathcal{W}^{(j)}[D^{-1}]_{j,j'}m(\tilde{\boldsymbol{R}}_{j'}, \boldsymbol{x}'). \tag{A.91}$$

The second equation (A.85) in matrix form becomes

$$\hat{G}(x, x') = \hat{g}(x, x') + \hat{g}(x, a)\mathcal{M}\hat{G}(a, x'). \tag{A.92}$$

where here we have "hatted" matrices

$$[\hat{G}(x, x')]_{j,j'} := G_{j,j'}(x, x'), \qquad [\hat{g}(x, x')]_{j,j'} = \delta_{j,j'}g_j(x, x'), \qquad \mathcal{M}_{j,j'} = \mathcal{W}^{(j)}m(\tilde{\boldsymbol{R}}_j, \tilde{\boldsymbol{R}}_{j'})\mathcal{W}^{(j')\dagger}. \tag{A.93}$$

The $\mathcal{M}$ matrix combines the property of the interactions in contacts $\mathcal{W}^{(j)}$ and their position in the non-SC system. Now we evaluate

$$\hat{G}(a, x') = [1 - \hat{g}(a, a)\mathcal{M}]^{-1}\hat{g}(a, x'), \tag{A.94}$$

and get the final expression of SC GF in terms of the bare GF and the properties of interaction between parts of the system:

$$\hat{G}(x, x') = \hat{g}(x, x') + \hat{g}(x, a)\mathcal{M}[1 - \hat{g}(a, a)\mathcal{M}]^{-1}\hat{g}(a, x'). \tag{A.95}$$

Spectral density

From the first equation, we infer the spectral density of the local system

$$\rho_n(\omega) = -\frac{1}{\pi}\text{Im}\int_\Omega d^{(d)}\boldsymbol{x}\,\text{tr}G_{SS}(\boldsymbol{x}, \boldsymbol{x}) \tag{A.96}$$

$$= \underbrace{-\frac{1}{\pi}\text{Im}\int_\Omega d^{(d)}\boldsymbol{x}\,\text{tr}m(\boldsymbol{x}, \boldsymbol{x})}_{=\rho_n^{(0)}(\omega)} -$$

$$-\frac{1}{\pi}\text{Im}\int_\Omega d^{(d)}\boldsymbol{x}\,\text{tr}\mathcal{W}^{(j)\dagger}g_j(a,a)\mathcal{W}^{(j)}[D^{-1}]_{j,j'}\int_\Omega d^{(d)}\boldsymbol{x}\,m(\tilde{\boldsymbol{R}}_{j'}, \boldsymbol{x})m(\boldsymbol{x}, \tilde{\boldsymbol{R}}_j) = \tag{A.97}$$

$$= \rho_n^{(0)}(\omega) + \frac{1}{\pi}\text{Im}\,\,\text{tr}\mathcal{W}^{(j)\dagger}g_j(a,a)\mathcal{W}^{(j)}[D^{-1}]_{j,j'}\frac{\partial m(\tilde{\boldsymbol{R}}_{j'}, \tilde{\boldsymbol{R}}_j)}{\partial\omega}. \tag{A.98}$$

59

From the second equation, we get

$$\rho_{\text{SC el-d}}(\omega) = -\frac{1}{\pi}\text{Im} \int_0^\infty dx \text{tr}\{\hat{G}(x,x)\} = \tag{A.99}$$

$$= \underbrace{-\frac{1}{\pi}\text{Im} \int_0^\infty dx \text{tr}\{\hat{g}(x,x)\}}_{=:\rho_{\text{SC el-d}}^{(0)}(\omega)} - \frac{1}{\pi}\text{Im} \ \text{tr}\left\{\mathcal{M}[1 - \hat{g}(a,a)\mathcal{M}]^{-1} \int_0^\infty dx \hat{g}(a,x)\hat{g}(x,a)\right\}$$

$$\tag{A.100}$$

$$= \rho_{\text{SC el-d}}^{(0)}(\omega) + \frac{1}{\pi}\text{Im} \ \text{tr}\left\{[1 - \hat{g}(a,a)\mathcal{M}]^{-1}\frac{\partial \hat{g}(a,a)}{\partial\omega}\mathcal{M}\right\} \tag{A.101}$$

$$= \rho_{\text{SC el-d}}^{(0)}(\omega) + \frac{1}{\pi}\text{Im} \ \text{tr}[D^{-1}]_{j,j'}m(\tilde{\boldsymbol{R}}_{j'},\tilde{\boldsymbol{R}}_j)\frac{\partial \mathcal{W}^{(j)\dagger}g_j(a,a)\mathcal{W}^{(j)}}{\partial\omega}. \tag{A.102}$$

Combining the results together we find the total spectral density

$$\rho(\omega) = \rho_n^{(0)}(\omega) + \rho_{\text{SC el-d}}^{(0)}(\omega) - \frac{1}{\pi}\text{Im} \ \text{tr}[D^{-1}]_{j,j'}\frac{\partial[D]_{j',j}}{\partial\omega} \tag{A.103}$$

$$= \rho_n^{(0)}(\omega) + \rho_{\text{SC el-d}}^{(0)}(\omega) - \frac{1}{\pi}\text{Im} \ \frac{\partial}{\partial\omega}\text{tr}\log[D]. \tag{A.104}$$

Applications of these formulas for particular systems, and obtaining formula for the current is a topic for another research.

B   Supplementary Information

B.1   Glossary

- ABS - Andreev states

- MBS - Majorana states

- DOS - density of states

- GF - Green's function

- BGF - boundary Green's function

- bare GF - Green's function of an uncoupled system

- NEGF - non-equilibrium Green's function

- BCS - model of superconductivity by Bardeen, Cooper, Schrieffer

- BdG - Bogoliubov-de-Gennes equations

- BTK - method from Blonder, Tinkham, Klapwijk

- JJ, - Josephson junction

- JC - Josephson current

- S - superconductor

- TS - topological superconductor

- non-SC - not a superconductive system

- SNS - junction between superconductor, normal metal and superconductor

- SIS, S-QD-S, SNS, TS-S-TS, ... - other junctions, where another material is placed instead of normal region and instead of conventional superconductor, a topological one

- 3TJJ, MTJJ - three-terminal Josephson junction, multiterminal Josephson junction

- QD - quantum dot

- SO, SOI - spin orbit, spin-orbit interaction

- SM - semiconductor

- CPR - current-phase relation

- SQUID - superconducting quantum interference device

- := - equals by definition, we often use it to emphasis that here we introduce the object (or when we use the equation, that defines the object);

- $\equiv$ - equals "from another side", we use it to emphasis that the object can also be expressed by another parameter.
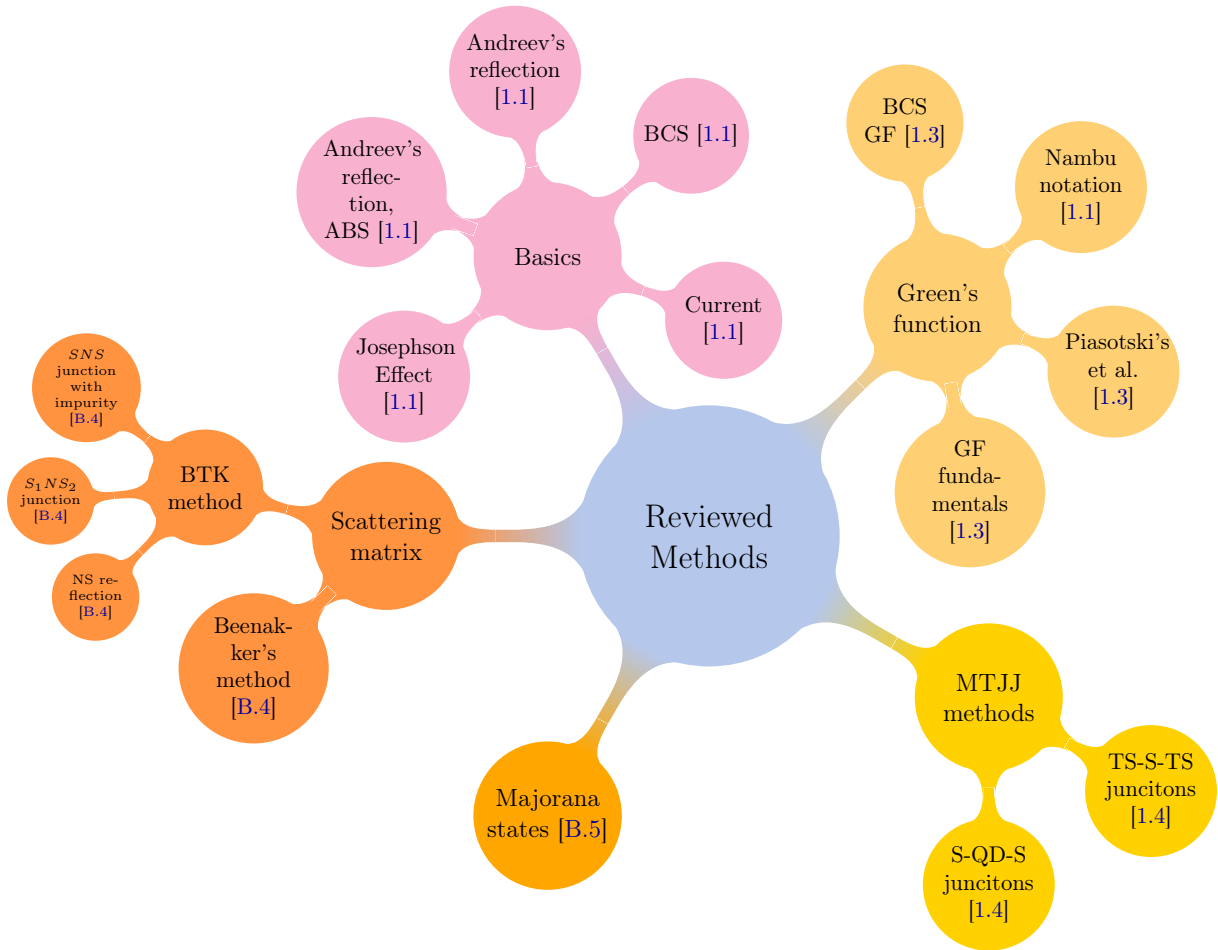
B.2   Mind Map

Figure 26: Mindmap of methods that are used or reviewed in this paper. Abbreviations are described in Sec. B.1. Numbers in links refer to the paragraphs, where a method is described.

B.3 List of Key Formulas

Formulas for General Multiterminal Josephson Junction with QD

$$H_{\text{full}} = H_D + H_{SC} + H_T, \tag{B.1}$$

$$H_D = \frac{1}{2}D^\dagger h_D D, \qquad h_D := V\tau_z + \Delta_Z \sigma_z. \tag{B.2}$$

$$H_{SC} = \frac{1}{2}\sum_{j=1}^{N}\sum_{n=1,n'=1}^{\infty} C_{n,j}^\dagger \, h_{SC,j}^{n,n'} \, C_{n',j}, \tag{B.3}$$

$$h_{SC,j}^{n,n'} := -\tau_z(t_j\delta_{n',n+1} + t_j\delta_{n',n-1} + \mu\delta_{n',n}) + (\Delta_j e^{i\varphi_j}\tau_+ + \Delta_j e^{-i\varphi_j}\tau_-)\delta_{n',n}. \tag{B.4}$$

$$H_T = -\frac{1}{2}\sum_{j=1}^{N} t'_j(C_{1,j}^\dagger \tau_z D + \text{h.c.}). \tag{B.5}$$

$$[G_{0,0}^{0,0}(t)]_{a,b} := -i\Theta(t)\left\langle\{D_a(t),\ D_b^\dagger(0)\}\right\rangle, \tag{B.6}$$

$$[G_{n,n'}^{j,j'}(t)]_{a,b} := -i\Theta(t)\left\langle\{C_{n,j,a}(t),\ C_{n',j',b}^\dagger(0)\}\right\rangle, \tag{B.7}$$

$$[G_{0,n}^{0,j}(t)]_{a,b} := -i\Theta(t)\left\langle\{D_a(t),\ C_{n,j,b}^\dagger(0)\}\right\rangle, \tag{B.8}$$

$$[G_{n,0}^{j,0}(t)]_{a,b} := -i\Theta(t)\left\langle\{C_{n,j,a}(t),\ D_b^\dagger(0)\}\right\rangle. \tag{B.9}$$

$$[z - h_D - \Sigma(\omega)]G_{0,0}^{0,0}(\omega) = 1, \qquad \Sigma(\omega) := \sum_{j=1}^{N}(t'_j)^2\tau_z g_{1,1}^j(\omega)\tau_z. \tag{B.10}$$

$$\Sigma(\omega) \simeq -\sum_{j=1}^{N}\Gamma_j\frac{z - \Delta_j[e^{i\varphi_j}\tau_+ + e^{-i\varphi_j}\tau_-]}{\sqrt{\Delta_j^2 - z^2}}, \qquad \Gamma_j := \frac{(t'_j)^2}{t_j}, \tag{B.11}$$

$$\det\left(\omega - h_D - \Sigma(\omega)\right) = 0. \tag{B.12}$$

$$E_{\tau,\sigma} = \tau\left[1 + \sum_{j=1}^{N}\frac{\Gamma_j}{\Delta_j}\right]^{-1}\left(\sqrt{V^2 + |\sum_{j=1}^{N}\Gamma_j e^{i\varphi_j}|^2} + \sigma\Delta_Z\right). \tag{B.13}$$

$$J_j(\varphi) = -\frac{\pi}{\Phi_0}\frac{1}{\beta}\sum_{\omega_n}\text{tr}\frac{1}{i\omega_n - h_D - \Sigma(i\omega_n)}\frac{\partial\Sigma(i\omega_n)}{\partial\varphi_j}. \tag{B.14}$$

$$J_j(\varphi, T = 0) = -\frac{1}{2\Phi_0}\int d\omega\ \text{tr}\frac{1}{i\omega - h_D - \Sigma(i\omega)}\frac{\partial\Sigma(i\omega)}{\partial\varphi_j}. \tag{B.15}$$

Formulas for Two-Terminal Junction

$$E_{\tau,\sigma} = \tau E_J \sqrt{1 - D\sin^2 \frac{\varphi}{2}} + \sigma E_Z, \tag{B.16}$$

$$E_J := \frac{\sqrt{V^2 + (\Gamma_1 + \Gamma_2)^2}}{1 + \frac{\Gamma_1}{\Delta_1} + \frac{\Gamma_2}{\Delta_2}}, \qquad D := \frac{4\Gamma_2\Gamma_1}{V^2 + (\Gamma_1 + \Gamma_2)^2}, \qquad E_Z := \frac{\Delta_Z}{1 + \frac{\Gamma_1}{\Delta_1} + \frac{\Gamma_2}{\Delta_2}}. \tag{B.17}$$

$$J_1(\varphi) = = \frac{DE_J\pi}{2\Phi_0} \frac{\sinh\left(\beta E_J \sqrt{1 - D\sin^2 \frac{\varphi}{2}}\right)}{\cosh(\beta E_Z) + \cosh\left(\beta E_J \sqrt{1 - D\sin^2 \frac{\varphi}{2}}\right)} \frac{\sin\varphi}{\sqrt{1 - D\sin^2 \frac{\varphi}{2}}}. \tag{B.18}$$

Formulas for Three-Terminal Junction

For $\varphi := \varphi_1 - \varphi_3$; $\chi := \varphi_2 - \varphi_3$; $\Gamma_1 = \Gamma_2 = \Gamma_3$; $\Delta_1 = \Delta_2 = \Delta_3$.

$$E_{\tau,\sigma}(\varphi, \chi) = \tau E_J \sqrt{1 - D\Phi(\varphi,\chi)} + \sigma \tilde{\Delta}_Z, \tag{B.19}$$

$$E_J := \left[1 + 3\frac{\Gamma}{\Delta}\right]^{-1} \sqrt{V^2 + 9\Gamma^2}, \qquad\qquad D := \frac{9\Gamma^2}{V^2 + 9\Gamma^2},$$

$$\Phi(\varphi, \chi) := \frac{4}{9}\left(\sin^2 \varphi/2 + \sin^2 \chi/2 + \sin^2(\varphi/2 - \chi/2)\right), \qquad \tilde{\Delta}_Z := \frac{\Delta_Z}{1 + 3\frac{\Gamma}{\Delta}}. \tag{B.20}$$

Formulas for Multiterminal Josephson Junction with a General non-SC System

$$H_n = \frac{1}{2} \int_\Omega d^{(d)}\boldsymbol{x}\, \hat{\Psi}^\dagger(\boldsymbol{x}) \mathcal{H}_n(\boldsymbol{p},\,\boldsymbol{x}) \hat{\Psi}(\boldsymbol{x}), \quad \mathcal{H}_n(\boldsymbol{p},\,\boldsymbol{x}) = \begin{pmatrix} h(\boldsymbol{p},\,\boldsymbol{x}) & 0 \\ 0 & -h^*(\boldsymbol{p},\,\boldsymbol{x}) \end{pmatrix}, \tag{B.21}$$

$$\hat{\Psi}(\boldsymbol{x}) = \begin{pmatrix} \hat{\psi}(\boldsymbol{x}) \\ i\sigma_y \left[\hat{\psi}^\dagger(\boldsymbol{x})\right]^T \end{pmatrix}, \quad \hat{\psi}(\boldsymbol{x}) = \sum_{\alpha=1}^{N_c} \sum_{\sigma=\pm} \hat{\psi}_{\alpha\sigma}(\boldsymbol{x}) \,|\alpha\sigma\rangle, \tag{B.22}$$

$$h(\boldsymbol{p},\,\boldsymbol{x}) = \sum_{\alpha,\alpha'=1}^{N_c} \sum_{\sigma,\sigma'=\pm} h_{\alpha\sigma,\alpha'\sigma'}(\boldsymbol{p},\,\boldsymbol{x}) \,|\alpha\sigma\rangle \langle\alpha'\sigma'|, \tag{B.23}$$

$$H_E = \frac{1}{2} \sum_{j=1}^{N_e} \int_0^\infty dx\, \hat{\Upsilon}_j^\dagger(x) \mathcal{H}_j(p,x) \hat{\Upsilon}_j(x), \quad \mathcal{H}_j(p,x) := \begin{pmatrix} \left[\frac{p^2}{2m_j} - \mu_j\right] & \Delta_j \\ \Delta_j^* & -\left[\frac{p^2}{2m_j} - \mu_j\right] \end{pmatrix}, \tag{B.24}$$

$$\hat{\Upsilon}_j(x) = \begin{pmatrix} \hat{\chi}_j(x) \\ i\sigma_y \left[\hat{\chi}_j^\dagger(x)\right]^T \end{pmatrix}, \quad \hat{\chi}_j(x) = \sum_{\alpha=1}^{N_c} \sum_{\sigma=\pm} \hat{\chi}_{\alpha\sigma,j}(x) \,|\alpha\sigma\rangle, \quad \sigma_y = -i\sum_{\alpha=1}^{N_c} (|\alpha+\rangle \langle\alpha-| - \text{h.c.}), \tag{B.25}$$

64

$$H_T = \frac{1}{2} \sum_{j=1}^{N_e} \hat{\Upsilon}_j^\dagger(a) \mathcal{W}^{(j)} \hat{\Psi}(\tilde{\boldsymbol{R}}_j) + \text{h.c.,} \quad \mathcal{W}^{(j)} = \begin{pmatrix} W^{(j)} & 0 \\ 0 & -W^{(j)*} \end{pmatrix}, \tag{B.26}$$

$$W^{(j)} = \sum_{\alpha,\alpha'=1}^{N_c} \sum_{\sigma,\sigma'=\pm} W_{\alpha\sigma,\alpha'\sigma'}^{(j)} |\alpha\sigma\rangle \langle\alpha'\sigma'|. \tag{B.27}$$

$$\tilde{\boldsymbol{R}}_j = \begin{cases} \boldsymbol{R}_j, & \boldsymbol{R}_j \notin \partial\Omega, \\ \boldsymbol{R}_j - a\boldsymbol{n}_j, & \boldsymbol{R}_j \in \partial\Omega, \end{cases} \tag{B.28}$$

$$i\frac{d}{dt}\hat{\Upsilon}_j(x,t) = \mathcal{H}_j(p,\ x)\hat{\Upsilon}_j(x,t) + \delta(x-a)\mathcal{W}^{(j)}\hat{\Psi}(\tilde{\boldsymbol{R}}_j, t), \tag{B.29}$$

$$i\frac{d}{dt}\hat{\Psi}(\boldsymbol{x},t) = \mathcal{H}_n(\boldsymbol{p},\ \boldsymbol{x})\hat{\Psi}(\boldsymbol{x},t) + \sum_{j=1}^{N_e} \delta^{(d)}(\boldsymbol{x} - \tilde{\boldsymbol{R}}_j)\mathcal{W}^{(j)\dagger}\hat{\Upsilon}_j(a, t). \tag{B.30}$$

$$[G_{SS}(\boldsymbol{x}, \boldsymbol{x}'|t)]_{ab} := -i\Theta(t)\langle\{\hat{\Psi}_a(\boldsymbol{x},t), \hat{\Psi}_b^\dagger(\boldsymbol{x}',0)\}\rangle, \tag{B.31}$$

$$[G_{j,j'}(x, x'|t)]_{ab} := -i\Theta(t)\langle\{\hat{\Upsilon}_{a,j}(x,t), \hat{\Upsilon}_{b,j'}^\dagger(x',0)\}\rangle, \tag{B.32}$$

$$[G_{S,j'}(\boldsymbol{x}, x'|t)]_{ab} := -i\Theta(t)\langle\{\hat{\Psi}_a(\boldsymbol{x},t), \hat{\Upsilon}_{b,j'}^\dagger(x',0)\}\rangle, \tag{B.33}$$

$$[G_{j,S}(x, \boldsymbol{x}'|t)]_{ab} := -i\Theta(t)\langle\{\hat{\Upsilon}_{a,j}(x,t), \hat{\Psi}_b^\dagger(\boldsymbol{x}',0)\}\rangle. \tag{B.34}$$

$$[z - \mathcal{H}_j(p,\ x)]g_j(x,x') = \delta(\boldsymbol{x} - \boldsymbol{x}'), \tag{B.35}$$

$$(z - \mathcal{H}_n(\boldsymbol{p},\ \boldsymbol{x}))\, m(\boldsymbol{x}, \boldsymbol{x}') = \delta^{(d)}(\boldsymbol{x} - \boldsymbol{x}'). \tag{B.36}$$

$$D_{j,j'} := \delta_{j,j'} - m(\tilde{\boldsymbol{R}}_j, \tilde{\boldsymbol{R}}_{j'})\mathcal{W}^{(j')\dagger}g_{j'}(a,a)\mathcal{W}^{(j')}. \tag{B.37}$$

$$[\hat{G}(x,x')]_{j,j'} := G_{j,j'}(x,x'), \qquad [\hat{g}(x,x')]_{j,j'} = \delta_{j,j'}g_j(x,x'), \qquad \mathcal{M}_{j,j'} = \mathcal{W}^{(j)}m(\tilde{\boldsymbol{R}}_j, \tilde{\boldsymbol{R}}_{j'})\mathcal{W}^{(j')\dagger}.$$

$$\hat{G}(x,x') = \hat{g}(x,x') + \hat{g}(x,a)\mathcal{M}[1 - \hat{g}(a,a)\mathcal{M}]^{-1}\hat{g}(a,x'). \tag{B.38}$$

$$\rho(\omega) = \rho_n^{(0)}(\omega) + \rho_{\text{SC el-d}}^{(0)}(\omega) - \frac{1}{\pi}\text{Im}\frac{\partial}{\partial\omega}\text{tr}\log[D]. \tag{B.39}$$

B.4 Review of Scattering Matrix Methods

Here we will review some typical junctions with superconductors in the scattering matrix approach and the celebrated Beenakker's determinant equation. Such methods are classical ones that provide more understanding of SC junctions and often appear in articles about MTJJ.

BTK Formalism and Basic Contacts

NS Boundary

The "classical" for tunneling problems framework, is the famous method by Blonder, Tinkham and Klapwijk or BTK method [80, 79, 78]. Considers the NS boundary with δ-potential barrier on it. What will be the reflectance amplitudes and how the current will change thought it if the voltage is applied? To get the answer the BTK method tells us: one needs to write BdG equations, then apply a plane wave ansatz and determine amplitudes by the matching conditions (like in basic quantum mechanics). In more details, the method works as follows. First of all, for the spatially varying gap $\Delta(x)$ the one-dimensional BdG equations for the spinor wave function of a superconducting electrons $\psi_k = [u_k(x.t), v_k(x,t)]^T$ looks as follows:

$$\left[-\frac{\hbar^2}{2m} \nabla^2 + V(x) - \mu(x) \right] u_k(x,t) + \Delta(x) v_k(x,t) = i\hbar \frac{\partial u_k(x,t)}{\partial t} \tag{B.40}$$

$$-\left[-\frac{\hbar^2}{2m} \nabla^2 + V(x) - \mu(x) \right] v_k(x,t) + \Delta^*(x) u_k(x,t) = i\hbar \frac{\partial v_k(x,t)}{\partial t}, \tag{B.41}$$

where $V(x)$ is the potential. In general, it can be an arbitrary function that is significant near the boundary, but we will model the strength of the barrier by a delta-potential, so we will consider $V(x) = H\delta(x)$, where H is the parameter for the strength of the barrier[21]. Now, we can consider two particular cases of it. Deep in the superconducting region $\Delta(x), \mu(x)$, and $V(x)$ are constants, and the solutions are time-independent plane waves. Thus we use ansatz $u_k(x,t) \equiv u_k e^{ikx - iE_k t/\hbar}$ and $v_k(x,t) \equiv v_k e^{ikx - iE_k t/\hbar}$ and from BdG equations for $V(x) = 0$, we get the spinor-amplitudes of the wavefunctions for S and N regions with fixed energy. For each energy E_k, there are 4 corresponding k values, $\pm k_{\pm}$, where $\frac{\hbar^2 k_{\pm}^2}{2m} = \mu \pm \sqrt{E_k^2 - |\Delta|^2}$. The obtained amplitudes give us the reason to use the following ansatz:

$$\psi_{\text{inc}}^N = \begin{bmatrix} 1 \\ 0 \end{bmatrix} e^{ik_+ x}, \tag{B.42}$$

$$\psi_{\text{refl}}^N = a \begin{bmatrix} 0 \\ 1 \end{bmatrix} e^{ik_- x} + b \begin{bmatrix} 1 \\ 0 \end{bmatrix} e^{-ik_+ x}, \tag{B.43}$$

$$\psi_{\text{trans}}^S = c \begin{bmatrix} u_0^2 \\ v_0^2 \end{bmatrix} e^{ik_+ x} + d \begin{bmatrix} v_0^2 \\ u_0^2 \end{bmatrix} e^{-ik_- x}, \tag{B.44}$$

where v_0, u_0 are such that $1 - v_0^2 = u_0^2 = \frac{1}{2} \left(1 + \frac{\left(E^2 - \Delta^2\right)^{1/2}}{E} \right)$ and a, b, c, d are some parameters. This ansatz is illustrated in Fig. 27. On the region of normal metal, the

---

[21]Notation of H as a parameter of a barrier, not a Hamiltonian originates from [80].

spectrum is linear and in SC region the spectrum is parabolic and gaped from zero (the main feature of the superconductors is that only above the gap Δ the excitations can exist).
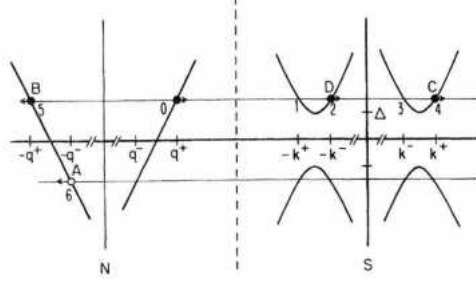

Figure 27: Schematic diagram of energy vs momentum at NS interface. The $\circ$ denote holes, and $\bullet$ - electrons; the arrows point in the direction of movement. (0) - incident electron, $(2,4)$ - transmitted and $(5,6)$ reflected particles. Credit: [80].

The boundary conditions $\psi^N(0) = \psi^S(0) = \psi(0)$ and $\frac{\hbar}{2m}\frac{d\psi^S(0)}{dx} - \frac{\hbar}{2m}\frac{d\psi^N(0)}{dx} = H\psi(0)$ will allow us to get the Andreev reflection $A(E)$ and normal reflection $B(E)$ amplitudes. For example, for $E < \Delta$

$$A(E) = |a(E)|^2 = \frac{\Delta^2}{E^2 + (\Delta^2 - E^2)(1+2Z^2)^2}; \qquad (B.45)$$

$$B(E) = |b(E)|^2 = 1 - A; \qquad (B.46)$$

where $Z := mH/\hbar^2 k_F$ is the dimensionless barrier height. The reflection amplitudes and bound states are closely related to the current as we will discuss below. If the voltage V is applied, the current can be obtained by

$$I_{\text{NS}}(V) \propto \int_{-\infty}^{\infty} [f(E-eV) - f(E)] \left[1 + |a(E)|^2 - |b(E)|^2\right] dE, \qquad (B.47)$$

where $f(E)$ is the Fermi distribution function. Physically, it tells us that Andreev reflection increases, while the normal reflection reduces tunneling current and the number of tunneling electrons is obtained by a Fermi distribution. Totally, for different values of $Z := mH/\hbar^2 k_F$ the behavior of the current, which is obtained by the BTK method, is shown in Fig. 28. This plot has an intuitive explanation: if there is no barrier, the Andreev reflection gives an electron and a hole, thus the current is twice as classical one. When potential is increased, electrons start to give excitation over the SC gap, thus they lose energy and the current diminishes. Then, the strength of the barrier is increased, fewer electrons can tunnel, and with strong Z only excitations with voltage higher than gap can appear. Also, as a very typical in SC and in experimental articles, one can plot the derivative $\frac{dI}{dV}$ versus V and see exactly the position of the gap.

Supercurrent Through a S_1NS_2 Junction

The easiest generalization of SNS junction is the junction between SC with different gaps (S_1NS_2). We will choose $\Delta_2 > \Delta_1$ and review it shortly following [77]. The BdG
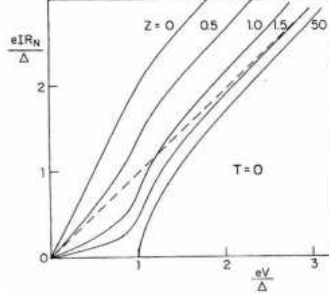
Figure 28: Current vs voltage for various barrier strengths $Z := mH/\hbar^2 k_F$ at $T = 0$. These curves attain their asympototic limits only for very high voltages. For example, the tunnel junction ($Z = 50$) curve will be within 1% of the normal-state curve (dotted line) only when $eV \geq 7\Delta$. Credit: [80].

equations for this case are

$$
\begin{pmatrix} H(x) - \mu & \Delta(x) \\ \Delta^*(x) & -[H^*(x) - \mu] \end{pmatrix} \begin{pmatrix} u(x) \\ v(x) \end{pmatrix} = E \begin{pmatrix} u(x) \\ v(x) \end{pmatrix}, \qquad \Delta(x) = \begin{cases} \Delta_1 e^{i\phi_1}, & x < 0, \\ 0, & 0 < x < L, \\ \Delta_2 e^{i\phi_2}, & x > L; \end{cases}
$$

$$
H(x) := -\frac{\hbar^2}{2m}\frac{d^2}{dx^2}.
$$

The amplitudes $u(x), v(x)$ can be obtained with the usual BTK method by plane waves ansatzes. These will be used in the Josephson current, which can be computed by counting currents from electrons with a certain energy:

$$
J_Q(x) = e \sum_n f_n \cdot \{J_{u_n}(x) + J_{v_n}(x)\} \tag{B.48}
$$

where n numerates states, $f_n := f(E_n) = \frac{1}{1+e^{E_n/k_B T}}$, and the $J_{u_n}(x)$, $J_{v_n}(x)$ are Schrödinger currents carried by the waves $u_n(x)$ and $v_n(x)$: $J_{u_n}(x) = \frac{\hbar}{m} \operatorname{Im}\{u_n^*(x)[\nabla u_n(x)]\}$; $J_{v_n}(x) = \frac{\hbar}{m} \operatorname{Im}\{v_n^*(x)[\nabla v_n(x)]\}$. But what are the allowed energy for this model? Since there are two different gaps Δ_1, Δ_2, there are three regions: below the lowest Δ, between them and higher then highest Δ. Thus the total current is sum of three terms:

$$
I(\phi) = \underbrace{I_1(\phi)}_{|E|<\Delta_1} + \underbrace{I_2(\phi)}_{E_1<|E|<\Delta_2} + \underbrace{I_3(\phi)}_{|E|>\Delta_2}. \tag{B.49}
$$

Here the $\phi =: \phi_2 - \phi_1$ is a phase difference, the most only parameter that we can vary if we constructed the junction. The Andreev levels are obtain from th transmission amplitude, by analyzing its poles. For $E \geq 0$ they are given by

$$
-\arccos\left(\frac{E}{\Delta_1}\right) - \arccos\left(\frac{E}{\Delta_2}\right) + \frac{2LE}{\hbar v_F} \pm \phi = 2\pi n, \tag{B.50}
$$

where L is the length of a contact, n is an integer, $v_F := \sqrt{2\mu/m}$ is the Fermi velocity. This is a generalization of Eq. (1.19).

For a reference we give also a formula for terms of the total currents, each of which can be obtained from Eq. (B.48). The current from purely Andreev levels is:

$$
I_1(\phi) = \sum_n \left\{I_n^+(\phi)f\left(E_n^+(\phi)\right) + I_n^-(\phi)f\left(E_n^-(\phi)\right)\right\}; \qquad I_n^\pm(\phi) = \mp\frac{ev_F}{L+\xi_1\left(E_n^\pm(\phi)\right)+\xi_2\left(E_n^\pm(\phi)\right)}, \tag{B.51}
$$

where $\xi_{1,2}(E) := \xi_{1,2}\frac{\Delta_{1,2}}{\sqrt{\Delta_{1,2}^2 - E^2}}$ and $\xi_{1,2} := \hbar v_F/2\,|\Delta_{1,2}|$. Currents $I_2(\phi)$ and $I_3(\phi)$ are from continuous part of the spectrum, and can be expressed as:

$$I_2(\phi) = \frac{2e}{h}\left(\int_{\Delta_1}^{\Delta_2} - \int_{-\Delta_2}^{-\Delta_1}\right)\left|u_1^2 - v_1^2\right|\left(\frac{1}{D(E,-\phi)} - \frac{1}{D(E,\phi)}\right)f(E)dE; \qquad (B.52)$$

$$I_3(\phi) = \frac{e}{h}\left(\int_{-\infty}^{-\Delta_2} + \int_{\Delta_2}^{\infty}\right)\left(\left|u_1^2 - v_1^2\right| + \left|u_2^2 - v_2^2\right|\right)\left(\frac{1}{D'(E,-\phi)} - \frac{1}{D'(E,\phi)}\right)f(E)dE; \qquad (B.53)$$

where

$$D(E,\phi) := u_1^2 + v_1^2 - 2u_1v_1\cos\left[\frac{|E|}{\Delta_1}\frac{L}{\xi_1} + \phi - \arccos\left(\frac{|E|}{\Delta_2}\right)\right]; \qquad (B.54)$$

$$D'(E,\phi) := u_1^2u_2^2 + v_1^2v_2^2 - 2u_1u_2v_1v_2\cos\left[\frac{|E|}{\Delta_1}\frac{L}{\xi_1} + \phi\right]; \qquad (B.55)$$

and $2u_{1,2}^2 = 1 + \frac{\sqrt{E^2 - \Delta_{1,2}^2}}{E}$; $2v_{1,2}^2 = 1 - \frac{\sqrt{E^2 - \Delta_{1,2}^2}}{E}$ (coherence factors from BCS theory). Formula for I_3 tells us that for a point contact there is no current from purely continuous spectrum at all (term $I_3(L \ll \xi_1, \xi_2) = 0$). These explicit expressions allow us to plug there ϕ and use simple mathematics to obtain the current (since all parameters Δ are fixed, and we have just functions of ϕ). One can see that these formulas are big, which is a typical feature of scattering matrix approaches and the biggest its disadvantage. Generalization
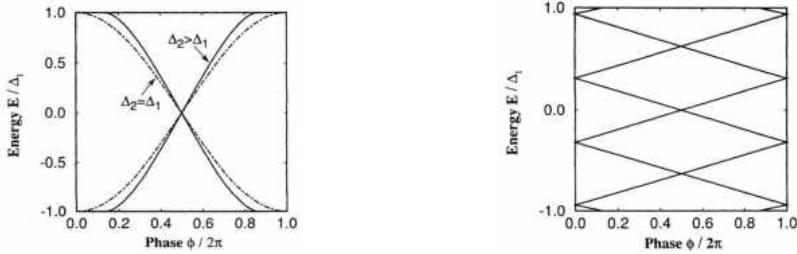

Figure 29: Left: ABS for point-contact junction with $\Delta_2/\Delta_1 = 1.5$ (solid) and $\Delta_2/\Delta_1 = 1.0$ (dashed). Right: ABS for a long SNS contact with $\Delta_2/\Delta_1 = 1.5$. Credit: [77].

to a higher number of channels, terminals is a challenge. For us it is good to see these formulas once, however, some works use this approach and obtain a generalization of these formulas for multiterminal case [32].

Let us finish this example by showing physics. As in SNS case, for a point-contact junction the Andreev levels from Eq. (B.50) is not much changed compared to symmetric contact. They are expressed by

$$E^{\pm} = \pm\frac{\Delta_1\Delta_2\sin(\phi)}{\sqrt{\Delta_1^2 + \Delta_2^2 - 2\Delta_1\Delta_2\cos(\phi)}} \qquad (B.56)$$

and depicted in Fig. 29. We see again the typical Andreev levels. The another typical case, for a long junction is shown on the right of the same figure. In this case, there are much more levels.

Also, formulas (B.51), (B.52) and (B.53) provide an answer on a question: from which regions of energy there is more contribution to the current, from discrete or from continuum? The plot of these exact expressions for a point-contact junction is shown in Fig. 30. At nearly symmetric case there are major contributions from the Andreev levels (I_1), and in very asymmetric from continuous spectra (I_2). Currents for finite temperature can be
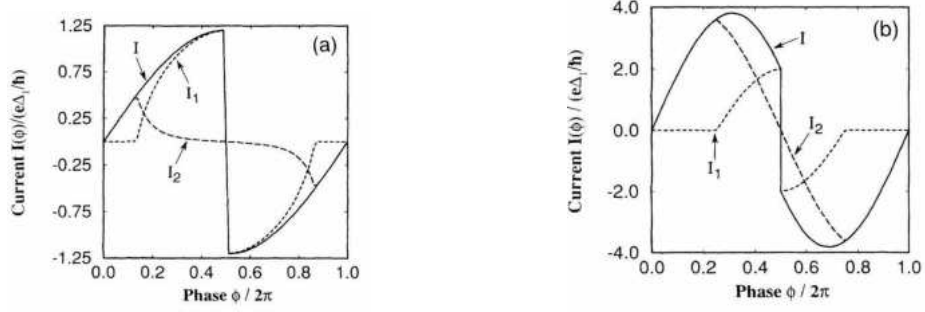

Figure 30: Total supercurrent $I(\phi)$ (solid) through a point-contact junction at $T = 0$ when the asymmetry is (a) $\Delta_2/\Delta_1 = 1.5$ and (b) $\Delta_2/\Delta_1 = 200$. The critical current in (b) is much bigger than in (a), and the CPR is changed. Credit: [77].

obtained with the same formulas. All these total currents are the generalization of the basic Josephson relation $I = I_c \sin \phi$, which for this case has a discontinuity at $\phi = \pi$, since carriers are changed from left-going to right-going.

SNS Junction with Impurity

The simplest multiterminal structure one can imagine is just an SNS contact with something that scatters, and the most basic candidate is a δ-potential. Andreev levels of such model can be obtained from the BdG equations[73]:

$$H(x) := \frac{1}{2m}\left(-i\hbar\frac{d}{dx} - eA(x)\right)^2 + V(x);$$

$$\begin{pmatrix} H(x) - \mu & \Delta(x) \\ \Delta^*(x) & -[H^*(x) - \mu] \end{pmatrix}\begin{pmatrix} u(x) \\ v(x) \end{pmatrix} = E\begin{pmatrix} u(x) \\ v(x) \end{pmatrix}, \qquad V(x) := V_s\delta(x-a), \qquad 0 \le a \le L;$$

$$\Delta(x) := \begin{cases} \Delta e^{i\phi_1}, & x < 0, \\ 0, & 0 < x < L, \\ \Delta e^{i\phi_2}, & x > L. \end{cases}$$

(B.57)

Here we state that that particle is described by the usual quantum mechanical hamiltonian, that there is a δ-potential at distance a from the left boundary inside the SNS junction, and that order parameter is different by phase at the left and at the right boundary. Now the equation for the Andreev levels (1.19) will be modified:

$$2\arccos\left(\frac{E}{\Delta}\right) + \frac{L}{\xi_0}\frac{E}{\Delta} \pm \alpha = 2\pi n, \tag{B.58}$$

where $\xi_0 = \hbar v_F/2\Delta$ and "effective phase" α is such that $\cos(\alpha) = T\cos(\phi) + R\cos\left[\left(\frac{L-2a}{\xi_0}\right)\left(\frac{E}{\Delta}\right)\right]$, $\hbar k_F := \sqrt{2m\mu}$ and μ is the Fermi energy Here the transmission probability $T = 1 - R = \frac{1}{1+(mV_s/\hbar^2 k_F)^2}$ obtained from the well-known

70

quantum mechanical problem of scattering on δ-potential. In the limit $T \to 1$ we recover the Andreev levels for the clean junction, since $\alpha \to \phi$. In the opposite limit of small transmission, where $T \to 0$, α also becomes small and is nearly independent of the actual phase difference ϕ. If the junction is long compared to the healing length ($L > \xi_0$), and if an impurity is present ($T \neq 1$), α also depends on the particle's energy and the impurity position $|L - 2a|$.

The Josephson current can be obtained as in the previous model, but the formulas become even bigger. We have again the contributions from discrete and continuous spectrum. The first one is a generalization of (B.51) and the second it an Eq. (B.53), but with $u_1 = u2$, since the junction is symmetric. Instead of providing large formulas, we will review some physics. For the short junction the Eq. B.58 gives the well-known formula for the Andreev levels

$$E^\pm = \pm\Delta \cos(\alpha/2) = \pm\Delta\sqrt{1 - T\sin^2(\phi/2)}, \tag{B.59}$$

where $\cos(\alpha) = T\cos(\phi) + R$. The δ-potential induces $R \neq 0$ and the gap $E_{\text{gap}} = 2\Delta\sqrt{R}$ appears (see Fig. 31, left). For the current at zero temperature and for short junction we

Figure 31: Left: ABS for a short junction. Right: Josephson current with impurity (solid) and unperturbed junction (dotted) Credit: [73].

also have a simple formula:

$$I(\phi) = \frac{e\Delta}{\hbar}T\sin(\alpha/2)\frac{\sin(\phi)}{\sin(\alpha)}, \tag{B.60}$$

where effective phase α was introduced above and T is a transmission amplitude. We can see on the right of Fig. 31, that current is strongly suppressed from the case of no impurity.

Beenakker's Determinant Equation

Now we will make a very short review of famous and fertile Beenakker's approach [71], which has been used for numerous junctions, including multiterminal ones. For example, analysis of the first observation of Josephson effect in 3- and 4-terminal junctions was done by it [39]. The main idea is that the DOS ρ of the SC junction can be obtained by the determinantal expression

$$\rho(\varepsilon) = -\frac{1}{\pi}\operatorname{Im}\frac{d}{d\varepsilon}\ln\det\left[1 - R_{\text{A}}(\varepsilon + i0^+)S_{\text{N}}(\varepsilon + i0^+)\right] + \rho_0(\varepsilon). \tag{B.61}$$

Here ρ_0 is the ϕ-independent terem, R_{A} is the Andreev reflection matrix, S_{N} is the scattering matrix of the junction in the normal state (see below); $\varepsilon > 0$ is the excitation

energy of Bogoliubov quasiparticles (superpositions of electrons and holes). We assume that both left and right gaps are Δ_0 and phase is $\pm\phi/2$. Because of electron and hole degree of freedom, the scattering matrices have a block structure, where two blocks are uncoupled and related by particle-hole symmetry:

$$S_{\mathrm{N}}(\varepsilon) := \begin{pmatrix} s_0(\varepsilon) & 0 \\ 0 & s_0^*(-\varepsilon) \end{pmatrix}, \tag{B.62}$$

Any normal reflection at the NS interface is taken into account in S_{N}. The Andreev reflection matrix has the block structure

$$R_{\mathrm{A}}(\varepsilon) := i\alpha(\varepsilon) \begin{pmatrix} 0 & r_{\mathrm{A}} \\ r_{\mathrm{A}}^* & 0 \end{pmatrix}, \qquad r_{\mathrm{A}} := \begin{pmatrix} e^{i\phi/2}\sigma_y & 0 \\ 0 & e^{-i\phi/2}\sigma_y \end{pmatrix},$$

$$\alpha(\varepsilon) = e^{-i\arccos(\varepsilon/\Delta_0)} = \varepsilon/\Delta_0 - i\sqrt{1 - \varepsilon^2/\Delta_0^2}. \tag{B.63}$$

The blocks r_{A}^* and r_{A} describe Andreev reflection from, respectively, electron to hole and hole to electron, in opposite spin bands. Another formula for DOS that is obtained from (B.61) by substituting terms is:

$$\rho(\varepsilon) = -\frac{1}{\pi}\operatorname{Im}\frac{d}{d\varepsilon}\ln\det\left[1 - M(\varepsilon + i0^+)\right] + \rho_0(\varepsilon), \qquad M(\varepsilon) := -\alpha(\varepsilon)^2 r_{\mathrm{A}}^* s_0^*(-\varepsilon) r_{\mathrm{A}} s_0(\varepsilon). \tag{B.64}$$

As was shown in Sec. 1.1, the free energy is $F = -k_{\mathrm{B}}T\int_0^\infty d\varepsilon\,\rho(\varepsilon)\ln\left[2\cosh(\varepsilon/2k_{\mathrm{B}}T)\right]$, thus we can express also it in terms of M:

$$F = \frac{i}{4\pi}\int_{-\infty}^{\infty} d\varepsilon\,\tanh(\varepsilon/2k_{\mathrm{B}}T)\ln\det\left[1 - M(\varepsilon + i0^+)\right] + F_0, \tag{B.65}$$

where F_0 the ϕ-independent term. The rest of this method is the calculation of this setup for the analyzed model. There are several famous ways to do it. For example, one can proceed by summing over Matsubara frequencies:

$$F = -k_{\mathrm{B}}T\sum_{p=0}^{\infty}\ln\det\left[1 - M\left(i\omega_p + i\gamma\right)\right], \qquad \omega_p = (2p+1)\pi k_{\mathrm{B}}T. \tag{B.66}$$

More importantly, we see that the bound stated can be obtained by equating the $\det\left[1 - M(\varepsilon + i0^+)\right]$ to zero, since its $(-1)\log[\,]$ will be infinite. This is a famous starting point for calculation of ABS for any junction, ans especially for multiterminal ones. For example, this approach gives ABS for three-terminal JJ by [22, 23]:

$$\frac{E}{\Delta} = \pm\frac{1}{2}\sqrt{1 + \operatorname{Tr}\left(S\mathbf{e}^{i\phi}S^*\mathbf{e}^{-i\phi}\right)}, \tag{B.67}$$

where $\mathbf{e}^{\pm i\phi}$ a diagonal matrix with the phases in each lead and S is the scattering matrix of the inner region. This can be simplified to

$$E = \pm\frac{\Delta}{2}\sqrt{1 + \sum_{l,j} T_{lj}e^{-i(\phi_l - \phi_j)}}, \tag{B.68}$$

where T_{lj} are the transmission probabilities for the quasiparticle that travel from the l'th lead to the j'th terminal and connected to the elements of the S-matrix by $T_{lj} = |s_{lj}|^2$.

A proper review of Beenakker's determinant method and its application can take hundreds of pages, so let us finish with the example. As mentioned above, the current also can be obtained by the determinant formula. For example, for Hamiltonian $H = \begin{pmatrix} -i\sigma_z \hat{v}\partial/\partial x & \Delta \\ \Delta^* & --i\sigma_z \hat{v}\partial/\partial x \end{pmatrix}$ with help of Matsubara Green function one can obtain

$$I = -\frac{e}{\hbar}\frac{\partial}{\partial\varphi}T\sum_{\omega}\ln\det\left[1 - S_N S_A(\omega)\right],$$

where

$$S_N := \begin{pmatrix} S & 0 \\ 0 & -S^* \end{pmatrix}, \qquad S := \begin{pmatrix} r_L & t_{LR} \\ t_{RL} & r_R \end{pmatrix} \qquad S_A = -i\begin{pmatrix} 0 & r_A \\ r_A^* & 0 \end{pmatrix} \qquad r_A := \begin{pmatrix} e^{-\theta_L + i\varphi_L} & 0 \\ 0 & e^{-\theta_R + i\varphi_R} \end{pmatrix}, \quad \theta := \operatorname{arcsinh}\frac{\omega}{\Delta}.$$

Where r_R, r_L, t_{RL}, t_{LR} are blocks that contain reflection and transmission amplitudes respectively. The formulas are big, but they can be simplify to the Eq. 1.25 (see [88]).

B.5 Review of Majorana Fermions

As mentioned in the introduction, Majorana states and the models that contain them are very important concepts in modern condensed matter physics. Since some models of MTJJ were proposed to host Majorana states and our method can be generalized to different Hamiltonians of normal region, we can not but mention some main concepts. This short review will be used in the following section, where we will discuss topological multiterminal junctions and potentially can be a background for further research with our method. We will follow [63].

The most famous model is a models of a SC-SM-SC junction (superconductor-semiconductor-superconductor). The SM and SC Hamiltonians are:

$$H_w := \frac{1}{2}\int dx\Psi^\dagger(x)\mathcal{H}(x)\Psi(x), \qquad \mathcal{H}_w(x) := \left(-\frac{\hbar^2\partial_x^2}{2m^*} - \mu - i\alpha\partial_x\sigma_y\right)\tau_z + V_Z\sigma_x; \tag{B.69}$$

$$H_{\mathrm{SC}} = \int_{-\infty}^{\infty} dx\left(\Delta(x)\psi_\uparrow^\dagger(x)\psi_\downarrow^\dagger(x) + h.c.\right). \tag{B.70}$$

The SM Hamiltonian takes into account the so-called Rashba spinorbit (SO) interaction (term $i\alpha\partial_x\sigma_y$) and the existence of parallel to the nanowire axis magnetic field B (term $V_Z\sigma_x$, where $V_Z = \frac{1}{2}g\mu_B B$ is the usual Zeeman energy with effective g-factor). The usual Nambu notation is assumed (for example, the wave function $\Psi(x) = (\psi_\uparrow^\dagger, \psi_\downarrow^\dagger, \psi_\downarrow, -\psi_\uparrow)$ is a Nambu spinor).

Another model with Majoranas that will be used in our review and for which our method can be applicable is a model of topological superconductors They can be modeled, for example, as a low-energy limit of a Kitaev chain, and its Hamiltonian looks as follows:

$$H_{TS} = \int_0^{\infty} dx\Psi_{TS}^\dagger(x)\left(-iv_F\partial_x\sigma_z + \Delta\sigma_y\right)\Psi_{TS}(x). \tag{B.71}$$

Here the pairing gap Δ is induced by proximity effect and can be considered as real and positive; $\Psi_{TS}(x) = \left(c_r, c_l^\dagger\right)^T$ is the Nambu spinor, it contains right- and left-moving fermion operators $c_{r,l}(x)$. One can see that the difference between the conventional SC is the dispersion relation.

The model (B.69) has a discretized version, which looks as follows [17]:

$$H_{\text{wire}} = \frac{1}{2} \sum_j \left[\Psi_j^\dagger \hat{h} \Psi_j + \left(\Psi_j^\dagger \hat{t} \Psi_{j+1} + \text{h.c.} \right) \right], \qquad \begin{aligned} \hat{h} &:= (2t - \mu)\sigma_z\tau_0 + V_x\sigma_0\tau_x + \Delta\sigma_x\tau_0, \\ \hat{t} &:= -t\sigma_z\tau_0 + i\alpha\sigma_z\tau_z, \\ \Psi_j^T &= \left(c_{j\uparrow}, c_{j\downarrow}, c_{j\downarrow}^\dagger, -c_{j\uparrow}^\dagger \right). \end{aligned}$$

Here $\hat{h}$ is responsible for a on-site energy and the $\hat{t}$ is a hopping matrix. Often the discretized models are analyzed more conveniently, and after one can take a continuous limit (as done in the main part of this thesis).
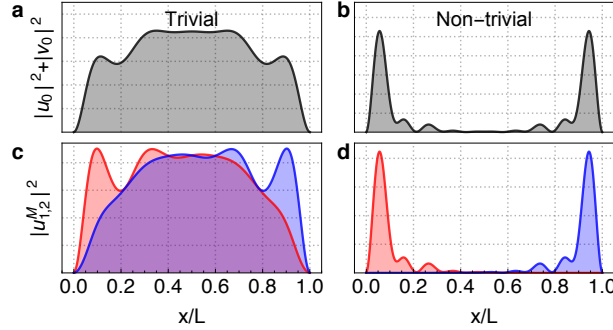

Figure 32: Wavefunction of the lowest energy state ψ_0 in a uniform $L = 1\mu m$ Majorana nanowire for a trivial $V_Z = 0.5V_Z^c$ (a) and a non-trivial $V_Z = 1.4V_Z^c$ (b) cases. (c,d) Wavefunctions of the corresponding Majorana components $u_{1,2}^M(x)$ in the Majorana basis. In the trivial regime the left (red) and right (blue) Majorana components strongly overlap (c), whereas in the topological regime they move apart and concentrate at the ends of the nanowire (d). Credit: [63].

One can find a lot of physics from these Hamiltonians, was was reviewed in the introduction. The excitations of this model can be described by self-conjugation operators (which are known from field theory as Majorana operators) $\gamma_1 := \gamma_1^\dagger$ and $\gamma_2 := \gamma_2^\dagger$. These can be obtained from unitary rotation $\gamma_1 := \psi_0^\dagger + \psi_0$, $\gamma_2 := i(\psi_0^\dagger - \psi_0)$, where the later operators are defined from the wave function in the model as $\psi_n := \int dx \sum_\sigma \left[u_{n\sigma}(x)\psi_\sigma(x) + v_{n\sigma}(x)\psi_\sigma^\dagger(x) \right]$. Here and $u_{n\sigma}(x), v_{n\sigma}(x)$ are the wavefunctions of electron and hole. The "big" value of V_Z is crucial for having the localization of the Majorana modes: if $V_Z > V_Z^c$ then we have a non-trivial topological regime and the wave-functions are localized. If $V_Z < V_Z^c$ then the regime is non-topological and the wave-functions are overlap strongly. This is illustrated in Fig. 32.

The GF approach is very useful for a theoretical description of Majorana wires. The computation of the Green's function of the discrete model is discussed in the [17] and the example of application can be found in [16]. They are given by

$$G(\tau) := -\langle \mathcal{T}_\tau \Psi_{\text{TS}}(\tau)\Psi_{\text{TS}}^\dagger(0) \rangle_0 = T \sum_\omega e^{-i\omega\tau} G_j(\omega); \qquad G(\omega) = \frac{1}{i\omega}\left(\sqrt{\omega^2 + \Delta^2}\,\tau_0 + \Delta\tau_x \right).$$

Here $\Psi_{\text{TS}} = (\psi\ \psi^\dagger)^T$ is a Nambu spinor and $\mathcal{T}_\tau$ is the time-ordering operator. The frequencies ω are the fermionic Matsubara frequencies ($\omega = 2\pi(n+1/2)/\beta$). This function can be used for description of multiterminal junctions with topological superconductors.

A good review of numerous models that host Majoranas is done by Alicea [61] and experimental detection schemes are discussed in [60, 63, 65]. Example of Majorana states in Josephson junction with special properties can be found in [64] and the analysis of the junction during topological phase transition was done by Murthy et al. [24]. Multiterminal junctions with Majorana wires are analyzed in [16, 17].

B.6   Some Derivations

B.6.1   Derivations for the Main Theory

Derivation of dot's Hamiltonian in Nambu formalism

Here we will show that

$$H_D := \sum_{\sigma=\pm}(V + \sigma\Delta_Z)d_\sigma^\dagger d_\sigma, \qquad \Leftrightarrow \qquad H_D = \frac{1}{2}D^\dagger\Big[V\tau_z + \Delta_Z\sigma_z\Big]D + \text{const}; \quad D := \begin{pmatrix} d_+ \\ d_- \\ d_-^\dagger \\ -d_+^\dagger \end{pmatrix}.$$

Let us do it in the opposite direction.

$$H_D = \frac{1}{2}D^\dagger\Big[V\tau_z + \Delta_Z\sigma_z\Big]D =$$

$$= \frac{1}{2}\begin{pmatrix} d_+^\dagger & d_-^\dagger & d_- & -d_+ \end{pmatrix}\begin{pmatrix} \Delta_Z + V & 0 & 0 & 0 \\ 0 & V - \Delta_Z & 0 & 0 \\ 0 & 0 & \Delta_Z - V & 0 \\ 0 & 0 & 0 & -\Delta_Z - V \end{pmatrix}\begin{pmatrix} d_+ \\ d_- \\ d_-^\dagger \\ -d_+^\dagger \end{pmatrix} =$$

$$= \frac{1}{2}\Big((\Delta_Z + V)d_+^\dagger d_+ + (V - \Delta_Z)d_-^\dagger d_- + (\Delta_Z - V)d_- d_-^\dagger + (-\Delta_Z - V)(-d_+)(-d_+^\dagger)\Big) =$$

$$= \frac{1}{2}\Big((\Delta_Z + V)d_+^\dagger d_+ + (V - \Delta_Z)d_-^\dagger d_- + (\Delta_Z - V)(1 - d_- d_-^\dagger) + (-\Delta_Z - V)(1 - d_+ d_+^\dagger)\Big) =$$

$$= (\Delta_Z + V)d_+^\dagger d_+ + (V - \Delta_Z)d_-^\dagger d_- - V.$$

Thus with const=V we got the initial Hamiltonian (2.2).

Derivation of SC's Hamiltonian in Nambu formalism for the discrete model

Here we will show that

$$H_{SC} := \sum_{j=1}^{N}\Bigg(-t_j\sum_{n=1}^{\infty}\sum_{\sigma=\pm}(c_{n,\sigma,j}^\dagger c_{n+1,\sigma,j} + c_{n+1,\sigma,j}^\dagger c_{n,\sigma,j}) + \Delta_j\sum_{n=1}^{\infty}(e^{i\varphi_j}c_{n,+,j}^\dagger c_{n,-,j}^\dagger + \text{h.c.}) -$$

$$-\mu\sum_{\sigma=\pm}\sum_{n=1}^{\infty}c_{n,\sigma,j}^\dagger c_{n,\sigma,j}\Bigg)$$

is equivalent to one in terms of $C_{n,j} := \begin{pmatrix} c_{n,+,j} & c_{n,-,j} & c_{n,-,j}^\dagger & -c_{n,+,j}^\dagger \end{pmatrix}^T$:

$$H_{SC} = \frac{1}{2}\sum_{j=1}^{N}\Bigg(-t_j\sum_{n=1}^{\infty}(C_{n,j}^\dagger\tau_z C_{n+1,j} + C_{n+1,j}^\dagger\tau_z C_{n,j}) + \Delta_j\sum_{n=1}^{\infty}(e^{i\varphi_j}C_{n,j}^\dagger\tau_+ C_{n,j} + \text{h.c.}) -$$

$$-\mu\sum_{n=1}^{\infty}C_{n,j}^\dagger\tau_z C_{n,j}\Bigg) + \text{const}.$$

We will do in the opposite direction and by each part in the sum over j. The first part:

$$\frac{1}{2}(C_{n,j}^\dagger \tau_z C_{n+1,j} + C_{n+1,j}^\dagger \tau_z C_{n,j}) =$$

$$= \frac{1}{2}(c_{n,+,j}^\dagger \; c_{n,-j}^\dagger \; c_{n,-j} \; -c_{n,+j}) \begin{pmatrix} 1 & 0 & 0 & 0 \\ 0 & 1 & 0 & 0 \\ 0 & 0 & -1 & 0 \\ 0 & 0 & 0 & -1 \end{pmatrix} \begin{pmatrix} c_{n+1,+,j} \\ c_{n+1,-j} \\ c_{n+1,-j}^\dagger \\ -c_{n+1,+j}^\dagger \end{pmatrix} + \frac{1}{2}(c_{n+1,+,j}^\dagger \; c_{n+1,-j}^\dagger \; c_{n+1,-j} \; -c_{n+1,+j}) \begin{pmatrix} 1 & 0 & 0 & 0 \\ 0 & 1 & 0 & 0 \\ 0 & 0 & -1 & 0 \\ 0 & 0 & 0 & -1 \end{pmatrix} \begin{pmatrix} c_{n,+,j} \\ c_{n,-j} \\ c_{n,-j}^\dagger \\ -c_{n,+j}^\dagger \end{pmatrix} =$$

$$= \frac{1}{2}\Big(c_{n,+,j}^\dagger c_{n+1,+,j} + c_{n,-j}^\dagger c_{n+1,-j} - c_{n,-j}c_{n+1,-j}^\dagger - (-c_{n,+j})(-c_{n+1,+j}^\dagger) +$$

$$+ c_{n+1,+,j}^\dagger c_{n,+,j} + c_{n+1,-j}^\dagger c_{n,-j} - c_{n+1,-j}c_{n,-j}^\dagger - (-c_{n+1,+j})(-c_{n,+j}^\dagger) \Big) =$$

$$= c_{n+1,+,j}^\dagger c_{n,+,j} + c_{n+1,-j}^\dagger c_{n,-j} - c_{n+1,-j}c_{n,-j}^\dagger - c_{n+1,+j}c_{n,+j}^\dagger.$$

This the exactly the term we needed. All was easy, since all operators in each term commute (the key transformation is the anticommutation relation). Now, the second part:

$$\frac{1}{2}(e^{i\varphi_j} C_{n,j}^\dagger \tau_+ C_{n,j} + \text{h.c.}) =$$

$$= \frac{1}{2}e^{i\varphi_j}(c_{n,+,j}^\dagger \; c_{n,-j}^\dagger \; c_{n,-j} \; -c_{n,+j}) \begin{pmatrix} 0 & 0 & 1 & 0 \\ 0 & 0 & 0 & 1 \\ 0 & 0 & 0 & 0 \\ 0 & 0 & 0 & 0 \end{pmatrix} \begin{pmatrix} c_{n,+,j} \\ c_{n,-j} \\ c_{n,-j}^\dagger \\ -c_{n,+j}^\dagger \end{pmatrix} + \frac{1}{2}e^{-i\varphi_j}(c_{n,+,j}^\dagger \; c_{n,-j}^\dagger \; c_{n,-j} \; -c_{n,+j}) \begin{pmatrix} 0 & 0 & 0 & 0 \\ 0 & 0 & 0 & 0 \\ 1 & 0 & 0 & 0 \\ 0 & 1 & 0 & 0 \end{pmatrix} \begin{pmatrix} c_{n,+,j} \\ c_{n,-j} \\ c_{n,-j}^\dagger \\ -c_{n,+j}^\dagger \end{pmatrix} =$$

$$= \frac{1}{2}e^{i\varphi_j}\Big(c_{n,+,j}^\dagger c_{n,-j}^\dagger + c_{n,-j}^\dagger(-c_{n,+j}^\dagger) \Big) + \frac{1}{2}e^{-i\varphi_j}\Big(c_{n,-j}c_{n,+,j} + (-c_{n,+j})c_{n,-j} \Big) =$$

$$= \frac{1}{2}e^{i\varphi_j}\Big(c_{n,+,j}^\dagger c_{n,-j}^\dagger + c_{n,+,j}^\dagger c_{n,-j}^\dagger \Big) + \frac{1}{2}e^{-i\varphi_j}\Big(c_{n,-j}c_{n,+,j} + c_{n,-j}c_{n,+,j} \Big) =$$

$$= e^{i\varphi_j} c_{n,+,j}^\dagger c_{n,-j}^\dagger + e^{-i\varphi_j} c_{n,-j}c_{n,+,j}.$$

Another, slightly simpler way is to obtain only the first term and then to take h.c. of it to get the second term. Also, note that this is the place where we wee exactly, why there is a minus sign in the last component of the Nambu spinor, it generates the essential minus to obtain the required term. Finally, the last term:

$$\frac{1}{2}C_{n,j}^\dagger \tau_z C_{n,j} = \frac{1}{2}\big(c_{n,+,j}^\dagger \; c_{n,-j}^\dagger \; c_{n,-j} \; -c_{n,+j}\big) \begin{pmatrix} 1 & 0 & 0 & 0 \\ 0 & 1 & 0 & 0 \\ 0 & 0 & -1 & 0 \\ 0 & 0 & 0 & -1 \end{pmatrix} \begin{pmatrix} c_{n,+,j} \\ c_{n,-j} \\ c_{n,-j}^\dagger \\ -c_{n,+j}^\dagger \end{pmatrix} =$$

$$= \frac{1}{2}\big(c_{n,+,j}^\dagger c_{n,+,j} + c_{n,-j}^\dagger c_{n,-j} - c_{n,-j}c_{n,-j}^\dagger - (-c_{n,+j})(-c_{n,+j}^\dagger)\big) =$$

$$= \frac{1}{2}\big(c_{n,+,j}^\dagger c_{n,+,j} - c_{n,+j}c_{n,+j}^\dagger + c_{n,-j}^\dagger c_{n,-j} - c_{n,-j}c_{n,-j}^\dagger\big) =$$

$$= \frac{1}{2}\big(c_{n,+,j}^\dagger c_{n,+,j} - (-c_{n,+j}^\dagger c_{n,+j} + 1) + c_{n,-j}^\dagger c_{n,-j} - (-c_{n,-j}^\dagger c_{n,-j} + 1)\big) =$$

$$= c_{n,+,j}^\dagger c_{n,+,j} + c_{n,-j}^\dagger c_{n,-j} - 1.$$

And this is the term in the initial Hamiltonian (2.8) (as usual, we neglect the constant term). Thus all terms coincide and the Hamiltonians are equivalent.

Derivation of tunneling Hamiltonian in Nambu formalism for the discrete model

Here we will prove that

$$H_T := -\sum_{j=1}^{N} t'_j \sum_{\sigma=\pm} (c^\dagger_{1,\sigma,j} d_\sigma + d^\dagger_\sigma c_{1,\sigma,j}). \qquad \Leftrightarrow \qquad H_T = -\frac{1}{2}\sum_{j=1}^{N} t'_j \sum_{\sigma=\pm} (C^\dagger_{1,j}\tau_z D + D^\dagger \tau_z C_{1,j}).$$

We do it again from the opposite direction:

$$H_T = -\tfrac{1}{2}(c^\dagger_{1,+j}\ c^\dagger_{1,-j}\ c_{1,-j}\ -c_{1,+j})\begin{pmatrix}1 & 0 & 0 & 0\\ 0 & 1 & 0 & 0\\ 0 & 0 & -1 & 0\\ 0 & 0 & 0 & -1\end{pmatrix}\begin{pmatrix}d_+\\ d_-\\ d^\dagger_-\\ -d^\dagger_+\end{pmatrix} - \tfrac{1}{2}(d^\dagger_+\ d^\dagger_-\ d_-\ -d_+)\begin{pmatrix}1 & 0 & 0 & 0\\ 0 & 1 & 0 & 0\\ 0 & 0 & -1 & 0\\ 0 & 0 & 0 & -1\end{pmatrix}\begin{pmatrix}c_{1,+j}\\ c_{1,-j}\\ c^\dagger_{1,-j}\\ -c^\dagger_{1,+j}\end{pmatrix} =$$

$$= -\frac{1}{2}\left(c^\dagger_{1,+,j}d_+ + c^\dagger_{1,-j}d_- - c_{1,-j}d^\dagger_- - c_{1,+j}d^\dagger_+ + d^\dagger_+ c_{1,+,j} + d^\dagger_- c_{1,-j} - d_- c^\dagger_{1,-j} - d_+ c^\dagger_{1,+j}\right) =$$

$$= -\frac{1}{2}\left(c^\dagger_{1,+,j}d_+ + c^\dagger_{1,-j}d_- - c_{1,-j}d^\dagger_- - c_{1,+j}d^\dagger_+\right).$$

This is the term in non-Nambu formalism (2.15).

Derivation of the Heisenberg equations for the discrete model

Here we will derive the Heisenberg equations for the Nambu fields $C_{n,j}$ and D.

We will use $i\frac{d}{dt}C_{n,ja}(t) = [C_{n,ja}(t), H_{\text{tot}}]$ and we will change the names of inner indices $j \to p, n \to k, n' \to l$, we compute:

$$[C_{nja}, H_D] = \frac{1}{2}\left(C_{nja}D^\dagger_b h^{bc}_D D_c - D^\dagger_b h^{bc}_D D_c C_{nja} = C_{nja}D^\dagger_b h^{bc}_D D_c - (-1)^2 D^\dagger_b h^{bc}_D D_c C_{nja}\right) = 0;$$

$$[C_{n,ja}, H_{SC}] = \frac{1}{2}\left[C_{n,ja}\sum_{p,k,l} C^\dagger_{k,pb}\ [h^{k,l}_{SC,p}]^{bc}\ C_{l,pc} - \sum_{p,k,l} C^\dagger_{k,pb}\ [h^{k,l}_{SC,p}]^{bc}\ C_{l,pc}C_{n,ja}\right] =$$

$$= \tfrac{1}{2}\left[\sum_{p,k,l}(-C^\dagger_{k,pb}C_{n,ja} + \delta_{kn}\delta_{pj}\delta_{ab})\ [h^{k,l}_{SC,p}]^{bc}\ C_{l,pc} - \sum_{p,k,l} \underbrace{C^\dagger_{k,pb}\ [h^{k,l}_{SC,p}]^{bc}}_{=C_{k,pr}P_{rb}}\ (P_{ac}\delta_{jp}\delta_{nl} - C_{n,ja}C_{l,pc})\right] =$$

$$= \tfrac{1}{2}\left[-\sum_{p,k,l} C^\dagger_{k,pb}C_{n,ja}\ [h^{k,l}_{SC,p}]^{bc}\ C_{l,pc} + \sum_l [h^{n,l}_{SC,j}]^{ac}\ C_{l,jc} - \sum_k C_{k,jr}\ \underbrace{P_{rb}\ [h^{k,n}_{SC,j}]^{bc}\ P_{ac}}_{=-[h^{k,n}_{SC,j}]^{ra*}=-[h^{k,n}_{SC,j}]^{ar}} + \sum_{p,k,l} C^\dagger_{k,pb}\ [h^{k,l}_{SC,p}]^{bc}\ C_{n,ja}C_{l,pc}\right] =$$

$$= \sum_l [h^{n,l}_{SC,j}]^{ac}\ C_{l,jc} = \left[\sum_l [h^{n,l}_{SC,j}]\ C_{l,j}\right]_a.$$

Let us remind, that here each $h^{k,l}_{SC,p}$ operator is a matrix of 4×4 dimensions, so two extra indices mean taking the row's and column's element. At the last step of the transformation we notice that the first and the fourth terms are the same but with different sign.

$$[C_{n,ja}, H_T] = -\tfrac{1}{2}\Big[C_{n,ja}\sum_{p=1}t'_p C^\dagger_{1,pb}\tau_z^{bc}D_c + C_{n,ja}\sum_{p=1}t'_p D^\dagger_b\tau_z^{bc}C_{1,pc} - \sum_{p=1}t'_p C^\dagger_{1,pb}\tau_z^{bc}D_c C_{n,ja} - \sum_{p=1}t'_p D^\dagger_b\tau_z^{bc}C_{1,pc}C_{n,ja}\Big] =$$

$$= -\frac{1}{2}\Big[\sum_{p=1}t'_p(-C^\dagger_{1,pb}C_{n,ja} + \delta_{n,1}\delta_{pj}\delta_{ab})\tau_z^{bc}D_c + \sum_{p=1}t'_p(-D^\dagger_b C_{n,ja})\tau_z^{bc}C_{1,pc}-$$

$$-\sum_{p=1}t'_p C^\dagger_{1,pb}\tau_z^{bc}\underbrace{D_c C_{n,ja}}_{=-C_{n,ja}D_c} - \sum_{p=1}t'_p\underbrace{D^\dagger_b}_{=D_d P_{db}}\tau_z^{bc}C_{1,pc}C_{n,ja}\Big] =$$

$$= -\frac{1}{2}\Big[t'_j\delta_{n,1}\tau_z^{ac}D_c - \sum_{p=1}t'_p D_d\underbrace{P_{db}\tau_z^{bc}P_{ca}}_{-\tau_z^{da}}\delta_{n1}\delta_{pj}\Big] =$$

$$=[-\delta_{n,1}\ t'_j\ \tau_z\ D]_a.$$

After restoring t-dependence and summing terms, we have

$$i\frac{d}{dt}C_{nj}(t) = \sum_l h_{SC,j}^{n,l}\ C_{l,j}(t) - \delta_{n,1}\ t'_j\ \tau_z\ D(t).$$

And this is the (2.18). The Eq. (2.19) is derived by exactly the same approach.

Derivation of the Dyson equation for Green's functions for the discrete model

The Dyson equation for $[G_{0,0}^{0,0}(t)]_{a,b} := -i\Theta(t)\langle\{D_a(t),\ D_b^\dagger(0)\}\rangle$ is derived as follows. We evaluate:

$$i\frac{d}{dt}[G_{0,0}^{0,0}(t)]_{a,b} = \underbrace{\delta(t)\langle\{D_a(t),\ D_b^\dagger(0)\}\rangle}_{=\delta(t)\langle\{D_a(0),\ D_b^\dagger(0)\}\rangle=\delta_{ab}\delta(t)} - i\Theta(t)\langle\{i\frac{dD_a(t)}{dt},\ D_b^\dagger(0)\}\rangle$$

$$= \delta(t)\delta_{ab} - i\Theta(t)\langle\{h_D^{ac}D_c(t),\ D_b^\dagger(0)\}\rangle - i\Theta(t)\langle\{\sum_{j=1}(-1)t'_j\tau_z^{ac}C_{1,jc}(t),\ D_b^\dagger(0)\}\rangle =$$

$$= \delta(t)\delta_{ab} - i\Theta(t)h_D^{ac}\underbrace{\langle\{D_c(t),\ D_b^\dagger(0)\}\rangle}_{=[G_{0,0}^{0,0}(t)]_{a,b}} - \sum_{j=1}t'_j\tau_z^{ac}\underbrace{(-i)\Theta(t)\langle\{C_{1,jc}(t),\ D_b^\dagger(0)\}\rangle}_{=[G_{1,0}^{j,0}(t)]_{cb}}.$$

Thus, in the matrix form we will get

$$\left(i\frac{d}{dt} - h_D\right)G_{0,0}^{0,0}(t) + \sum_{j=1}t'_j\tau_z G_{1,0}^{j,0}(t) = \delta(t)$$

Now, to use transformation $F[f](z) := \int_0^\infty dt e^{izt}f(t)$, the formulas below are used:

$$F[i\frac{d}{dt}[G_{0,0}^{0,0}(t)]_{a,b}](z) = \int_0^\infty dt e^{izt}i\frac{d}{dt}[G_{0,0}^{0,0}(t)]_{a,b} =$$

$$= ie^{izt}[G_{0,0}^{0,0}(t)]_{a,b}|_0^\infty - i\cdot iz\int_0^\infty dt e^{izt}[G_{0,0}^{0,0}(t)]_{a,b} = z[G_{0,0}^{0,0}(z)]_{a,b},$$

$$F[h_D[G_{0,0}^{0,0}(t)]_{a,b}](z) = h_D[G_{0,0}^{0,0}(z)]_{a,b},$$

$$F[\sum_{j=1}t'_j\tau_z[G_{1,0}^{j,0}(t)]_{ab}](z) = \sum_{j=1}t'_j\tau_z[G_{1,0}^{j,0}(z)]_{ab}.$$

$$F[\delta(t)](z) = 1,$$

and we will have:

$$[z - h_D]G_{0,0}^{0,0}(\omega) + \sum_{j=1}^{N} t'_j \tau_z G_{1,0}^{j,0}(\omega) = 1,$$

Now, we will derive the Dyson eq. for $[G_{n,n'}^{j,j'}(t)]_{a,b} := -i\Theta(t)\langle\{C_{n,j,a}(t),\ C_{n',j',b}^{\dagger}(0)\}\rangle$, we evaluate:

$$i\frac{d}{dt}[G_{n,n'}^{j,j'}(t)]_{a,b} = \delta(t)\underbrace{\langle\{C_{n,j,a}(t),\ C_{n',j',b}^{\dagger}(0)\}\rangle}_{=\delta_{nn'}\delta_{jj'}\delta_{ab}} - i\Theta(t)\langle\{i\frac{dC_{n,j,a}(t)}{dt},\ C_{n',j',b}^{\dagger}(0)\}\rangle =$$

$$= \delta(t)\delta_{nn'}\delta_{jj'}\delta_{ab} + \sum_l(-i\Theta(t))\langle\{[h_{SC,j}^{n,l}]^{ad}C_{l,jd}(t), C_{n',j',b}^{\dagger}(0)\}\rangle - (-i\Theta(t))\langle\{\delta_{n,1}t'_j\tau_z^{ad}D_d(t), C_{n',j',b}^{\dagger}(0)\}\rangle =$$

$$= \delta(t)\delta_{nn'}\delta_{jj'}\delta_{ab} + \sum_l[h_{SC,j}^{n,l}]^{ad}\underbrace{(-i\Theta(t))\langle\{C_{l,jd}(t),C_{n',j',b}^{\dagger}(0)\}\rangle}_{=[G_{l,n'}^{j,j'}]_{db}} - \delta_{n,1}t'_j\tau_z^{ad}\underbrace{(-i\Theta(t))\langle\{D_d(t), C_{n',j',b}^{\dagger}(0)\}\rangle}_{=[G_{0,n'}^{0,j'}]_{db}}.$$

Also, $i\frac{d}{dt}[G_{n,n'}^{j,j'}(t)]_{a,b} \equiv \sum_l i\frac{d}{dt}[G_{l,n'}^{j,j'}(t)]_{a,b}\delta_{l,n}$, thus in matrix notation we will have:

$$\sum_l i\frac{d}{dt}G_{l,n'}^{j,j'}(t)\delta_{l,n} = \delta(t)\delta_{nn'}\delta_{jj'}\delta_{ab} + \sum_l h_{SC,j}^{n,l}\ G_{l,n'}^{j,j'} - \delta_{n,1}t'_j\tau_z G_{0,n'}^{0,j'} \tag{B.72}$$

$$\sum_l\left[i\delta_{l,n}\frac{d}{dt} - h_{SC,j}^{n,l}\right]G_{l,n'}^{j,j'} + \delta_{n,1}t'_j\tau_z G_{0,n'}^{0,j'} = \delta(t)\delta_{nn'}\delta_{jj'}. \tag{B.73}$$

The Fourier transform is done exactly as for the example above.

The other two Dyson equations (2.24) can be derived the same way.

Assumed formulas for the main derivation of bare Green's function $g_{1,1}^j$ for the discrete model

In quantum mechanics, we can set any set of basis vectors. For the case of a boundary the following set of functions is sufficient

$$\psi_k(n) = \sqrt{\frac{2}{\pi}}\sin(kn), \quad k \in [0,\pi], \quad n \in \mathbb{N}. \tag{B.74}$$

These satisfy

$$\sum_{n=1}^{\infty}\psi_k(n)\psi_{k'}^{\dagger}(n) = \delta(k-k'), \qquad \int_0^{\pi}dk\psi_k^{\dagger}(n)\psi_k(n') = \delta_{n,n'}. \tag{B.75}$$

These are the completeness and the orthogonality relations. After acting with the Hamiltonian $h_{SC,j}^{n,n'} := -\tau_z(t_j\delta_{n',n+1} + t_j\delta_{n',n-1} + \mu\delta_{n',n}) + (\Delta_j e^{i\varphi_j}\tau_+ + \Delta_j e^{-i\varphi_j}\tau_-)\delta_{n',n}$ on these

vectors, with help of $\sin x + \sin y = 2\sin\frac{x+y}{2}\cos\frac{x-y}{2}$ one has:

$$\sum_{n'=1}^{\infty} h_{SC,j}^{n,n'}\psi_k(n') = \sqrt{\frac{2}{\pi}}\sum_{n'=1}^{\infty}\Big[-\tau_z(t_j\delta_{n',n+1} + t_j\delta_{n',n-1} + \mu\delta_{n',n})\sin(kn') +$$

$$+ (\Delta_j e^{i\varphi_j}\tau_+ + \Delta_j e^{-i\varphi_j}\tau_-)\delta_{n',n}\sin(kn')\Big] =$$

$$= \sqrt{\frac{2}{\pi}}\Big[-\tau_z t_j(\sin(k(n+1)) + \sin(k(n-1))) + \mu\sin(kn) + (\Delta_j e^{i\varphi_j}\tau_+ + \Delta_j e^{-i\varphi_j}\tau_-)\sin(kn)\Big] =$$

$$= \sqrt{\frac{2}{\pi}}\Big[-\tau_z t_j\cdot 2\sin(kn)\cos(k) + \mu\sin(kn) + (\Delta_j e^{i\varphi_j}\tau_+ + \Delta_j e^{-i\varphi_j}\tau_-)\sin(kn)\Big] =$$

$$= h_k^j\psi_k(n), \qquad h_k^j := -\tau_z(2t_j\cos(k) + \mu) + (\Delta_j e^{i\varphi_j}\tau_+ + \Delta_j e^{-i\varphi_j}\tau_-).$$

Now, we obtain the expression of the Green's function, that is defined as a solution of

$$zG_{n,n'} - \sum_{n=1}^{\infty} h_{n-n''}G_{n'',n'} = \delta_{n,n'}. \tag{B.76}$$

If we decompose as

$$G_{n,n'} = \int_0^{\pi} dk\,\psi_k(n)G_k(n'), \tag{B.77}$$

we will have

$$zG_k(n') - h_k^j G_k(n') = \psi_k(n'), \tag{B.78}$$

$$G_k(n') = \frac{\psi_k(n')}{z - h_k^j}, \tag{B.79}$$

hence

$$G_{n,n'} = \int_0^{\pi} dk\,\frac{\psi_k(n)\psi_k(n')}{z - h_k^j}. \tag{B.80}$$

This is called Lehmann's representation. This is how the (2.37) was obtained.

Derivation of $G_{n,0}^{j,0}(\omega)$ in terms of $-g_{n,1}^j(\omega)$

We define $g_{n'',n'}^j(\omega)$ as a solution of

$$\sum_{n''}[z\delta_{n,n''} - h_{SC,j}^{n,n''}]g_{n'',n'}^j(\omega) = \delta_{n,n'}. \tag{B.81}$$

To work with the it we need to understand this equation well. Here only n, n' are external indices, we can treat them as a matrix indices and imagine l.h.s. as a product of a matrix $[z - h_{SC,j}]$ and a vector-column $g^j(\omega)$, and the r.h.s. as the identity matrix. Thus, in this notation, $g^j(\omega) = [z - h_{SC,j}]^{-1}$ and has a type of a matrix (or in index notation $[g^j(\omega)]_{n,n''} = g_{n,n''}^j(\omega) = [[z - h_{SC,j}]^{-1}]_{n,n'}$). Another important feature of $g_{n'',n'}^j(\omega)$ is that

it doesn't have same number of indices as $G_{n'',n'}^{j,j'}(\omega)$. This is because it describes only two pints (n and n') in j-th SC lead. Now, the Eq. (2.32) can be transformed as

$$\sum_{n''}[z\delta_{n,n''} - h_{SC,j}^{n,n''}]G_{n'',0}^{j,0}(\omega) = -\delta_{n,1}t'_j\tau_z G_{0,0}^{0,0}(\omega), \tag{B.82}$$

$$\sum_n g_{n',n}^j(\omega) \cdot \sum_{n''}\left[z\delta_{n,n''} - h_{SC,j}^{n,n''}\right]G_{n'',0}^{j,0}(\omega) = -\sum_n g_{n',n}^j(\omega)\,\delta_{n,1}\,t'_j\,\tau_z G_{0,0}^{0,0}(\omega) \tag{B.83}$$

$$\sum_{n''}\sum_n\left[z\delta_{n,n''} - h_{SC,j}^{n,n''}\right]g_{n',n}^j(\omega)G_{n'',0}^{j,0}(\omega) = -\sum_n g_{n',n}^j(\omega)\cdot\,\delta_{n,1}\,t'_j\,\tau_z G_{0,0}^{0,0}(\omega) \tag{B.84}$$

$$\sum_{n''}\delta_{n',n''}G_{n'',0}^{j,0}(\omega) = -\sum_n g_{n',n}^j(\omega)\,\delta_{n,1}\,t'_j\,\tau_z G_{0,0}^{0,0}(\omega) \tag{B.85}$$

$$G_{n',0}^{j,0}(\omega) = -g_{n',1}^j(\omega)t'_j\tau_z G_{0,0}^{0,0}(\omega) \tag{B.86}$$

$$G_{n,0}^{j,0}(\omega) = -g_{n,1}^j(\omega)t'_j\tau_z G_{0,0}^{0,0}(\omega), \quad j \neq 0. \tag{B.87}$$

At the second line we multiplied the whole sum (with fixed n) by $g_{n',n}^j(\omega)$ (with some unknown fixed n') and then summed all possible l.h.s. and r.h.s. over all n. Thus the (2.34) is proven.

Derivation of the bare Green's function $g_{1,1}^j$ for the discrete model

The BGF approach proposes the calculation of the GF by the following formula

$$G_{1,1} = G_0^{(0)} - G_1^{(0)}[G_0^{(0)}]^{-1}G_{-1}^{(0)} \tag{B.88}$$

where the translationally invariant SC GF is

$$G_{n-n'}^{(0)}(z) := \int_{-\pi}^{\pi}\frac{dk}{2\pi}\frac{e^{ik(n-n')}}{z - (-2t\cos k - \mu)\tau_z - \Delta_j\left[e^{i\varphi_j}\tau_+ + e^{-i\varphi_j}\tau_-\right]}. \tag{B.89}$$

Here compared to main theory we have a basis of plane waves $|\psi\rangle = \frac{e^{ikn}}{\sqrt{2\pi}}$. For only this calculation we will introduce $\bar{\boldsymbol{\Delta}} := \Delta_j\left[e^{i\varphi_j}\tau_+ + e^{-i\varphi_j}\tau_-\right]$ to make formulas shorter. Considering this integral in the wide-band limit $t \gg \Delta_j$, we approximate it by linearizing near the Fermi points $\mu = 0$, $k = \pm\frac{\pi}{2}$:

$$G_{n-n'}^{(0)}(z) \approx e^{i\frac{\pi}{2}(n-n')}\int_{-\infty}^{\infty}\frac{dq}{2\pi}\frac{e^{iq(n-n')}}{z - 2tq\tau_z - \bar{\boldsymbol{\Delta}}} + e^{-i\frac{\pi}{2}(n-n')}\int_{-\infty}^{\infty}\frac{dq}{2\pi}\frac{e^{iq(n-n')}}{z + 2tq\tau_z - \bar{\boldsymbol{\Delta}}}. \tag{B.90}$$

We are interested in

$$G_0^{(0)}(z) \approx \frac{1}{t}\int_{-\infty}^{\infty}\frac{d\bar{q}}{2\pi}\frac{z + \bar{\boldsymbol{\Delta}}}{z^2 - \bar{q}^2 - \Delta_j^2} = -\frac{1}{t}\int_{-\infty}^{\infty}\frac{d\bar{q}}{2\pi}\frac{z + \bar{\boldsymbol{\Delta}}}{(\bar{q} - k_+)(\bar{q} - k_-)}; \qquad k_\pm(z) := \pm z\sqrt{1 - \frac{\Delta_0^2}{z^2}}. \tag{B.91}$$

The inversion is done the same way like in the main derivation. Closing the integration contour in the upper half-plane, we obtain

$$G_0^{(0)}(z) \approx -\frac{i}{2t}\frac{z + \bar{\boldsymbol{\Delta}}}{k_+} = -\frac{i}{2t}\frac{1 + \frac{\bar{\boldsymbol{\Delta}}}{z}}{\sqrt{1 - \frac{\Delta_j^2}{z^2}}}; \qquad [G_0^{(0)}(z)]^{-1} = 2ti\frac{1 - \frac{\bar{\boldsymbol{\Delta}}}{z}}{\sqrt{1 - \frac{\Delta_j^2}{z^2}}}. \tag{B.92}$$

Analogously,

$$G_1^{(0)}(z) \approx \frac{i\tau_z}{t} \int_{-\infty}^{\infty} \frac{d\bar{q}}{2\pi} \frac{\bar{q} e^{i\frac{\bar{q}}{2t}}}{z^2 - \bar{q}^2 - \Delta_j^2} = -\frac{i\tau_z}{t} \int_{-\infty}^{\infty} \frac{d\bar{q}}{2\pi} \frac{\bar{q} e^{i\frac{\bar{q}}{2t}}}{(\bar{q} - k_+)(\bar{q} - k_-)} \approx \frac{\tau_z}{2t}; \qquad \text{(B.93)}$$

$$G_{-1}^{(0)}(z) \approx -\frac{i\tau_z}{t} \int_{-\infty}^{\infty} \frac{d\bar{q}}{2\pi} \frac{\bar{q} e^{-i\frac{\bar{q}}{2t}}}{z^2 - \bar{q}^2 - \Delta_j^2} = G_1^{(0)}(z), \qquad \text{(B.94)}$$

where the last equality is obtained by re-defining the integration variable $\bar{q} \to -\bar{q}$. Collecting together all the contribution, we have

$$G_{1,1} = -\frac{i}{2t} \frac{1 + \frac{\bar{\Delta}}{z}}{\sqrt{1 - \frac{\Delta_j^2}{z^2}}} - \frac{\tau_z}{2t} 2ti \frac{1 - \frac{\bar{\Delta}}{z}}{\sqrt{1 - \frac{\Delta_j^2}{z^2}}} \frac{\tau_z}{2t} = -\frac{i}{t} \frac{1 + \frac{1}{z}\Delta_j \left[e^{i\varphi_j}\tau_+ + e^{-i\varphi_j}\tau_-\right]}{\sqrt{1 - \frac{\Delta_j^2}{z^2}}}. \qquad \text{(B.95)}$$

And this is the same result (2.41).

Derivation of the equation of ABS

Here we will derive the DOS for the QD model (2.43). The density of states $\rho(\omega) = \int \delta(\omega - E_s)$ can be obtained by the fundamental relation (1.30), which for our discrete model looks like:

$$\rho(\omega) = -\frac{1}{\pi} \sum_{\forall m} \text{Im} \ \text{tr} \ \widehat{G}_{m,m}(\omega + i\eta). \qquad \text{(B.96)}$$

Here the trace is taken over the spin and particle-hole indices, and $\widehat{G}_{m,m'}(\omega + i\eta)$ is the full retarded ($z = \omega + i\eta$) Green's function of the system. In another words, in this notation we consider m and m' as all allowed points in our "sun-junction" 10, so

$$\rho(\omega) = -\frac{1}{\pi} \text{Im} \ \text{tr} G_{0,0}^{0,0}(\omega + i\eta) - \frac{1}{\pi} \sum_{j=1}^{N} \sum_{n=1}^{\infty} \text{Im} \ \text{tr} G_{n,n}^{j,j}(\omega + i\eta). \qquad \text{(B.97)}$$

To calculate it, we continue to exploit the Dyson equations (2.29), (2.30),(2.31) and (2.32). From them we have

$$G_{n,n'}^{j,j'}(\omega) = g_{n,n'}^{j}(\omega)\delta_{j,j'} - t_j' g_{n,1}^{j}(\omega)\tau_z G_{0,n'}^{0,j'}(\omega), \qquad \text{(B.98)}$$

$$G_{0,n'}^{0,j'}(\omega) = -g_D(\omega) \sum_{j''=1}^{N} t_{j''}' \tau_z G_{1,n'}^{j'',j'}(\omega), \qquad \text{(B.99)}$$

where the dot's GF is defined as a solution of

$$[z - h_D]g_D(\omega) = 1. \qquad \text{(B.100)}$$

Derivation of (B.98) is easily done by looking at l.h.s. of (2.30) as on matrix equation and by inverting matrices. Together these equations give

$$G_{n,n'}^{j,j'}(\omega) = g_{n,n'}^{j}(\omega)\delta_{j,j'} + \sum_{j''=1}^{N} t_j' t_{j''}' g_{n,1}^{j}(\omega)\tau_z g_D(\omega)\tau_z G_{1,n'}^{j'',j'}(\omega). \qquad \text{(B.101)}$$

83

From this, we find by setting $n = 1$ that

$$G_{1,n'}^{j,j'}(\omega) = g_{1,n'}^j(\omega)\delta_{j,j'} + \sum_{j''=1}^{N} g_{1,1}^j(\omega) \cdot t_j' t_{j''}' \tau_z g_D(\omega) \tau_z \cdot G_{1,n'}^{j'',j'}(\omega). \tag{B.102}$$

Now, we switch to the fully matrix notation. We define the block matrices

$$\hat{g}_{j,j'}(n, n') := g_{n,n'}^j(\omega)\delta_{j,j'}, \qquad \hat{t}_{j,j''} := t_j' t_{j''}' \tau_z g_D(\omega) \tau_z, \qquad \hat{G}_{j,j'}(n, n') := G_{n,n'}^{j,j'}(\omega). \tag{B.103}$$

We think about arguments in brackets as indices of the matrix, that is determined by each j and each j'. The sum in (B.102) is a tensor contraction by index j'', thus in matrix notation it is a multiplication of a matrix to the hatted $\hat{G}$. Thus we write a solution as

$$\hat{G}(1, n') = (1 - \hat{g}(1, 1)\hat{t})^{-1}\hat{g}(1, n'), \tag{B.104}$$

This formula in matrix notation gives the GF from (B.98) as

$$\hat{G}(n, n') = \hat{g}(n, n') + \hat{g}(n, 1)\hat{t}(1 - \hat{g}(1, 1)\hat{t})^{-1}\hat{g}(1, n'). \tag{B.105}$$

Now we are ready to compute the DOS. We substitute the known already (2.35) and the $\hat{G}(n, n')$ and transform:

$$\rho(\omega) = -\frac{1}{\pi}\text{Im}\,\text{tr}[z - h_D - \Sigma(\omega)]^{-1} - \frac{1}{\pi}\sum_{n=1}^{\infty}\text{Im}\,\text{Tr}\hat{G}(n, n) =$$

$$= \rho_{SC}^{(0)}(\omega) - \frac{1}{\pi}\text{Im}\,\text{tr}[z - h_D - \Sigma(\omega)]^{-1} - \frac{1}{\pi}\text{Im}\,\text{Tr}\left[\hat{t}(1 - \hat{g}(1, 1)\hat{t})^{-1}\sum_{n=1}^{\infty}\hat{g}(1, n)\hat{g}(n, 1)\right] =$$

$$= \rho_{SC}^{(0)}(\omega) - \frac{1}{\pi}\text{Im}\,\text{tr}[g_D^{-1}(\omega) - \Sigma(\omega)]^{-1} + \frac{1}{\pi}\text{Im}\,\text{Tr}\left[\hat{t}(1 - \hat{g}(1, 1)\hat{t})^{-1}\frac{\partial\hat{g}(1, 1)}{\partial\omega}\right]. \tag{B.106}$$

Here we have used the widely-known for GF specialists identity $\sum_{n=1}^{N} G_{1,n}G_{n,1} = -\frac{\partial G_{1,1}}{\partial\omega}$ (see[1]). Now we do the final transformation. We define $\mathcal{T}_j := t_j'\tau_z$ and rewrite

$$\hat{t} \equiv \mathcal{T}g_D(\omega)\mathcal{T}^T. \tag{B.107}$$

Now indices of $\hat{t}$ are distributed between $\mathcal{T}_j$ matrices. The sign "transpose" makes the column-vector $\mathcal{T}_j$ a row, such that by indices j, j'' we have a number (1×1 object). Now, by applying Woodbury matrix identity[22] and identifying $\Sigma(\omega) := \mathcal{T}^T\hat{g}(1, 1)\mathcal{T}$ (in the previous notation the definition looked like $\Sigma(\omega) := \sum_{j=1}^{N}\left(t_j'\right)^2\tau_z g_{1,1}^j(\omega)\tau_z$) the multiplier under trace will be

$$(1 - \hat{g}(1, 1)\mathcal{T}g_D(\omega)\mathcal{T}^T)^{-1} = (\hat{g}^{-1}(1, 1) - \mathcal{T}g_D(\omega)\mathcal{T}^T)^{-1}\hat{g}^{-1}(1, 1) =$$
$$= 1 + \hat{g}(1, 1)\mathcal{T}(g_D^{-1}(\omega) - \mathcal{T}^T\hat{g}(1, 1)\mathcal{T})^{-1}\mathcal{T}^T = \tag{B.108}$$
$$= 1 + \hat{g}(1, 1)\mathcal{T}(g_D^{-1}(\omega) - \Sigma(\omega))^{-1}\mathcal{T}^T.$$

---

[22]$(A + UCV)^{-1} = A^{-1} - A^{-1}U\left(C^{-1} + VA^{-1}U\right)^{-1}VA^{-1}$

And we do the final step of the final transformation:

$$\rho(\omega) = \rho_{SC}^{(0)}(\omega) - \frac{1}{\pi} \mathrm{Im} \, \mathrm{tr}[g_D^{-1}(\omega) - \Sigma(\omega)]^{-1} +$$
$$\frac{1}{\pi} \mathrm{Im} \, \mathrm{tr} \left[g_D(\omega) \left(1 + \Sigma(\omega)(g_D^{-1}(\omega) - \Sigma(\omega))^{-1} \right) \frac{\partial \Sigma(\omega)}{\partial \omega} \right] = \tag{B.109}$$

$$= \rho_{SC}^{(0)}(\omega) - \frac{1}{\pi} \mathrm{Im} \, \mathrm{tr} \left[(g_D^{-1}(\omega) - \Sigma(\omega))^{-1} \underbrace{\frac{\partial g_D^{-1}(\omega)}{\partial \omega}}_{\equiv 1} \right] + \frac{1}{\pi} \mathrm{Im} \, \mathrm{tr} \left[(g_D^{-1}(\omega) - \Sigma(\omega))^{-1} \frac{\partial \Sigma(\omega)}{\partial \omega} \right] =$$

$$= \rho_{SC}^{(0)}(\omega) - \frac{1}{\pi} \mathrm{Im} \, \mathrm{tr} \left[\frac{\partial}{\partial \omega} \log \left(g_D^{-1}(\omega) - \Sigma(\omega) \right) \right] =$$

$$= \rho_{SC}^{(0)}(\omega) - \frac{1}{\pi} \mathrm{Im} \, \frac{\partial}{\partial \omega} \log \det \left[g_D^{-1}(\omega) - \Sigma(\omega) \right] =$$

$$= \underbrace{\rho_{SC}^{(0)}(\omega) + \rho_D^{(0)}(\omega)}_{\text{bare DOS}} + \underbrace{\left(-\frac{1}{\pi} \mathrm{Im} \, \frac{\partial}{\partial \omega} \log \det \left[1 - g_D(\omega)\Sigma(\omega) \right] \right)}_{\text{tunneling contribution}}. \tag{B.110}$$

Thus we have proven (2.43).

Derivation of spectrum in two terminals for the discrete model

$$E_{\tau,\sigma} = \tau \left[1 + \frac{\Gamma_1}{\Delta_1} + \frac{\Gamma_2}{\Delta_2} \right]^{-1} \left(\sqrt{V^2 + |\Gamma_1 e^{i\varphi_1} + \Gamma_2 e^{i\varphi_2}|^2} + \sigma \Delta_Z \right) = \tag{B.111}$$

$$= \frac{\tau}{1 + \frac{\Gamma_1}{\Delta_1} + \frac{\Gamma_2}{\Delta_2}} \sqrt{V^2 + \Gamma_1^2 + \Gamma_2^2 + 2\Gamma_1\Gamma_2 \cos(\varphi_1 - \varphi_2)} + \sigma \frac{\Delta_Z}{1 + \frac{\Gamma_1}{\Delta_1} + \frac{\Gamma_2}{\Delta_2}} \tag{B.112}$$

$$= \frac{\tau}{1 + \frac{\Gamma_1}{\Delta_1} + \frac{\Gamma_2}{\Delta_2}} \sqrt{V^2 + (\Gamma_1 + \Gamma_2)^2 - 2\Gamma_1\Gamma_2 + 2\Gamma_1\Gamma_2 \cos(\varphi_1 - \varphi_2)} + \sigma E_Z, \tag{B.113}$$

$$= \frac{\sqrt{V^2 + (\Gamma_1 + \Gamma_2)^2} \tau}{1 + \frac{\Gamma_1}{\Delta_1} + \frac{\Gamma_2}{\Delta_2}} \sqrt{1 - 2\Gamma_1\Gamma_2 \frac{1}{V^2 + (\Gamma_1 + \Gamma_2)^2} \cdot 2 \frac{1 - \cos\varphi}{2}} + \sigma E_Z, \tag{B.114}$$

$$= \tau E_J \sqrt{1 - D \sin^2 \frac{\varphi}{2}} + \sigma E_Z, \tag{B.115}$$

where

$$E_J := \frac{\sqrt{V^2 + (\Gamma_1 + \Gamma_2)^2}}{1 + \frac{\Gamma_1}{\Delta_1} + \frac{\Gamma_2}{\Delta_2}}, \qquad D := \frac{4\Gamma_2\Gamma_1}{V^2 + (\Gamma_1 + \Gamma_2)^2}, \qquad E_Z := \frac{\Delta_Z}{1 + \frac{\Gamma_1}{\Delta_1} + \frac{\Gamma_2}{\Delta_2}}. \tag{B.116}$$

This is the (2.61).

Derivation of the approximation of the current for two terminals

The general expression for the Josephson current (2.54) can be simplified for the case of two terminals by usage of the Sokhotski–Plemelj theorem as follows:

$$I_1 = \frac{1}{\Phi_0}\text{Im}\int_{-\infty}^{+\infty} d\omega f(\omega)\text{tr}\frac{1}{\omega + i\eta - h_D - \Sigma(\omega)}\frac{\partial\Sigma(\omega + i\eta)}{\partial\varphi_1} = \tag{B.117}$$

$$= -\frac{\pi}{\Phi_0}\sum_{\tau,\sigma=\pm}\int d\omega f(\omega)\delta\left(\omega - \tau\omega_A - \sigma E_Z\right)\frac{\partial}{\partial\varphi_1}\left(\Sigma(0) + \omega\left.\frac{d\Sigma(\omega)}{d\omega}\right|_{\omega=0}\right) = \tag{B.118}$$

$$= -\frac{\pi}{\Phi_0}\Big(f(\omega_A + E_Z) + f(\omega_A - E_Z) - f(-\omega_A + E_Z) - f(-\omega_A - E_Z)\Big)\frac{\partial}{\partial\varphi_1}\omega_A = \tag{B.119}$$

$$= -\frac{\pi}{\Phi_0}\left(-\frac{2\text{sh}(\beta\omega_A)}{\text{ch}(\beta\omega_A) + \text{ch}(\beta E_Z)}\right)\frac{\partial}{\partial\varphi_1}\omega_A = \tag{B.120}$$

$$= \frac{2\pi E_J}{\Phi_0}\frac{\text{sh}(\beta\omega_A)}{\text{ch}(\beta\omega_A) + \text{ch}(\beta E_Z)}\frac{\partial\sqrt{1 - D\sin^2\frac{\varphi}{2}}}{\partial\varphi_1}\;{}_{\varphi:=\underline{\varphi_2}-\varphi_1} \tag{B.121}$$

$$= \frac{2\pi E_J}{\Phi_0}\frac{\text{sh}(\beta\omega_A)}{\text{ch}(\beta\omega_A) + \text{ch}(\beta E_Z)}\frac{D\cdot 2\sin\frac{\varphi}{2}\cos\frac{\varphi}{2}}{4\sqrt{1 - D\sin^2\frac{\varphi}{2}}} = \tag{B.122}$$

$$= \frac{\pi D E_J}{2\Phi_0}\frac{\text{sh}(\beta\omega_A)}{\text{ch}(\beta\omega_A) + \text{ch}(\beta E_Z)}\frac{\sin\varphi}{\sqrt{1 - D\sin^2\frac{\varphi}{2}}}. \tag{B.123}$$

Thus we have (2.64).

Derivation of spectrum in three terminals for the discrete model

$$E_{\tau,\sigma} = \tau\left[1 + 3\frac{\Gamma}{\Delta}\right]^{-1}\left(\sqrt{V^2 + \Gamma^2(3 + 2\cos(\varphi - \chi) + 2\cos\varphi + 2\cos\chi)} + \sigma\Delta_Z\right) =$$

$$= \tau\left[1 + 3\frac{\Gamma}{\Delta}\right]^{-1}\left(\sqrt{V^2 + 3\Gamma^2 - 4\Gamma^2\left(-\frac{3}{2} + \frac{1-\cos(\varphi-\chi)}{2} + \frac{1-\cos\varphi}{2} + \frac{1-\cos\chi}{2}\right)} + \sigma\Delta_Z\right) =$$

$$= \tau\left[1 + 3\frac{\Gamma}{\Delta}\right]^{-1}\left(\sqrt{V^2 + 9\Gamma^2 - 4\Gamma^2\left(\sin^2\frac{(\varphi-\chi)}{2} + \sin^2\frac{\varphi}{2} + \sin^2\frac{\chi}{2}\right)} + \sigma\Delta_Z\right).$$

Thus

$$E_{\tau,\sigma} = \tau E_J\sqrt{1 - D\Phi(\varphi,\chi)} + \sigma\tilde{\Delta}_Z, \tag{B.124}$$

86

where we introduce $\Phi(\varphi, \chi)$ and D with special coefficients, such that $D \in [0,1]$,

$$E_J := \left[1 + 3\frac{\Gamma}{\Delta}\right]^{-1} \sqrt{V^2 + 9\Gamma^2}, \tag{B.125}$$

$$D := \frac{9\Gamma^2}{V^2 + 9\Gamma^2}, \tag{B.126}$$

$$\Phi(\varphi, \chi) := \frac{4}{9}\left(\sin^2 \varphi/2 + \sin^2 \chi/2 + \sin^2(\varphi/2 - \chi/2)\right), \tag{B.127}$$

$$\tilde{\Delta}_Z := \frac{\Delta_Z}{1 + 3\frac{\Gamma}{\Delta}}. \tag{B.128}$$

And we have (2.67). Note that with ore definition, the function $\Phi(\varphi, \chi)$ has a maximal value of 1, and the D is allowed to be from 0 to 1.

B.6.2 Derivations for Sec. A.1

Derivation of normal Hamiltonian in Nambu space for the continuous model

Here we will prove that

$$H_{\rm n} = \sum_{\sigma,\sigma'=\pm} \int_\Omega dx \hat{\psi}_\sigma^\dagger(x) h_{\sigma,\sigma'}(p,x)\hat{\psi}_{\sigma'}(x) \qquad \Leftrightarrow \qquad H_{\rm n} \equiv \frac{1}{2}\int_\Omega dx\ \hat{\Psi}^\dagger(x)\mathcal{H}_{\rm n}(p,x)\hat{\Psi}(x),$$

where $\mathcal{H}_{\rm n}(p,x) := \begin{pmatrix} h(p,x) & 0 \\ 0 & -\sigma_y h^*(p,x)\sigma_y \end{pmatrix}$; $h(p,x) := \sum_{\sigma,\sigma'=\pm} h_{\sigma,\sigma'}(p,x)|\sigma\rangle\langle\sigma'|$; $\hat{\Psi}(x) := \begin{pmatrix} \hat{\psi}(x) \\ i\sigma_y\left[\hat{\psi}^\dagger(x)\right]^T \end{pmatrix}$; $\hat{\psi}(x) := \sum_{\sigma=\pm} \hat{\psi}_\sigma(x)|\sigma\rangle$.

We will omit the arguments (p,x), (x) and prove to the other direction:

$$\hat{\Psi}^\dagger \mathcal{H}_{\rm n} \hat{\Psi} = \begin{pmatrix} \hat{\psi}_+^\dagger & \hat{\psi}_-^\dagger & \hat{\psi}_- & -\hat{\psi}_+ \end{pmatrix} \begin{pmatrix} h_{++} & h_{+-} & 0 & 0 \\ h_{-+} & h_{--} & 0 & 0 \\ 0 & 0 & -h_{--} & h_{-+}^* \\ 0 & 0 & h_{+-}^* & -h_{++} \end{pmatrix} \begin{pmatrix} \hat{\psi}_+ \\ \hat{\psi}_- \\ \hat{\psi}_-^\dagger \\ -\hat{\psi}_+^\dagger \end{pmatrix} =$$

$$= \begin{pmatrix} \hat{\psi}_+^\dagger h_{++} + \hat{\psi}_-^\dagger h_{+-} & \hat{\psi}_+^\dagger h_{-+} + \hat{\psi}_-^\dagger h_{--} & -\hat{\psi}_- h_{--} - \hat{\psi}_+ h_{-+}^* & \hat{\psi}_- h_{+-}^* - (-\hat{\psi}_+)h_{++} \end{pmatrix} \begin{pmatrix} \hat{\psi}_+ \\ \hat{\psi}_- \\ \hat{\psi}_-^\dagger \\ -\hat{\psi}_+^\dagger \end{pmatrix} =$$

$$= \hat{\psi}_+^\dagger h_{++}\hat{\psi}_+ + \hat{\psi}_-^\dagger h_{+-}\hat{\psi}_+ + \hat{\psi}_+^\dagger h_{-+}\hat{\psi}_- + \hat{\psi}_-^\dagger h_{--}\hat{\psi}_- - \hat{\psi}_- h_{--}\hat{\psi}_-^\dagger - \hat{\psi}_+ h_{-+}^*\hat{\psi}_-^\dagger - \hat{\psi}_- h_{+-}^*\hat{\psi}_+^\dagger - \hat{\psi}_+ h_{++}\hat{\psi}_+^\dagger =$$

$$= 2\left(\hat{\psi}_+^\dagger h_{++}\hat{\psi}_+ + \hat{\psi}_-^\dagger h_{+-}\hat{\psi}_+ + \hat{\psi}_+^\dagger h_{-+}\hat{\psi}_- + \hat{\psi}_-^\dagger h_{--}\hat{\psi}_-\right) + \mathrm{const}\cdot\delta(0),$$

where at the last step we used anticommutative identities and the hermiticity of the Hamiltonian $(H = H^{*T})$[23]. We remind that h-s are just complex functions, so ψ-s can go through it. Then, the factor 2 cancels with factor $1/2$ from the Nambu Hamiltonian and we get the exactly the term under the integral of non-Nambu Hamiltonian (2.2).

---

[23]Because of which, for example, $h_{-+}^* = h_{+-}$

Derivation of SC Hamiltonian in Nambu space for the continuous model

Here we will prove that

$$H_{\text{SC}} := \sum_{\sigma=\pm} \int_0^\infty dx \hat{\chi}_\sigma^\dagger(x) \left[\frac{p^2}{2m} - \mu \right] \hat{\chi}_\sigma(x) + \int_0^\infty dx \left[\Delta \hat{\chi}_+^\dagger(x)\hat{\chi}_-^\dagger(x) + \Delta^* \hat{\chi}_-(x)\hat{\chi}_+(x) \right]$$

is equivalent to

$$H_{\text{SC}} = \frac{1}{2} \int_0^\infty dx \hat{\Upsilon}^\dagger(x) \mathcal{H}_{\text{SC}}(p,x) \hat{\Upsilon}(x), \quad \mathcal{H}_{\text{SC}}(p,x) = \begin{pmatrix} \left[\frac{p^2}{2m} - \mu \right] & i\Delta\sigma_y \\ -i\Delta^*\sigma_y & -\left[\frac{p^2}{2m} - \mu \right] \end{pmatrix},$$

where $\hat{\Upsilon}(x) = \begin{pmatrix} \hat{\chi}(x) \\ i\sigma_y \left[\hat{\chi}^\dagger(x) \right]^T \end{pmatrix}$, $\hat{\chi}(x) = \sum_{\sigma=\pm} \hat{\chi}_\sigma(x) |\sigma\rangle$. We will omit dependence on $(p,x),(x)$ and do as before:

$$\hat{\Upsilon}^\dagger \mathcal{H}_{\text{SC}} \hat{\Upsilon} = \begin{pmatrix} \hat{\chi}^\dagger & \hat{\chi}^T(-i\sigma_y) \end{pmatrix} \begin{pmatrix} \left[\frac{p^2}{2m} - \mu \right] & \Delta \\ \Delta^* & -\left[\frac{p^2}{2m} - \mu \right] \end{pmatrix} \begin{pmatrix} \hat{\chi} \\ i\sigma_y \hat{\chi}^{\dagger T} \end{pmatrix} =$$

$$= \begin{pmatrix} \hat{\chi}^\dagger \left[\frac{p^2}{2m} - \mu \right] + \hat{\chi}^T(-i\sigma_y)\Delta^* & \hat{\chi}^\dagger \Delta - (\hat{\chi}^T(-i\sigma_y)) \left[\frac{p^2}{2m} - \mu \right] \end{pmatrix} \begin{pmatrix} \hat{\chi} \\ i\sigma_y \hat{\chi}^{\dagger T} \end{pmatrix} =$$

$$= \hat{\chi}^\dagger \left[\frac{p^2}{2m} - \mu \right] \hat{\chi} + \hat{\chi}^T(-i\sigma_y)\Delta^* \hat{\chi} + \hat{\chi}^\dagger \Delta (i\sigma_y \hat{\chi}^{\dagger T}) - (\hat{\chi}^T(-i\sigma_y)) \left[\frac{p^2}{2m} - \mu \right] (i\sigma_y \hat{\chi}^{\dagger T}) =$$

$$= \hat{\chi}^\dagger \left[\frac{p^2}{2m} - \mu \right] \hat{\chi} + \Delta^* \begin{pmatrix} \chi_+ & \chi_- \end{pmatrix} \begin{pmatrix} 0 & -1 \\ 1 & 0 \end{pmatrix} \begin{pmatrix} \chi_+ \\ \chi_- \end{pmatrix} + \Delta \begin{pmatrix} \chi_+^\dagger & \chi_-^\dagger \end{pmatrix} \begin{pmatrix} 0 & 1 \\ -1 & 0 \end{pmatrix} \begin{pmatrix} \chi_+^\dagger \\ \chi_-^\dagger \end{pmatrix} - \left[\frac{p^2}{2m} - \mu \right] \begin{pmatrix} \chi_+ & \chi_- \end{pmatrix} \begin{pmatrix} \chi_+^\dagger \\ \chi_-^\dagger \end{pmatrix} =$$

$$= \left[\frac{p^2}{2m} - \mu \right] (\chi_+^\dagger \chi_+ + \chi_-^\dagger \chi_-) + \Delta^*(\chi_- \chi_+ - \chi_+ \chi_-) + \Delta(-\chi_-^\dagger \chi_+^\dagger + \chi_+^\dagger \chi_-^\dagger) + \left[\frac{p^2}{2m} - \mu \right] (-\chi_+ \chi_+^\dagger - \chi_- \chi_-^\dagger) =$$

$$= 2 \left(\left[\frac{p^2}{2m} - \mu \right] (\chi_+^\dagger \chi_+ + \chi_-^\dagger \chi_-) + \Delta \chi_+^\dagger \chi_-^\dagger + \Delta^* \chi_- \chi_+ \right).$$

Now the equivalence with (A.8) is obvious. Also, this formula can also be found, for example, in [1] and the similar one in [66].

Derivation of the Heisenberg equations for the continuous model

Here we will derive the Heisenberg equations for the Nambu fields $\hat{\Psi}$ and $\hat{\Upsilon}$. We will use $i\frac{d}{dt}\hat{\Upsilon}(x,t) = \left[\hat{\Upsilon}(x,t), H_{\text{tot}} \right]$ and for it we compute:

$$\left[\hat{\Upsilon}_a(x), H_n \right] = \int_\Omega dx' \hat{\Upsilon}_a(x) \frac{1}{2} \hat{\Psi}_b^\dagger(x') \mathcal{H}_n^{bc}(p',x') \hat{\Psi}_c(x') - \int_\Omega dx' \frac{1}{2} \hat{\Psi}_b^\dagger(x') \mathcal{H}_n^{bc}(p',x') \hat{\Psi}_c(x') \hat{\Upsilon}_a(x) =$$

$$= \int_\Omega dx' \hat{\Upsilon}_a(x) \frac{1}{2} \hat{\Psi}_b^\dagger(x') \mathcal{H}_n^{bc}(p',x') \hat{\Psi}_c(x') - \int_\Omega dx'(-1)^2 \frac{1}{2} \hat{\Upsilon}_a(x) \hat{\Psi}_b^\dagger(x') \mathcal{H}_n^{bc}(p',x') \hat{\Psi}_c(x') = 0;$$

$$\left[\hat{\Upsilon}_a(x), H_{SC}\right] = \hat{\Upsilon}_a(x)\int dx' \frac{1}{2}\hat{\Upsilon}_b^\dagger(x')\mathcal{H}_{SC}^{bc}(p',x')\hat{\Upsilon}_c(x') - \int dx' \frac{1}{2}\hat{\Upsilon}_b^\dagger(x')\mathcal{H}_{SC}^{bc}(p',x')\hat{\Upsilon}_c(x')\hat{\Upsilon}_a(x) =$$

$$= \int dx' \frac{1}{2}(-\hat{\Upsilon}_b^\dagger(x')\hat{\Upsilon}_a(x) + \delta_{ab}\delta(x-x'))\mathcal{H}_{SC}^{bc}(p',x')\hat{\Upsilon}_c(x')-$$

$$- \int dx' \frac{1}{2}\hat{\Upsilon}_b^\dagger(x')\mathcal{H}_{SC}^{bc}(p',x')(-\hat{\Upsilon}_a(x)\hat{\Upsilon}_c(x') + \mathcal{C}_{ca}\delta(x-x')) =$$

$$= - \int dx' \frac{1}{2}\hat{\Upsilon}_b^\dagger(x')\hat{\Upsilon}_a(x)\mathcal{H}_{SC}^{bc}(p',x')\hat{\Upsilon}_c(x') + \frac{1}{2}\mathcal{H}_{SC}^{ac}(p,x)\hat{\Upsilon}_c(x)+$$

$$+ \int dx' \frac{1}{2}\hat{\Upsilon}_b^\dagger(x')\mathcal{H}_{SC}^{bc}(p',x')\hat{\Upsilon}_a(x)\hat{\Upsilon}_c(x') - \frac{1}{2}\hat{\Upsilon}_b^\dagger(x)\mathcal{H}_{SC}^{bc}(p,x)\mathcal{C}_{ca} =$$

$$= - \int dx' \frac{1}{2}\hat{\Upsilon}_b^\dagger(x')\hat{\Upsilon}_a(x)\mathcal{H}_{SC}^{bc}(p',x')\hat{\Upsilon}_c(x') + \int dx' \frac{1}{2}\hat{\Upsilon}_b^\dagger(x')\mathcal{H}_{SC}^{bc}(p',x')\hat{\Upsilon}_a(x)\hat{\Upsilon}_c(x')$$

$$+ \frac{1}{2}\mathcal{H}_{SC}^{ac}(p,x)\hat{\Upsilon}_c(x) - \frac{1}{2}\underbrace{\hat{\Upsilon}_b^\dagger(x)}_{=\hat{\Upsilon}_d\mathcal{C}_{bd}}\mathcal{H}_{SC}^{bc}(p,x)\mathcal{C}_{ca} =$$

$$= \int dx' \frac{1}{2}\hat{\Upsilon}_b^\dagger(x')\underbrace{\left[\mathcal{H}_{SC}^{bc}(p',x'), \hat{\Upsilon}_a(x)\right]}_{=0}\hat{\Upsilon}_c(x') + \frac{1}{2}\mathcal{H}_{SC}^{ac}(p,x)\hat{\Upsilon}_c(x) - \frac{1}{2}\hat{\Upsilon}_d\underbrace{\mathcal{C}_{bd}\mathcal{H}_{SC}^{bc}(p,x)\mathcal{C}_{ca}}_{=-\mathcal{H}_{SC}^{da*}=-\mathcal{H}_{SC}^{ad}} =$$

$$= \mathcal{H}_{SC}^{ac}(p,x)\hat{\Upsilon}_c(x) \equiv [\mathcal{H}_{SC}(p,x)\hat{\Upsilon}(x)]_a.$$

Here we used the fact that each component $\mathcal{H}_{SC}^{bc}$ is a scalar function, so it commutes with spinor $\hat{\Upsilon}_c(x)$ and that from charge-symmetry properties $(C_{ab}\hat{\Upsilon}_b^\dagger = \hat{\Upsilon}_a)$ we have[24] $\hat{\Upsilon}_b C_{ab} = \hat{\Upsilon}_b^\dagger$, since $C_{ab}^\dagger = C_{ab}$. Also, it is important to use the fact that that $\mathcal{H}_{SC}$ is Hermitian, since this is the main property to use the transformations like $\mathcal{C}_{bd}\mathcal{H}_{SC}^{bc}(p,x)\mathcal{C}_{ca} = -\mathcal{H}_{SC}^{da*} = \mathcal{H}_{SC}^{ad}$.

$$\left[\hat{\Upsilon}_a(x), H_T\right] = \frac{1}{2}\Big(\hat{\Upsilon}_a(x)\hat{\Upsilon}_b^\dagger(a)\mathcal{W}^{bc}\hat{\Psi}_c(\tilde{R}) + \underbrace{\hat{\Upsilon}_a(x)\hat{\Psi}_b^\dagger(\tilde{R})}_{=-\hat{\Psi}_b^\dagger(\tilde{R})\hat{\Upsilon}_a(x)}\mathcal{W}^{\dagger bc}\hat{\Upsilon}_c(a)-$$

$$- \hat{\Upsilon}_b^\dagger(a)\mathcal{W}^{bc}\underbrace{\hat{\Psi}_c(\tilde{R})\hat{\Upsilon}_a(x)}_{=-\hat{\Upsilon}_a(x)\hat{\Psi}_c(\tilde{R})} - \hat{\Psi}_b^\dagger(\tilde{R})\mathcal{W}^{\dagger bc}\hat{\Upsilon}_c(a)\hat{\Upsilon}_a(x)\Big) =$$

$$= \frac{1}{2}\Big(\delta_{ab}\delta(x-a)\mathcal{W}^{bc}\hat{\Psi}_c(\tilde{R}) - \hat{\Psi}_b^\dagger(\tilde{R})\mathcal{W}^{\dagger bc}\mathcal{C}_{ab}\delta(x-a)\Big) =$$

$$= \frac{1}{2}\Big(\delta_{ab}\delta(x-a)\mathcal{W}^{bc}\hat{\Psi}_c(\tilde{R}) - \hat{\Psi}_r(\tilde{R})\underbrace{\mathcal{C}_{br}\mathcal{W}^{\dagger bc}\mathcal{C}_{ab}}_{-\mathcal{W}^{ra*}=-\mathcal{W}^{ar}}\delta(x-a)\Big) =$$

$$= \delta(x-a)\mathcal{W}^{ac}\hat{\Psi}_c(\tilde{R}) \equiv [\delta(x-a)\mathcal{W}\hat{\Psi}(\tilde{R})]_a$$

After collecting terms and restoring t-dependence, we got

$$i\frac{d}{dt}\hat{\Upsilon}(x,t) = \mathcal{H}_{SC}(p,x)\hat{\Upsilon}(x,t) + \delta(x-a)\mathcal{W}\hat{\Psi}(\tilde{R},t),$$

---

[24]To be more mathematically strict, one can also agree about the positions of row and column indices of spinors (Ψ and Υ). We are not fixing much attention to it, since in case of doubt one can imagine matrices, rows, columns. Also, we omit upper-lower position of indices and agree that we sum over each repeated index despite its position.

which is the Eq. (A.17). Analogous we get the Eq. (A.18). There is no value of writing the analogous derivation and as the one before, it is straightforward and bulky.

Derivative of the Dyson equations for the continuous model

Here we will find the Dyson equation for $[G_{\text{NN}}(x, x'|t)]_{ab} := -i\Theta(t)\langle\{\hat{\Psi}_a(x,t), \hat{\Psi}_b^\dagger(x',0)\}\rangle$. We evaluate:

$$i\frac{d}{dt}[G_{\text{NN}}(x,x'|t)]_{ab} = \underbrace{\delta(t)\langle\{\hat{\Psi}_a(x,t), \hat{\Psi}_b^\dagger(x',0)\}\rangle}_{=\delta(t)\langle\{\hat{\Psi}_a(x,0),\hat{\Psi}_b^\dagger(x',0)\}\rangle=\delta(t)\delta(x-x')\delta_{ab}} - i\Theta(t)\langle\{i\frac{d\hat{\Psi}_a(x,t)}{dt}, \hat{\Psi}_b^\dagger(x',0)\}\rangle =$$

$$= \delta(t)\delta(x-x')\delta_{ab} - i\Theta(t)\langle\{\mathcal{H}_n^{ac}(p,x)\hat{\Psi}_c(x,t), \hat{\Psi}_b^\dagger(x',0)\}\rangle - i\Theta(t)\langle\{\delta(x-\tilde{R})\mathcal{W}^{\dagger ac}\hat{\Upsilon}_c(a,t), \hat{\Psi}_b^\dagger(x',0)\}\rangle =$$

$$= \delta(t)\delta(x-x')\delta_{ab} + \mathcal{H}_n^{ac}(p,x)\underbrace{(-i\Theta(t))\langle\{\hat{\Psi}_c(x,t), \hat{\Psi}_b^\dagger(x',0)\}\rangle}_{=[G_{NN}(x,x'|t)]_{cb}} + \delta(x-\tilde{R})\mathcal{W}^{\dagger ac}\underbrace{(-i\Theta(t))\langle\{\hat{\Upsilon}_c(a,t), \hat{\Psi}_b^\dagger(x',0)\}\rangle}_{=[G_{SN}(a,x'|t)]_{cb}}.$$

Note that purely the expression $\langle\{\hat{\Psi}_a(x,t), \hat{\Psi}_b^\dagger(x',0)\}\rangle$ is in general case complex to evaluate and the $\delta(t)$ and $\Theta(t)$ allow us to proceed. Also, we consider the Hamiltonian as a complex function, thus we can easily take it out of averaging. Thus in matrix form, we have

$$\left(i\frac{d}{dt} - \mathcal{H}_n(p,x)\right)G_{\text{NN}}(x,x'|t) = \delta(x-\tilde{R})\mathcal{W}^\dagger G_{SN}(a,x'|t) + \delta(t)\delta(x-x'). \qquad \text{(B.129)}$$

Exactly the same way other Dyson Eq. (A.23) can be proven. To use transformation $F[f](z) := \int_0^\infty dt e^{izt}f(t)$, we prepare, for example, like

$$F[i\frac{d}{dt}G_{\text{NS}}](z) = \int_0^\infty dt e^{izt} i\frac{d}{dt}G_{\text{NS}}(t) = ie^{izt}G_{\text{NS}}(t)|_0^\infty - i\cdot iz\int_0^\infty dt e^{izt}G_{\text{NS}} = zG_{\text{NS}}(z),$$

$$F[\mathcal{H}_n G_{\text{NS}}](z) = \mathcal{H}_n G_{\text{NS}}(z),$$

$$F[\delta(x-\tilde{R})\mathcal{W}^\dagger G_{\text{SS}}](z) = \delta(x-\tilde{R})\mathcal{W}^\dagger G_{\text{SS}}(z).$$

Now, the eq. $\left(i\frac{d}{dt} - \mathcal{H}_n(p,x)\right)G_{\text{NS}}(x,x'|t) = \delta(x-\tilde{R})\mathcal{W}^\dagger G_{\text{SS}}(a,x'|t)$ will be transformed as

$$(z-\mathcal{H}_n)G_{\text{NS}}(z) = \delta(x-\tilde{R})\mathcal{W}^\dagger G_{\text{SS}}(z).$$

Other Dyson eq. (A.27) are transformed the same way.

Derivation of spectral density for the continuous model

Here we will find the formula for the $\rho_{\mathrm{n}}(\omega)$. Fist, we notice that (we use $z := \omega + i\eta, \eta \to 0$)

$$\frac{\partial}{\partial z}\big[z - \mathcal{H}_{\mathrm{n}}(p, x)\big]m(x, x') = \frac{\partial}{\partial z}\delta(x - x'),$$

$$m(x, x') + \big[z - \mathcal{H}_{\mathrm{n}}(p, x)\big]\frac{\partial m(x, x')}{\partial z} = 0,$$

$$\frac{\partial m(x, x')}{\partial z} = -\frac{1}{\big[z - \mathcal{H}_{\mathrm{n}}(p, x)\big]}m(x, x')$$

$$\frac{\partial m(x, x')}{\partial z}\delta(x' - x) = -\frac{\delta(x' - x)}{\big[z - \mathcal{H}_{\mathrm{n}}(p, x)\big]}m(x, x')$$

$$\frac{\partial m(x, x')}{\partial z}\delta(x' - x) = -m(x', x)m(x, x').$$

Here we see the importance of $m(x', x) \neq m(x, x')$ Analogously, the same formula for g is obtained. Now, with the help of $G_{\mathrm{NN}}(x, x') = m(x, x') + m(x, \tilde{R})\mathcal{W}^\dagger g(a, a)\mathcal{W}D^{-1}m(\tilde{R}, x')$ we will find the formula for $\rho_{\mathrm{n}}(\omega)$:

$$\rho_{\mathrm{n}}(\omega) = -\frac{1}{\pi}\mathrm{Im}\int_\Omega dx \mathrm{tr} G_{\mathrm{NN}}(x, x)$$

$$= \underbrace{-\frac{1}{\pi}\mathrm{Im}\int_\Omega dx \mathrm{tr}\, m(x, x)}_{=:\rho_{\mathrm{n}}^{(0)}(\omega)} - \frac{1}{\pi}\mathrm{Im}\,\mathrm{tr}\Big[m(x, \tilde{R})\mathcal{W}^\dagger g(a, a)\mathcal{W}D^{-1}\int_\Omega dx\, m(\tilde{R}, x)\Big]$$

$$= \rho_{\mathrm{n}}^{(0)}(\omega) - \frac{1}{\pi}\mathrm{Im}\,\mathrm{tr}\Big[m(x, \tilde{R})\mathcal{W}^\dagger g(a, a)\mathcal{W}D^{-1}\int_\Omega dx\, m(\tilde{R}, x)\Big] =$$

$$= \rho_{\mathrm{n}}^{(0)}(\omega) - \frac{1}{\pi}\mathrm{Im}\int_\Omega dx \mathrm{tr}\Big[\mathcal{W}^\dagger g(a, a)\mathcal{W}D^{-1}\int_\Omega dx\, m(\tilde{R}, x)m(x, \tilde{R})\Big] =$$

$$= \rho_{\mathrm{n}}^{(0)}(\omega) - \frac{1}{\pi}\mathrm{Im}\,\mathrm{tr}\Big[\mathcal{W}^\dagger g(a, a)\mathcal{W}D^{-1}\int_\Omega dx\, m(\tilde{R}, x)m(x, \tilde{R})\Big] =$$

$$= \rho_{\mathrm{n}}^{(0)}(\omega) + \frac{1}{\pi}\mathrm{Im}\,\mathrm{tr}\,\mathcal{W}^\dagger\, g(a, a)\,\mathcal{W}\,D^{-1}\frac{\partial m(\tilde{R}, \tilde{R})}{\partial z}.$$

Thus we have proven the (A.48).

Now, with the help of $G_{\mathrm{SS}}(x, x') = g(x, x') + g(x, a)\mathcal{M}[1 - g(a, a)\mathcal{M}]^{-1}g(a, x')$ find a

formula for the $\rho_{\mathrm{SC}}(\omega)$:

$$\rho_{\mathrm{SC}}(\omega) = -\frac{1}{\pi}\mathrm{Im}\int_0^\infty dx\mathrm{tr}\{G_{\mathrm{SS}}(x,x)\} =$$

$$= \underbrace{-\frac{1}{\pi}\mathrm{Im}\int_0^\infty dx\mathrm{tr}\{g(x,x)\}}_{=:\rho_{\mathrm{SC}}^{(0)}(\omega)} -\frac{1}{\pi}\mathrm{Im}\int_0^\infty dx\mathrm{tr}\left[g(x,a)\mathcal{M}[1-g(a,a)\mathcal{M}]^{-1}g(a,x)\right]$$

$$= \rho_{\mathrm{SC}}^{(0)}(\omega) - \frac{1}{\pi}\mathrm{Im}\ \mathrm{tr}\left[\mathcal{M}[1-g(a,a)\mathcal{M}]^{-1}\int_0^\infty dxg(a,x)g(x,a)\right]$$

$$= \rho_{\mathrm{SC}}^{(0)}(\omega) + \frac{1}{\pi}\mathrm{Im}\ \mathrm{tr}\left[\mathcal{M}[1-g(a,a)\mathcal{M}]^{-1}\frac{\partial g(a,a)}{\partial\omega}\right]$$

$$= \rho_{\mathrm{SC}}^{(0)}(\omega) + \frac{1}{\pi}\mathrm{Im}\ \mathrm{tr}\left[\mathcal{W}m(\tilde{R},\tilde{R})\mathcal{W}^\dagger[1-g(a,a)\mathcal{W}m(\tilde{R},\tilde{R})\mathcal{W}^\dagger]^{-1}\frac{\partial g(a,a)}{\partial\omega}\right].$$

Finally, one needs to use $(ABC)^{-1} = C^{-1}B^{-1}A^{-1}$ to simplify the expression under tr:

$$\mathcal{W}m(\tilde{R},\tilde{R})\mathcal{W}^\dagger[(m(\tilde{R},\tilde{R})\mathcal{W}^\dagger)^{-1}m(\tilde{R},\tilde{R})\mathcal{W}^\dagger - (m(\tilde{R},\tilde{R})\mathcal{W}^\dagger)^{-1}m(\tilde{R},\tilde{R})\mathcal{W}^\dagger g(a,a)\mathcal{W}m(\tilde{R},\tilde{R})\mathcal{W}^\dagger]^{-1}\frac{\partial g(a,a)}{\partial\omega}] =$$

$$= \mathcal{W}m(\tilde{R},\tilde{R})\mathcal{W}^\dagger(m(\tilde{R},\tilde{R})\mathcal{W}^\dagger)^{-1}[1 - m(\tilde{R},\tilde{R})\mathcal{W}^\dagger g(a,a)\mathcal{W}]^{-1}(m(\tilde{R},\tilde{R})\mathcal{W}^\dagger)\frac{\partial g(a,a)}{\partial\omega} =$$

$$= \mathcal{W}D^{-1}m(\tilde{R},\tilde{R})\mathcal{W}^\dagger\frac{\partial g(a,a)}{\partial\omega}$$

and finish our little proof:

$$\rho_{\mathrm{SC}}(\omega) = \rho_{\mathrm{SC}}^{(0)}(\omega) + \frac{1}{\pi}\mathrm{Im}\ \mathrm{tr}\left[\mathcal{W}D^{-1}m(\tilde{R},\tilde{R})\mathcal{W}^\dagger\frac{\partial g(a,a)}{\partial\omega}\right]. \qquad\qquad (B.130)$$

$$= \rho_{\mathrm{SC}}^{(0)}(\omega) + \frac{1}{\pi}\mathrm{Im}\ \mathrm{tr}D^{-1}m(\tilde{R},\tilde{R})\frac{\partial\mathcal{W}^\dagger g(a,a)\mathcal{W}}{\partial\omega}. \qquad\qquad (B.131)$$

We hope that by this point reader felt the whole beauty of the mathematical transformations.

B.7 Programming Code

Below there is a Python `.ipynb` code. created with the help of Chat GPT. We will omit not essential parts of the code not comment much, since this is a technical part of the thesis.

Preparation:

```python
import numpy as np; import matplotlib.pyplot as plt; import matplotlib as mpl

S0=np.array([[1,0],[0,1]]);    S1=np.array([[0,1],[1,0]]);
    S2=np.array([[0,-1j],[1j,0]]);
S3=np.array([[1,0],[0,-1]]);   Spl=np.array([[0,1],[0,0]]);
    Smn=np.array([[0,0],[1,0]]);
```

The code for two terminals is as follows.

```python
def h(v, dz):
 return v*np.kron(S3,S0)+dz*np.kron(S0,S3)

def sigm_two(g1,d1,ph1, g2,d2,ph2, om):
 return -np.kron(
                (g1/( np.sqrt(d1*d1-om*om) ) )*(om*S0 - d1*(np.exp(ph1*1j)*Spl +
    np.exp(-ph1*1j)*Smn) )
     +
     (g2/( np.sqrt(d2*d2-om*om)))*(om*S0 - d2*(np.exp(ph2*1j)*Spl +
    np.exp(-ph2*1j)*Smn) ),S0)

def d_det_two(v, dz, g1,d1,ph1, g2,d2,ph2, om):
 return np.linalg.det( om*np.kron(S0,S0) - h(v, dz) - sigm_two(g1,d1,ph1, g2,d2,ph2,
    om) )
```

```python
precision_phi = 600;        precision_z = 400

ve2= 1;          g1e2=1.3;        g2e2=1.4;
dze2=0.3;        d1e2=1.4;        d2e2=1.4;

Zran=np.linspace(-min(d1e2,d2e2)+0.0001, min(d1e2,d2e2)-0.0001, precision_z)
Phran=np.linspace(0, 2*np.pi, precision_phi)

def d_det_exp_two(phi):
 return np.array([d_det_two(ve2, dze2,  g1e2,d1e2,phi/2,  g2e2,d2e2,-phi/2, om)
      for om in Zran])
```

```python
res=np.array([ d_det_exp_two(phi) for phi in Phran])
res_two=np.swapaxes(res, 0, 1)
```

```python
cs_two = plt.contourf(Phran, Zran, np.where(np.log(np.abs(res_two))< -3, 50,
    np.log(np.abs(res_two))), 500)
```

The code for three terminals is analogous. Full versions of both codes is available by double clicking[25] on ▭. The code of the current for 3TJJ is available here: ▭. To play with ABS of 7 terminals one can double click on: ▭.

---

[25]Using Adobe Acrobat Reader

C Bibliography

[1] Piasotski, K., Pletyukhov, M., and Shnirman, A.: *Green's functions of quasi-one-dimensional layered systems and their application to josephson junctions.* 2023. https://arxiv.org/abs/2311.15338.

[2] Matute-Cañadas, F.J., Tosi, L., and Yeyati, A. Levy: *Quantum circuits with multiterminal josephson-andreev junctions.* PRX Quantum, 5(2), May 2024, ISSN 2691-3399. http://dx.doi.org/10.1103/PRXQuantum.5.020340.

[3] Sauls, J. A.: *Andreev bound states and their signatures.* Philosophical Transactions of the Royal Society A: Mathematical, Physical and Engineering Sciences, 376(2125):20180140, June 2018, ISSN 1471-2962. http://dx.doi.org/10.1098/rsta.2018.0140.

[4] Martín-Rodero, A. and Levy Yeyati, A.: *Josephson and andreev transport through quantum dots.* Advances in Physics, 60(6):899–958, December 2011, ISSN 1460-6976. http://dx.doi.org/10.1080/00018732.2011.624266.

[5] Vecino, E., Martín-Rodero, A., and Yeyati, A. Levy: *Josephson current through a correlated quantum level: Andreev states and π-junction behavior.* Physical Review B, 68(3), July 2003, ISSN 1095-3795. http://dx.doi.org/10.1103/PhysRevB.68.035105.

[6] Jacquet, R., Popoff, A., Imura, K. I., Rech, J., Jonckheere, T., Raymond, L., Zazunov, A., and Martin, T.: *Theory of nonequilibrium noise in general multiterminal superconducting hybrid devices: Application to multiple cooper pair resonances.* Physical Review B, 102(6), August 2020, ISSN 2469-9969. http://dx.doi.org/10.1103/PhysRevB.102.064510.

[7] Zalom, Peter, Žonda, M., and Novotný, T.: *Hidden symmetry in interacting-quantum-dot-based multiterminal josephson junctions.* Physical Review Letters, 132(12), March 2024, ISSN 1079-7114. http://dx.doi.org/10.1103/PhysRevLett.132.126505.

[8] Oosterkamp, T. H., Fujisawa, T., Wiel, W. G. van der, Ishibashi, K., Hijman, R. V., Tarucha, S., and Kouwenhoven, L. P.: *Microwave spectroscopy on a quantum-dot molecule*, 1998. https://arxiv.org/abs/cond-mat/9809142.

[9] Heinrich, Andreas J., Oliver, William D., Vandersypen, Lieven M. K., Ardavan, Arzhang, Sessoli, Roberta, Loss, Daniel, Jayich, Ania Bleszynski, Fernandez-Rossier, Joaquin, Laucht, Arne, and Morello, Andrea: *Quantum-coherent nanoscience.* Nature Nanotechnology, 16(12):1318–1329, November 2021, ISSN 1748-3395. http://dx.doi.org/10.1038/s41565-021-00994-1.

[10] Meng, T.: *Andreev bound states in josephson quantum dot devices.* March 2009. https://quantumtheory.physik.unibas.ch/people/meng/Tobias_Meng_diploma_thesis.pdf.

[11] Meitei, Thingujam Yaiphalemba, Krithivasan, Saikumar, Sen, Arijit, and Ali, Md Manirul: *Quantumness of electron transport in quantum dot devices through leggett–garg inequalities: A non-equilibrium green's function approach.* Physica A: Statistical Mechanics and its Applications, 655:130160, December 2024, ISSN 0378-4371. http://dx.doi.org/10.1016/j.physa.2024.130160.

[12] Chirolli, L., Greco, A., Crippa, A., Strambini, E., Cuoco, M., Amico, L., and Giazotto, F.: *Diode effect in fraunhofer patterns of disordered multi-terminal josephson junctions.* 2024. https://arxiv.org/abs/2411.19338.

[13] Padurariu, C., Jonckheere, T., Rech, J., Martin, T., and Feinberg, D.: *Tunable pseudogaps due to nonlocal coherent transport in voltage-biased three-terminal josephson junctions.* Physical Review B, 95(20), May 2017, ISSN 2469-9969. http://dx.doi.org/10.1103/PhysRevB.95.205437.

[14] Zazunov, A. and Egger, R.: *Supercurrent blockade in josephson junctions with a majorana wire.* Physical Review B, 85(10), March 2012, ISSN 1550-235X. http://dx.doi.org/10.1103/PhysRevB.85.104514.

[15] Mélin, R. and Feinberg, D.: *Transport theory of multiterminal hybrid structures.* The European Physical Journal B, 26(1):101–114, March 2002, ISSN 1434-6028. http://dx.doi.org/10.1140/epjb/e20020071.

[16] Zazunov, A., Egger, R., and Levy Yeyati, A.: *Low-energy theory of transport in majorana wire junctions.* Physical Review B, 94(1), July 2016, ISSN 2469-9969. http://dx.doi.org/10.1103/PhysRevB.94.014502.

[17] Zazunov, A., Egger, R., Alvarado, M., and Yeyati, A. Levy: *Josephson effect in multiterminal topological junctions.* Physical Review B, 96(2), July 2017, ISSN 2469-9969. http://dx.doi.org/10.1103/PhysRevB.96.024516.

[18] Zazunov, A., Yeyati, A. Levy, and Egger, R.: *Coulomb blockade of majorana-fermion-induced transport.* Physical Review B, 84(16), October 2011, ISSN 1550-235X. http://dx.doi.org/10.1103/PhysRevB.84.165440.

[19] Zazunov, A., Iks, A., Alvarado, M., Levy Yeyati, A., and Egger, R.: *Josephson effect in junctions of conventional and topological superconductors.* Beilstein Journal of Nanotechnology, 9:1659–1676, June 2018, ISSN 2190-4286. http://dx.doi.org/10.3762/bjnano.9.158.

[20] Shmidt, V.V., Müller, P., and Ustinov, A.V.: *The Physics of Superconductors: Introduction to Fundamentals and Applications.* Springer, 1997, ISBN 9783540612438. https://books.google.bg/books?id=8O8svNo_tWoC.

[21] Alvarado, M., Iks, A., Zazunov, A., Egger, R., and Yeyati, A. Levy: *Boundary green's function approach for spinful single-channel and multichannel majorana nanowires.* Physical Review B, 101(9), March 2020, ISSN 2469-9969. http://dx.doi.org/10.1103/PhysRevB.101.094511.

[22] Huamani Correa, Jorge Luis and Nowak, Michal P.: *Theory of universal diode effect in three-terminal josephson junctions.* SciPost Physics, 17(2), August 2024, ISSN 2542-4653. http://dx.doi.org/10.21468/SciPostPhys.17.2.037.

[23] Deb, Oindrila, Sengupta, K., and Sen, Diptiman: *Josephson junctions of multiple superconducting wires.* Phys. Rev. B, 97:174518, May 2018. https://link.aps.org/doi/10.1103/PhysRevB.97.174518.

[24] Murthy, C., Kurilovich, V. D., Kurilovich, P. D., Heck, B. van, G., Leonid I., and Nayak, C.: *Energy spectrum and current-phase relation of a nanowire josephson junction close to the topological transition.* Physical Review B, 101(22), June 2020, ISSN 2469-9969. http://dx.doi.org/10.1103/PhysRevB.101.224501.

[25] Heck, B. van, Mi, S., and Akhmerov, A. R.: *Single fermion manipulation via superconducting phase differences in multiterminal josephson junctions.* Physical Review B, 90(15), October 2014, ISSN 1550-235X. http://dx.doi.org/10.1103/PhysRevB.90.155450.

[26] D.A., Savinov: *Scattering-matrix approach to the theory of josephson transport in mesoscopic multiterminal nodes.* Physica C: Superconductivity and its Applications, 509:22–28, 2015, ISSN 0921-4534. https://www.sciencedirect.com/science/article/pii/S092145341400361X.

[27] Kornich, Viktoriia, Barakov, Hristo S., and Nazarov, Yuli V.: *Overlapping andreev states in semiconducting nanowires: Competition of one-dimensional and three-dimensional propagation.* Phys. Rev. B, 101:195430, May 2020. https://link.aps.org/doi/10.1103/PhysRevB.101.195430.

[28] Mélin, Régis: *Ultralong-distance quantum correlations in three-terminal josephson junctions.* Phys. Rev. B, 104:075402, Aug 2021. https://link.aps.org/doi/10.1103/PhysRevB.104.075402.

[29] Kornich, Viktoriia, Barakov, Hristo S., and Nazarov, Yuli V.: *Fine energy splitting of overlapping andreev bound states in multiterminal superconducting nanostructures.* Physical Review Research, 1(3), October 2019, ISSN 2643-1564. http://dx.doi.org/10.1103/PhysRevResearch.1.033004.

[30] Kokkeler, T.H.: *Usadel equation for a four terminal junction.* University of Twente, June 2021. https://essay.utwente.nl/87911/2/Masterthesis_Tim_Kokkeler_final_version.pdf.

[31] Kokkeler, T. H., Golubov, A. A., and Geurts, B. J.: *Testing superconducting pairing symmetry in multiterminal junctions.* Superconductor Science and Technology, 35(8):084005, jun 2022. https://dx.doi.org/10.1088/1361-6668/ac7675.

[32] Posadskii, A. F.: *Properties of Andreev states in multiterminal josephson junctions.* Master's thesis, MIPT, 2023.

[33] Riwar, Roman Pascal, Houzet, Manuel, Meyer, Julia S., and Nazarov, Yuli V.: *Multi-terminal josephson junctions as topological matter.* Nature Communications, 7(1), April 2016, ISSN 2041-1723. http://dx.doi.org/10.1038/ncomms11167.

[34] Peralta Gavensky, Lucila, Usaj, Gonzalo, and Balseiro, C. A.: *Multi-terminal josephson junctions: A road to topological flux networks.* Europhysics Letters, 141(3):36001, January 2023, ISSN 1286-4854. http://dx.doi.org/10.1209/0295-5075/acb2f6.

[35] Mélin, Régis, Winkelmann, Clemens B., and Danneau, Romain: *Magnetointerferometry of multiterminal josephson junctions.* Physical Review B, 109(12), March 2024, ISSN 2469-9969. http://dx.doi.org/10.1103/PhysRevB.109.125406.

[36] Hwang, Sun Yong, Giazotto, Francesco, and Sothmann, Björn: *Phase-coherent heat circulator based on multiterminal josephson junctions.* Phys. Rev. Appl., 10:044062, Oct 2018. https://link.aps.org/doi/10.1103/PhysRevApplied.10.044062.

[37] Piasotski, K., Svetogorov, A., Belzig, W., and Pletyukhov, M.: *Theory of three-terminal andreev spin qubits.* 2024. https://arxiv.org/abs/2411.11155.

[38] Holgaard, Ulrik Laurens Drejer: *Multi terminal josephson junctions.* Master thesis, 2018. https://nbi.ku.dk/english/theses/masters-theses/ulrik-laurens-d-holgaard/Ulrik_Holgaard_master_thesis_04092018.pdf.

[39] Pankratova, N., Lee, H., Kuzmin, R., Wickramasinghe, K., Mayer, W., *et al.*: *Multiterminal josephson effect.* Physical Review X, 10(3), September 2020, ISSN 2160-3308. http://dx.doi.org/10.1103/PhysRevX.10.031051.

[40] Coraiola, M., Haxell, D. Z., Sabonis, D., Hinderling, M., *et al.*: *Spin-degeneracy breaking and parity transitions in three-terminal josephson junctions.* Phys. Rev. X, 14:031024, Aug 2024. https://link.aps.org/doi/10.1103/PhysRevX.14.031024.

[41] Bardeen, J., Cooper, L. N., and Schrieffer, J. R.: *Theory of superconductivity.* Phys. Rev., 108:1175–1204, Dec 1957. https://link.aps.org/doi/10.1103/PhysRev.108.1175.

[42] Josephson, B.D.: *Possible new effects in superconductive tunnelling.* Physics Letters, 1(7):251–253, 1962, ISSN 0031-9163. https://www.sciencedirect.com/science/article/pii/0031916362913690.

[43] Andreev, A F: *Thermal conductivity of the intermediate state of superconductors.* Zh. Eksperim. i Teor. Fiz., 46, May 1964. https://www.osti.gov/biblio/4071988.

[44] Kulik, Igor O.: *Macroscopic quantization and the proximity effect in s-n-s junctions.* 1969. https://api.semanticscholar.org/CorpusID:115399493.

[45] Koelle, Dieter: *Basic properties of josephson junctions.* https://nanocohybri.eu/wp-content/uploads/2019/01/Koelle_1.pdf.

[46] Keldysh, L. V.: *Diagram technique for nonequilibrium processes.* Zh. Eksp. Teor. Fiz., 47:1515–1527, 1964.

[47] Martin, Paul C. and Schwinger, Julian: *Theory of many-particle systems. i.* Phys. Rev., 115:1342–1373, Sep 1959. https://link.aps.org/doi/10.1103/PhysRev.115.1342.

[48] Kulik, I.O., Yanson, I.K., and Gluck, P.: *Josephson Effect in Superconducting Tunneling Structures.* John Wiley & Sons, Incorporated, 1972, ISBN 9780470510506. https://books.google.bg/books?id=_KDUAQAACAAJ.

[49] *Wikipedia, Josephson effect.* Accessed: Dec 2024. https://en.wikipedia.org/wiki/Josephson_effect.

[50] Zazunov, A., Shumeiko, V. S., Bratus', E. N., Lantz, J., and Wendin, G.: *Andreev level qubit.* Physical Review Letters, 90(8), February 2003, ISSN 1079-7114. http://dx.doi.org/10.1103/PhysRevLett.90.087003.

[51] Clarke, John, Cleland, Andrew N., Devoret, Michel H., Esteve, Daniel, and Martinis, John M.: *Quantum mechanics of a macroscopic variable: The phase difference of a josephson junction.* Science, 239(4843):992–997, 1988. https://www.science.org/doi/abs/10.1126/science.239.4843.992.

[52] Blais, A., Grimsmo, A. L., Girvin, S. M., and Wallraff, A.: *Circuit quantum electrodynamics.* Reviews of Modern Physics, 93(2), May 2021, ISSN 1539-0756. http://dx.doi.org/10.1103/RevModPhys.93.025005.

[53] Despósito, M. A. and Levy Yeyati, A.: *Controlled dephasing of andreev states in superconducting quantum point contacts.* Physical Review B, 64(14), September 2001, ISSN 1095-3795. http://dx.doi.org/10.1103/PhysRevB.64.140511.

[54] Likharev, K.K. and Semenov, V.K.: *Rsfq logic/memory family: a new josephson-junction technology for sub-terahertz-clock-frequency digital systems.* IEEE Transactions on Applied Superconductivity, 1(1):3–28, 1991.

[55] You, J. Q. and Nori, Franco: *Atomic physics and quantum optics using superconducting circuits.* Nature, 474(7353):589–597, June 2011, ISSN 1476-4687. http://dx.doi.org/10.1038/nature10122.

[56] Padurariu, C. and Nazarov, Yu. V.: *Theoretical proposal for superconducting spin qubits.* Physical Review B, 81(14), April 2010, ISSN 1550-235X. http://dx.doi.org/10.1103/PhysRevB.81.144519.

[57] Chtchelkatchev, N. M. and Nazarov, Yu. V.: *Andreev quantum dots for spin manipulation.* Physical Review Letters, 90(22), June 2003, ISSN 1079-7114. http://dx.doi.org/10.1103/PhysRevLett.90.226806.

[58] Wees, B. J. van, Lenssen, K. M. H., and Harmans, C. J. P. M.: *Transmission formalism for supercurrent flow in multiprobe superconductor-semiconductor-superconductor devices.* Phys. Rev. B, 44:470–473, Jul 1991. https://link.aps.org/doi/10.1103/PhysRevB.44.470.

[59] Sau, Jay D., Lutchyn, Roman M., Tewari, Sumanta, and Das Sarma, S.: *Generic new platform for topological quantum computation using semiconductor heterostructures.* Physical Review Letters, 104(4), January 2010, ISSN 1079-7114. `http://dx.doi.org/10.1103/PhysRevLett.104.040502`.

[60] Beenakker, C.W.J.: *Search for majorana fermions in superconductors.* Annual Review of Condensed Matter Physics, 4(1):113–136, April 2013, ISSN 1947-5462. `http://dx.doi.org/10.1146/annurev-conmatphys-030212-184337`.

[61] Alicea, J.: *New directions in the pursuit of majorana fermions in solid state systems.* Reports on Progress in Physics, 75(7):076501, June 2012, ISSN 1361-6633. `http://dx.doi.org/10.1088/0034-4885/75/7/076501`.

[62] Aguado, Ramon: *Majorana quasiparticles in condensed matter.* La Rivista del Nuovo Cimento, (11):523–593, October 2017, ISSN 0393697X, 0393697X. `https://doi.org/10.1393/ncr/i2017-10141-9`.

[63] Prada, Elsa, San-Jose, Pablo, Moor, Michiel W. A. de, *et al.*: *From andreev to majorana bound states in hybrid superconductor–semiconductor nanowires.* Nature Reviews Physics, 2(10):575–594, September 2020, ISSN 2522-5820. `http://dx.doi.org/10.1038/s42254-020-0228-y`.

[64] Pientka, Falko, Keselman, Anna, Berg, Erez, Yacoby, Amir, Stern, Ady, and Halperin, Bertrand I.: *Topological superconductivity in a planar josephson junction.* Physical Review X, 7(2), May 2017, ISSN 2160-3308. `http://dx.doi.org/10.1103/PhysRevX.7.021032`.

[65] Leijnse, M. and Flensberg, K.: *Introduction to topological superconductivity and majorana fermions.* Semiconductor Science and Technology, 27(12):124003, November 2012, ISSN 1361-6641. `http://dx.doi.org/10.1088/0268-1242/27/12/124003`.

[66] Chamon, C., Jackiw, R., Nishida, Y., Pi, S. Y., and Santos, L.: *Quantizing majorana fermions in a superconductor.* Phys. Rev. B, 81:224515, Jun 2010. `https://link.aps.org/doi/10.1103/PhysRevB.81.224515`.

[67] Likharev, K. K.: *Superconducting weak links.* Rev. Mod. Phys., 51:101–159, Jan 1979. `https://link.aps.org/doi/10.1103/RevModPhys.51.101`.

[68] Golubov, A. A., Kupriyanov, M. Yu., and Il'ichev, E.: *The current-phase relation in josephson junctions.* Rev. Mod. Phys., 76:411–469, Apr 2004. `https://link.aps.org/doi/10.1103/RevModPhys.76.411`.

[69] Lesovik, Gordei B and Sadovskyy, Ivan A: *Scattering matrix approach to the description of quantum electron transport.* Physics-Uspekhi, 54(10):1007–1059, October 2011, ISSN 1468-4780. `http://dx.doi.org/10.3367/UFNe.0181.201110b.1041`.

[70] Zhu, Jian Xin: *Bogoliubov-de Gennes Method and Its Applications*, volume 924. 2016.

[71] Beenakker, C. W. J.: *Universal limit of critical-current fluctuations in mesoscopic josephson junctions.* Phys. Rev. Lett., 67:3836–3839, Dec 1991. `https://link.aps.org/doi/10.1103/PhysRevLett.67.3836`.

[72] Beenakker, C. W. J.: *Josephson effect in a junction coupled to an electron reservoir.* Applied Physics Letters, 125(12), September 2024, ISSN 1077-3118. http://dx.doi.org/10.1063/5.0215522.

[73] Chang, Li Fu and Bagwell, Philip F.: *Ballistic josephson-current flow through an asymmetric superconductor–normal-metal–superconductor junction.* Phys. Rev. B, 49:15853–15863, Jun 1994. https://link.aps.org/doi/10.1103/PhysRevB.49.15853.

[74] Eschrig, M.: *Theory of andreev bound states in s-f-s junctions and s-f proximity devices.* 2015. https://arxiv.org/abs/1509.07818.

[75] Žonda, M., Pokorný, V., Janiš, V., and Novotný, T.: *Perturbation theory of a superconducting 0-π impurity quantum phase transition.* Scientific Reports, 5(1), March 2015, ISSN 2045-2322. http://dx.doi.org/10.1038/srep08821.

[76] Meden, V: *The anderson–josephson quantum dot—a theory perspective.* Journal of Physics: Condensed Matter, 31(16):163001, February 2019, ISSN 1361-648X. http://dx.doi.org/10.1088/1361-648X/aafd6a.

[77] Bagwell, Philip F.: *Suppression of the josephson current through a narrow, mesoscopic, semiconductor channel by a single impurity.* Phys. Rev. B, 46:12573–12586, Nov 1992. https://link.aps.org/doi/10.1103/PhysRevB.46.12573.

[78] Shnirman, A. and Piasotski, K.: *Exercises to Superconductivity, Josephson effect and applications.* KIT-Fakultäten - KIT-Fakultät für Physik. https://www.tkm.kit.edu/english/teaching/4144_4151.php.

[79] Chen, Ching Tzu: *Scanning tunneling spectroscopy studies of high-temperature cuprate superconductors.* Dissertation (Ph.D.), 2006. https://resolver.caltech.edu/CaltechETD:etd-05222006-124257.

[80] Blonder, G. E., Tinkham, M., and Klapwijk, T. M.: *Transition from metallic to tunneling regimes in superconducting microconstrictions: Excess current, charge imbalance, and supercurrent conversion.* Phys. Rev. B, 25:4515–4532, Apr 1982. https://link.aps.org/doi/10.1103/PhysRevB.25.4515.

[81] Groth, Christoph W, Wimmer, Michael, Akhmerov, Anton R, and Waintal, Xavier: *Kwant: a software package for quantum transport.* New Journal of Physics, 16(6):063065, June 2014, ISSN 1367-2630. http://dx.doi.org/10.1088/1367-2630/16/6/063065.

[82] Wimmer, M.: *Quantum Transport in Nanostructures: From Computational Concepts to Spintronics in Graphene and Magnetic Tunnel Junctions.* Dissertationsreihe der Fakultät für Physik der Universität Regensburg. Univ.-Verlag Regensburg, 2009, ISBN 9783868450255. https://books.google.bg/books?id=WQtZngEACAAJ.

[83] Affleck, I., Caux, J. S., and Zagoskin, A. M.: *Andreev scattering and josephson current in a one-dimensional electron liquid.* Physical Review B, 62(2):1433–1445, July 2000, ISSN 1095-3795. http://dx.doi.org/10.1103/PhysRevB.62.1433.

[84] Zyuzin, Alexander, Alidoust, Mohammad, and Loss, Daniel: *Josephson junction through a disordered topological insulator with helical magnetization.* Phys. Rev. B, 93:214502, Jun 2016. https://link.aps.org/doi/10.1103/PhysRevB.93.214502.

[85] Heersche, Hubert B., Jarillo-Herrero, Pablo, Oostinga, Jeroen B., Vandersypen, Lieven M. K., and Morpurgo, Alberto F.: *Bipolar supercurrent in graphene.* Nature, 446(7131):56–59, March 2007, ISSN 1476-4687. http://dx.doi.org/10.1038/nature05555.

[86] Ryazanov, V. V., Oboznov, V. A., Veretennikov, A. V., Rusanov, A. Yu., Golubov, A. A., and Aarts, J.: *Coupling of two superconductors through a ferromagnet. sfs π-junctions and intrinsically-frustrated superconducting networks.* Physics-Uspekhi, 44(10S):81, oct 2001. https://dx.doi.org/10.1070/1063-7869/44/10S/S18.

[87] Eichler, A., Deblock, R., Weiss, M., Karrasch, C., Meden, V., Schönenberger, C., and Bouchiat, H.: *Tuning the josephson current in carbon nanotubes with the kondo effect.* Phys. Rev. B, 79:161407, Apr 2009. https://link.aps.org/doi/10.1103/PhysRevB.79.161407.

[88] Ioselevich, P. A., Ostrovsky, P. M., and Feigel'man, M. V.: *Josephson current between topological and conventional superconductors.* Physical Review B, 93(12), March 2016, ISSN 2469-9969. http://dx.doi.org/10.1103/PhysRevB.93.125435.

[89] Kuplevakhsky, S. V. and Fal'ko, I.I.: *Theory of superconducting junctions sfs and sf for temperatures close to critical.* 84(1), 1990.

[90] Koch, Jens, Manucharyan, V., Devoret, M. H., and Glazman, L. I.: *Charging effects in the inductively shunted josephson junction.* Physical Review Letters, 103(21), November 2009, ISSN 1079-7114. http://dx.doi.org/10.1103/PhysRevLett.103.217004.

[91] Cuevas, J. C., Martín-Rodero, A., and Yeyati, A. Levy: *Hamiltonian approach to the transport properties of superconducting quantum point contacts.* Physical Review B, 54(10):7366–7379, September 1996, ISSN 1095-3795. http://dx.doi.org/10.1103/PhysRevB.54.7366.

[92] Caroli, C., Combescot, R., Lederer, D., Nozieres, P., and Saint-James, D.: *A direct calculation of the tunnelling current. ii. free electron description.* 4(16):2598, nov 1971. https://dx.doi.org/10.1088/0022-3719/4/16/025.

[93] Khomyakov, P. A., Brocks, G., Karpan, V., Zwierzycki, M., and Kelly, P. J.: *Conductance calculations for quantum wires and interfaces: Mode matching and green's functions.* Physical Review B, 72(3), July 2005, ISSN 1550-235X. http://dx.doi.org/10.1103/PhysRevB.72.035450.

[94] Wilhelm, Frank K., Schön, Gerd, and Zaikin, Andrei D.: *Mesoscopic superconducting–normal metal–superconducting transistor.* Phys. Rev. Lett., 81:1682–1685, Aug 1998. https://link.aps.org/doi/10.1103/PhysRevLett.81.1682.

[95] Golubov, A. A., Kupriyanov, M. Yu., and Il'ichev, E.: *The current-phase relation in josephson junctions.* Rev. Mod. Phys., 76:411–469, Apr 2004. https://link.aps.org/doi/10.1103/RevModPhys.76.411.

[96] Belzig, Wolfgang, Wilhelm, Frank K, Bruder, Christoph, Schön, Gerd, and Zaikin, Andrei D: *Quasiclassical green's function approach to mesoscopic superconductivity.* Superlattices and Microstructures, 25(5–6):1251–1288, May 1999, ISSN 0749-6036. http://dx.doi.org/10.1006/spmi.1999.0710.

[97] Shelankov, A. and Ozana, M.: *Quasiclassical theory of superconductivity: a multiple interface geometry.* 1999. https://arxiv.org/abs/cond-mat/9905226.

[98] Choi, Mahn Soo, Lee, Minchul, Kang, Kicheon, and Belzig, W.: *Kondo effect and josephson current through a quantum dot between two superconductors.* Physical Review B, 70(2), July 2004, ISSN 1550-235X. http://dx.doi.org/10.1103/PhysRevB.70.020502.

[99] Karrasch, C., Oguri, A., and Meden, V.: *Josephson current through a single anderson impurity coupled to bcs leads.* Phys. Rev. B, 77:024517, Jan 2008. https://link.aps.org/doi/10.1103/PhysRevB.77.024517.

[100] Siano, F. and Egger, R.: *Josephson current through a nanoscale magnetic quantum dot.* Phys. Rev. Lett., 93:047002, Jul 2004. https://link.aps.org/doi/10.1103/PhysRevLett.93.047002.

[101] Luitz, D. J., Assaad, F. F., Novotný, T., Karrasch, C., and Meden, V.: *Understanding the josephson current through a kondo-correlated quantum dot.* Phys. Rev. Lett., 108:227001, May 2012. https://link.aps.org/doi/10.1103/PhysRevLett.108.227001.

[102] Cheng, Meng and Lutchyn, Roman M.: *Josephson current through a superconductor/semiconductor-nanowire/superconductor junction: Effects of strong spin-orbit coupling and zeeman splitting.* Phys. Rev. B, 86:134522, Oct 2012. https://link.aps.org/doi/10.1103/PhysRevB.86.134522.

[103] Driel, David van: *Qutech360: Andreev bound states: Spin and charge.* July Jul 2023. https://www.youtube.com/watch?v=4TLlhK-WYKk&ab_channel=QuTechAcademy.

[104] Bargerbos, Arno, Pita-Vidal, Marta, Žitko, Rok, Ávila, Jesús, Splitthoff, Lukas J., Grünhaupt, Lukas, *et al.*: *Singlet-doublet transitions of a quantum dot josephson junction detected in a transmon circuit.* PRX Quantum, 3(3), July 2022, ISSN 2691-3399. http://dx.doi.org/10.1103/PRXQuantum.3.030311.

[105] Nazarov, Y.V. and Blanter, Y.M.: *Quantum Transport: Introduction to Nanoscience.* Cambridge University Press, 2009, ISBN 9780521832465. https://books.google.bg/books?id=YNr4OcCExUcC.

[106] Abrikosov, A.A., Gorkov, L.P., and Dzyaloshinski, I.E.: *Methods of Quantum Field Theory in Statistical Physics.* Dover Books on Physics. Dover Publications, 2012, ISBN 9780486140155. https://books.google.bg/books?id=JYTCAgAAQBAJ.

[107] Levitov, L. S. and Shytov, A. V.: *Green's functions. theory and practice.* page 352, 2002. https://www.mit.edu/~levitov/book/.

[108] Kadanoff, L.P. and Baym, G.: *Quantum Statistical Mechanics: Green's Function Methods in Equilibrium and Nonequilibrium Problems.* Frontiers in Physics. A Lecture Note and Reprint Series. W.A. Benjamin, 1962, ISBN 9780805352016. https://books.google.bg/books?id=Y5I-AAAAIAAJ.

[109] Economou, E.N.: *Green's Functions in Quantum Physics.* Springer Series in Solid-State Sciences. Springer Berlin Heidelberg, 2006, ISBN 9783540288411. https://books.google.bg/books?id=HdJDAAAAQBAJ.

[110] Camsari, Kerem Y., Chowdhury, Shuvro, and Datta, Supriyo: *The Nonequilibrium Green Function (NEGF) Method,* page 1583–1599. Springer International Publishing, November 2022, ISBN 9783030798277. http://dx.doi.org/10.1007/978-3-030-79827-7_44.

[111] Coleman, Piers: *Introduction to Many-Body Physics.* Cambridge University Press, 2015.

[112] Danielewicz, P.: *Quantum theory of nonequilibrium processes, i.* Annals of Physics, 152(2):239–304, 1984, ISSN 0003-4916. https://www.sciencedirect.com/science/article/pii/0003491684900927.

[113] Pascal Simon, Michele Casula: *Introduction of many-body physics of fermions and bosons.* 2021. https://equipes2.lps.u-psud.fr/wp-content/uploads/2021/12/manybody.pdf.

[114] Mahan, G.D.: *Quantum transport equation for electric and magnetic fields.* Physics Reports, 145(5):251–318, 1987, ISSN 0370-1573. https://www.sciencedirect.com/science/article/pii/0370157387900044.

[115] Kiselyov, V.V.: *Non-relativistic mechanics of particles and fields: vector analysis and symmetries [in Russian].* 2022. https://sites.google.com/view/nrmech/μ.

[116] Zazunov, A., Shumeiko, V. S., Wendin, G., and Bratus', E. N.: *Dynamics and phonon-induced decoherence of andreev level qubit.* Physical Review B, 71(21), June 2005, ISSN 1550-235X. http://dx.doi.org/10.1103/PhysRevB.71.214505.

[117] Mineev, V.P and Samokhin, K.: *Introduction to Unconventional Superconductivity.* Taylor & Francis, 1999, ISBN 9789056992095. https://books.google.be/books?id=2BXYWT8m068C.

[118] Beenakker, C. W. J.: *Random-matrix theory of quantum transport.* Reviews of Modern Physics, 69(3):731–808, July 1997, ISSN 1539-0756. http://dx.doi.org/10.1103/RevModPhys.69.731.

[119] Beenakker, C.W.J. and Houten, H. van: *Quantum Transport in Semiconductor Nanostructures,* page 1–228. Elsevier, 1991. http://dx.doi.org/10.1016/S0081-1947(08)60091-0.